



## Characterisation of weak layers, physical controls on their global distribution and their role in submarine landslide formation

R. Gatter<sup>a,\*</sup>, M.A. Clare<sup>b</sup>, J. Kuhlmann<sup>a</sup>, K. Huhn<sup>a</sup>

<sup>a</sup> MARUM – Center for Marine Environmental Sciences, University of Bremen, Germany

<sup>b</sup> National Oceanography Centre, Southampton European Way, Southampton, UK

### ARTICLE INFO

#### Keywords:

Submarine landslide  
Slope failure  
Preconditioning factor  
Weak layer  
Failure plane  
Geotechnics

### ABSTRACT

Submarine landslides pose a hazard to coastal communities as they can generate powerful tsunamis, and threaten critical offshore infrastructure such as seafloor cable networks that underpin global communications. Such events can be orders of magnitude larger than their onshore equivalents. Despite the hazard they pose, many aspects of submarine landslides remain poorly understood, such as why they fail on low angle (<2°), seemingly stable slopes. Many studies have proposed that failure on low slope angles, and the large areal extent of submarine landslides, may be controlled by the presence of laterally-extensive weak layers embedded within the slope stratigraphy, which precondition slopes to failure. Little remains known, however, about the characteristics and processes that control and form weak layers. We conducted a comprehensive review of published submarine landslide studies that examine failure planes and apparent weak layers associated with historical and ancient submarine landslides. Based on a new global landslide catalogue that comprises 64 case studies, this review aims to investigate the types of sediment that form weak layers and to understand the controls on their global variability. Existing classification schemes are based on mechanical process(es), and do not readily enable a diagnosis of weak layers from unfailed sediments. Here, a new and complementary classification of weak layers based on lithology is introduced. This classification enables weak layer recognition from sediment cores (including those sampling unfailed sediments), and allows us to attribute failure mechanisms to different environmental settings where distinct types of weak layers are more likely. The results show that failure planes usually form in the vicinity of an interface between distinct lithologies that together comprise a weak layer. The weak layers of 22 of the 64 case studies were related to characteristic sediment sequences within the slope stratigraphy, of which 19 were classified based on direct measurements from sediment cores and in-situ measurements: 16 weak layers were classified as siliciclastic, four as volcanoclastic, and two as fossiliferous sediment sequences. Only three submarine landslides were related to clay-dominated weak layers. In addition, failure along lithological contrasts was inferred for six case studies. Based on global depositional models likely locations of these different types of weak layer can be inferred. These include oceanic gateways where long-term circulation can create distinct permeability interfaces within siliciclastic sequences, areas of high productivity where biogenic sediments may dominate, and regions that experience widespread ash fall from volcanic eruptions. We highlight that many submarine landslide studies have historically not collected sediment cores that characterise weak layers within intact sedimentary sequences and instead have focused on characterising the slope failure deposit. As weak layers can collapse or become heavily modified during failure, there is a widespread omission of key information required for geotechnical analysis to determine where and why certain slopes are predisposed to failure. We conclude by highlighting the need to combine detailed geotechnical measurements with sedimentological and geophysical analyses including grain-scale observations (e.g. micro-Computed Tomography 3D imagery), and emphasise the importance of a uniform workflow that will allow for a better comparison between individual studies.

\* Corresponding author at: MARUM – Center for Marine Environmental Sciences, University of Bremen, Leobener Str. 8, 28359 Bremen, Germany.

E-mail address: [rgatter@marum.de](mailto:rgatter@marum.de) (R. Gatter).

<https://doi.org/10.1016/j.earscrev.2021.103845>

Received 20 April 2021; Received in revised form 22 October 2021; Accepted 24 October 2021

Available online 28 October 2021

0012-8252/© 2021 The Authors.

Published by Elsevier B.V. This is an open access article under the CC BY-NC-ND license

(<http://creativecommons.org/licenses/by-nc-nd/4.0/>).

## 1. Introduction

Submarine landslides are gravity-driven mass movements that occur in a variety of underwater slope settings worldwide (e.g. Lee et al., 2007). They can be many orders of magnitude larger than their terrestrial counterparts (Hühnerbach et al., 2004; Korup et al., 2007), involving up to thousands of cubic kilometres of sediment (e.g. Watts and Masson, 1995; Hafidason et al., 2004; Winkelmann et al., 2008). Submarine landslides and their resulting sediment density flows are thus one of the most important processes for transporting large amounts of sediment from the continental slope to the deep ocean (e.g. Talling et al., 2007; Korup, 2012; Talling, 2014). The socio-economic consequences of submarine landslides can be severe, ranging from damage to important seafloor infrastructure such as telecommunication cables and gas and oil production equipment (Piper et al., 1999; Ruffman and Hann, 2006; Thomas et al., 2010; Carter et al., 2014; Pope et al., 2017a) to the generation of devastating and deadly tsunamis (Tappin et al., 2001; Ruffman and Hann, 2006; ten Brink et al., 2009; Hsu et al., 2009; Harbitz et al., 2014; Løvholt et al., 2019). Continued growth in coastal populations and development (i.e. cities and harbours), and increased reliance on subsea energy and communication transfer (e.g. Carter et al., 2014) has led to a growth in research of submarine landslides over the past decades.

Some of the largest submarine landslides have been identified on extremely low angle slopes ( $<2^\circ$ ) along continental margins (such as offshore Norway, e.g. Evans et al., 2005; or offshore NW Africa, e.g. Krastel et al., 2019); however, such slopes should theoretically be stable according to conventional standard slope stability concepts (e.g. Leynaud et al., 2007). This contrast between theoretical predictions and observed reality highlights the need to identify additional factors that contribute towards slope failure in the subaqueous realm. Many hypotheses have been put forward concerning factors that control the initiation of submarine landslides (e.g. Hampton et al., 1996; Locat and Lee, 2002; Masson et al., 2006; Lee et al., 2007; Leynaud et al., 2009). Seismic shaking and slope over-steepening were initially inferred to be the dominant triggers for submarine landslides since the early work of Morgenstern (1967); however, more recent studies have shown that in addition to such short-term triggering mechanisms, longer term pre-conditioning factors play a crucial role in the formation of submarine landslides. In particular, the occurrence of so-called *weak layers* embedded within the slope stratigraphy appear to control the localisation of submarine landslides and their failure planes (e.g. Masson et al., 2006; L'Heureux et al., 2012; Locat et al., 2014).

Movement of submarine landslides seems to initiate along distinct sediment horizons. These horizons are somehow predisposed to failure, and have been termed as 'weak layers' (e.g. Masson et al., 2006, 2010; Locat et al., 2014). Slides have often been observed to follow failure planes at different stratigraphic levels, forming a stepped, staircase-like profile (e.g. AFEN Slide, Wilson et al., 2004; Gatter et al., 2020; Grand Banks, Mosher and Piper, 2007; Schulten et al., 2019a; Flemish Cap Slides, Cameron et al., 2014; Sahara Slide, Georgiopoulou et al., 2010; Li et al., 2017). This phenomenon has been related to weak layers at different stratigraphic depths that become active under different strength thresholds (O'Leary, 1991).

### 1.1. The weak layer concept

The concept of weak layers that control the location and depth of submarine landslides is widely established (e.g. Lewis, 1971; O'Leary, 1991; Masson et al., 2006; L'Heureux et al., 2012; Locat et al., 2014; Rodríguez-Ochoa et al., 2015). The concept suggests that specific sediment layers are the focus of effective stress reduction due to external forcing and therefore, serve as preferential failure planes of submarine landslides (e.g. Masson et al., 2006, 2010; Locat et al., 2014). That is to say that effective stress reduction, and thereby failure, is focused along weak layers as their shear strength is transiently reduced and/or the

acting shear stress exceeds the shear strength of the layer.

Although a growing number of studies have pointed towards the significance of such weak layers in the inception of submarine landslides, very little is known about their characteristics, nature and global variability (e.g. Lewis, 1971; O'Leary, 1991; Masson et al., 2010; Locat et al., 2014; Huhn et al., 2020). A first attempt to define and classify weak layers from a geotechnical perspective was carried out by Locat et al. (2014). They defined a weak layer as "a layer (or band) consisting of sediment or rock that has strength potentially or actually sufficiently lower than that of adjacent units (strength contrast) to provide a potential focus for the development of a surface of rupture". Based on this definition and their observations, they proposed a classification in which weak layers are categorised into *inherited* and *induced* weak layers. This definition clarified that in addition to weak layers with inherently lower shear strength (e.g. under-consolidated sediments), weak layers could also originate from strength reduction e.g. due to changes in pore pressure or as a result of other sedimentological, geochemical or geomechanical processes, which in turn may also influence pore pressure conditions (Fig. 1). In particular, the layering of sediments with different physical and geotechnical properties (especially permeability and shear strength) was identified to enable focused shearing and the formation of weak layers (e.g. L'Heureux et al., 2012; Locat et al., 2014). Notably, this layering is not limited to 'traditional' siliciclastic clay-sand sequences, but was also recognised in volcanoclastic and fossiliferous sediments that are common in many marine settings (e.g. Harders et al., 2010; Urlaub et al., 2018).

The processes that form and activate weak layers, as well as their role in the formation of submarine landslides, however, are still subject to debate (e.g. Locat and Lee, 2002; Lastras et al., 2004; Leynaud et al., 2009; Harders et al., 2010; Masson et al., 2010; Wiemer and Kopf, 2015; Madhusudhan et al., 2017; Cukur et al., 2020). In light of the increasing focus on and seeming importance of weak layers (e.g. Talling et al., 2014; Huhn et al., 2020), it is timely to review the current state of knowledge and their controls on submarine landslide formation.

### 1.2. Objectives

Here, a global catalogue of case studies is presented that examine the basal surface and potential weak layers of submarine landslides. Based on this compilation, three main questions are addressed:

- What types of sediment are capable of forming weak layers and how diverse is the nature of weak layers worldwide? We explore which types of sediment and associated physical and geotechnical properties may create weak layers through an analysis of a new global landslide catalogue, which includes submarine slope failures that have been linked to weak layers. A new classification system for weak layers is presented, wherein specific properties of different sediment types are attributed to their implications for slope failure. This new classification is intended to complement, rather than compete with established geomechanical-based classifications such as Locat et al. (2014).
- What are the physical controls on where different types of weak layers form? We provide a general model to explain how and why different types of weak layers dominate in different environmental settings, based on the new classification scheme.
- What are the limitations of our submarine landslide catalogue and the outstanding challenges in identifying and characterising weak layers? How can future studies extend our understanding? Several studies have pointed towards the importance of a multi-disciplinary investigation of submarine landslides in order to identify and understand the processes that control slope failure (e.g. Vanneste et al., 2014). We investigate whether multi-disciplinary investigations are common practice for the identification and characterisation of failure planes and weak layers, and make some specific recommendations for future studies to fill outstanding knowledge gaps.



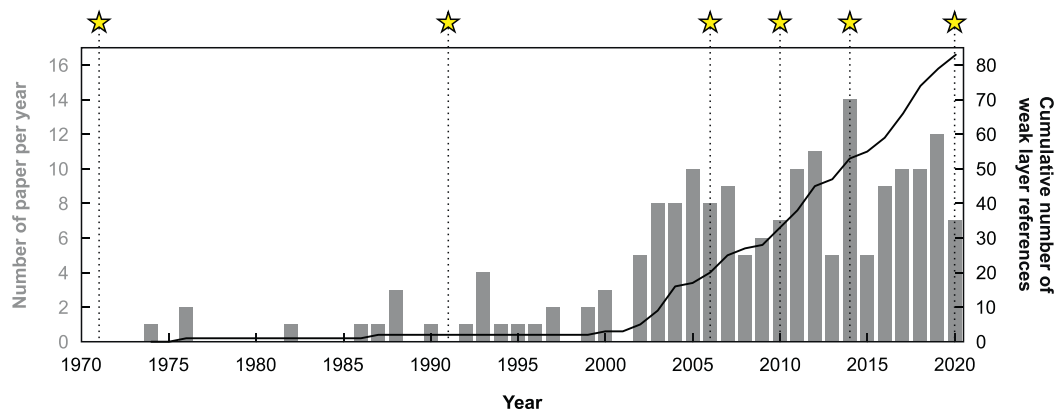


**Fig. 2.** Literature on submarine landslides with information about their glide or failure planes and weak layers increased over the years. In total, 187 references that describe 64 individual case studies were selected for this review. Review papers that initiated key discussion on the presence and importance of weak layers are represented as stars (Lewis, 1971; O’Leary, 1991; Masson et al., 2006, 2010; Locat et al., 2014; Huhn et al., 2020).

studies cover submarine landslides, or landslide complexes from various environmental settings worldwide. The selected references include mainly peer-reviewed papers as well as technical reports and conference proceedings. The catalogue shows an evident increase in literature on submarine landslide studies in general over the years, with a particular growth in the recognition of glide and failure planes and weak layers (Fig. 2). The increase can be attributed to both, the recognition of submarine landslides as a relevant geohazard that requires more attention as well as advances in seafloor surveying techniques, sampling and in-situ measurement equipment, and analytical methods. We recognise that there are a number of limitations to this study because the catalogue is based on published data and inherent restrictions to the findings within these publications. These limitations are further discussed in Section 3.3. In the following, the information of the case studies is summarised in terms of (1) the methods and analyses applied to investigate the selected submarine landslides, in particular their failure planes and weak layers, and (2) the observations and inferences made regarding failure planes and weak layers.

### 2.1. Applied methods and analyses

All 64 selected case studies included identification of submarine landslides from hydroacoustic (multi-beam and side-scan sonar) data. Basal surfaces of submarine landslides were further delineated using geophysical data, which included 2D and 3D seismic, and sub-bottom profiler data. Hydroacoustic and geophysical datasets enable the collection of basic morphometric features of the landslides (e.g. area, volume, slope angle), including identification of the basal surface (see Supplementary data A.1). As legacy seafloor data from 30+ years ago is generally of lower resolution than from more recent studies, they typically only provided limited information about basal surfaces. Therefore, if more than one reference was available for a case study, preference was given to that with higher resolution data and information obtained from advanced analytical techniques.

In addition to hydroacoustic and geophysical data, 53 of the 64 case studies also recovered sediment cores (Fig. 3A, Table 1). Different coring devices were used, including gravity, piston, MeBo (*Meeresboden Bohrergerät* or seafloor drill rig; Freudenthal and Wefer, 2007, 2013), and hydraulic piston and rotary cores from deep ocean drilling programmes (IODP – *International Ocean Discovery Program* and ODP – *Ocean Drilling Program*). Not all cores, however, sampled sediment layers relevant to the study of potential weak layers, i.e. ideally failure plane equivalent sediments outside the slide area or the basal surface of the landslide inside the slide area. Of the 53 case studies with sediment cores, the relevant sediments were sampled in only 24 cases.

A detailed investigation of these 24 case studies, which cored and

sampled the basal surface or failure plane equivalent sediments, revealed that 23 were subject to further analyses (Fig. 3C). MSCL (multi-sensor core logging) measurements were available for cores of five case studies. Data from MSCL and geotechnical analyses (i.e. water content, fall-cone/vane shear tests, PSD (particle size distribution), Atterberg limits, oedometer tests, direct shear tests and/or triaxial tests) were available for another five studies. Seven case studies reported MSCL, geotechnical analyses and XRF (X-ray fluorescence) data, while the remaining six studies reported only geotechnical data.

In general, data from MSCL as well as standard geotechnical analyses (water content, fall-cone/vane shear tests and PSD analyses) become readily available, but advanced geotechnical tests are rare (Fig. 4). Of the 53 case studies with sediment cores, MSCL and water content measurements were available for 28 case studies, undrained shear strength information from fall cone and vane shear tests for 23, and PSD measurements for 25 case studies. Atterberg limits and oedometer tests, on the other hand, were available for cores of 14 and 15 case studies, respectively. Direct shear tests were performed on cores of 11 and triaxial tests on sediment cores of 12 case studies.

Furthermore, of the 64 case studies, nine used in-situ measurements to characterise landslide materials (Fig. 3A; Table 1). Free-fall and pushed cone penetration testing with pore pressure response (FF-CPTu and CPTu) were the primary geotechnical tools used for offshore in-situ measurements. In total, in-situ measurements were available for nine case studies, of which eight included measurements of the relevant sediment layers.

Combining data from both sediment cores and in-situ measurements, 26 of the 64 case studies obtained information from the basal surface of the landslide or failure plane equivalent sediments outside the slide area. In six cases, information was obtained from in-situ measurements and sediment cores. Two case studies had only in-situ measurements, and the remaining 18 studies had only sediment cores that sampled the relevant sediments (Fig. 3A, Table 1). A detailed investigation of these 26 case studies revealed that six obtained data from outside the slide area (i.e. the undisturbed sediments equivalent to the failure plane), 11 from within the slide area (i.e. the basal surface of the landslide), and eight from inside and outside the slide area (Fig. 3B, Table 1). Therefore, these 26 case studies may allow for deeper insight and analysis of weak layers.

### 2.2. Observations and inferences regarding failure planes and weak layers

The synthesised data on submarine landslides and their weak layers (Table 1) show that various sediment types and failure mechanisms have been inferred to control the formation of weak layers and the generation of submarine landslides. The main failure mechanisms invoked to form

**Table 1**

Summary of selected case studies, the deployed methods, and information about the failure plane, weak layer and failure mechanism.

Slide name	Location	Available data		Classification			Selected references	
		Sediment cores	In-situ	Inferred failure plane lithology	Weak layer lithology	Potential failure mechanism		Weak layer type* (after Locat et al., 2014)
1 AFEN Slide	Offshore northern UK, Faroe-Shetland Channel	IN	N/A	Sand-clay interface	Sand-clay sequence; contourite (?)	Strain softening behaviour of a sensitive clay layer, or liquefaction (transient pore pressure generation) along a widespread sandy layer	Induced*	Madhusudhan et al. (2017); Gatter et al. (2020)
2 Agadir Slide	Offshore NW Africa, Atlantic Ocean	NO	N/A	Cannot be classified based on available data	Cannot be classified based on available data	No information	Cannot be deduced from available data	Krastel et al. (2016); Li et al. (2018)
3 Amazon Fan (WMTD)	Offshore NE Brazil, Atlantic Ocean	IN	IN	Cannot be classified based on available data	Cannot be classified based on available data	No information	Cannot be deduced from available data	Piper et al. (1997); Maslin et al. (2005); Maslin (2009)
4 Ana Slide (Eivissa Channel Slides)	Offshore Balearic Islands, Eivissa Channel	NO	IN, OUT	Coarse-fine-grained sediment interface	Coarse-fine-grained sediment sequence	Excess pore pressure generation at coarse-fine-grained sediment interface due to methane gas charging and liquefaction	Inherited or induced*	Berndt et al. (2012); Lafuerza et al. (2012)
5 Andøya Slide	Offshore Norway, Norwegian Sea	NO	N/A	Cannot be classified based on available data	Cannot be classified based on available data	No information	Cannot be deduced from available data	Laberg et al. (2000)
6 Baiyun Slide	Offshore China, Pearl River Mouth Basin, northern South China Sea	NO	N/A	Coarse-fine-grained sediment interface* (?)	Coarse-fine-grained sediment sequence (?); turbidite (?); contourite (?)	Excess pore pressure generation due to free gas charging	Inherited or induced*	Li et al. (2014a, 2014b); Wang et al. (2017); Sun et al. (2017, 2018)
7 Baraza Slide	Offshore Spain, NW Alboran Sea	N/A	N/A	Cannot be classified based on available data	Cannot be classified based on available data	Excess pore pressure (?)	Cannot be deduced from available data	Casas et al. (2011)
8 Betsiamites (-Colombier) Slides	Offshore Betsiamites River, Canada, Lower St. Lawrence Estuary	NO	OUT	Silty layer	Silt-clay sequence*	Excess pore pressure generation along silt-clay interface due to rapid sedimentation and liquefaction	Induced*	Cauchon-Voyer et al. (2008, 2011, 2012)
9 BIG'95 Slide	Offshore Columbretes Islands, Balearic Sea	NO	N/A	Cannot be classified based on available data	Cannot be classified based on available data	Excess pore pressure (?)	Cannot be deduced from available data	Urgeles et al. (2003, 2006); Lastras et al. (2004, 2007)
10 Bjørnøyrenna (Bear Island Fan) Slide	Offshore Norway, Barents Sea	N/A	N/A	Cannot be classified based on available data	Cannot be classified based on available data	No information	Cannot be deduced from available data	Laberg and Vorren (1993)
11 Bowl Slide	Offshore eastern Australia, Great Barrier Reef, Coral Sea	NO	N/A	Cannot be classified based on available data	Cannot be classified based on available data	No information	Cannot be deduced from available data	Clarke et al. (2016); Puga-Bernabéu et al. (2019)
12 Brattøra Slide	Offshore Norway, Trondheimsfjorden	IN	OUT	Clay layer; turbidite	Clay layer; sand-clay sequence*; turbidite	Excess pore pressure generation due to groundwater flow and strain softening behaviour of weak, sensitive clays	Induced*	L'Heureux et al. (2010, 2011)
13 Brunei Slide	Offshore Brunei, South China Sea	N/A	N/A	Cannot be classified based on	Cannot be classified based on available data	Excess pore pressure (?)	Cannot be deduced from	Gee et al. (2007)

(continued on next page)

Table 1 (continued)

Slide name	Location	Available data		Classification				Selected references	
		Sediment cores	In-situ	Inferred failure plane lithology	Weak layer lithology	Potential failure mechanism	Weak layer type* (after Locat et al., 2014)		
14	Byron Slide	Offshore Byron Bay, eastern Australia, South Pacific Ocean	NO	N/A	available data Cannot be classified based on available data	Cannot be classified based on available data	No information	available data Cannot be deduced from available data	Clarke et al. (2016); Mollison et al. (2020)
15	Cap Blanc Slide	Offshore NW Africa, Atlantic Ocean	IN	N/A	Diatom ooze; diatom ooze-clay interface	Diatom ooze-clay sequence	Excess pore pressure generation and further strength reduction due to particle breakage	Induced*	Urlaub et al. (2018, 2020)
16	Cape Fear Slide	Offshore eastern US, Atlantic Ocean	NO	N/A	Cannot be classified based on available data	Cannot be classified based on available data	Excess pore pressure generation due to gas escape from gas hydrates	Cannot be deduced from available data	Schmuck and Paull (1993); Paull et al. (1996)
17	Crete Slide	Offshore Crete, Cretan Sea	NO	NO	Cannot be classified based on available data	Cannot be classified based on available data	No information	Cannot be deduced from available data	Strozyk et al. (2010a, 2010b)
18	Cudgen Slide	Offshore eastern Australia, South Pacific Ocean	NO	N/A	Cannot be classified based on available data	Cannot be classified based on available data	No information	Cannot be deduced from available data	Clarke et al. (2016)
19	Currituck Slide	Offshore eastern US, Atlantic Ocean	NO	N/A	Cannot be classified based on available data	Cannot be classified based on available data	Excess pore pressure (?)	Cannot be deduced from available data	Prior et al. (1986); Hill et al. (2017)
20	Dakar Slide	Offshore NW Africa, Atlantic Ocean	N/A	N/A	Cannot be classified based on available data	Cannot be classified based on available data	No information	Cannot be deduced from available data	Meyer et al. (2012); Krastel et al. (2019)
21	East Sea Slides I	Offshore Korea, Ulleung Basin, East Sea	NO	N/A	Cannot be classified based on available data	Cannot be classified based on available data	No information	Cannot be deduced from available data	Cukur et al. (2016); Horozal et al. (2019)
22	East Sea Slides II	Offshore Korea, Ulleung Basin, East Sea	IN	N/A	Sand layer* (?)	Sand layer (?); sand-clay sequence* (?)	No information	Cannot be deduced from available data	Horozal et al. (2019); Cukur et al. (2020)
23	Finneidfjord Slide	Offshore Norway, Finneidfjord	IN, OUT	IN, OUT	Clay layer; turbidite	Sand-clay sequence; turbidite	Excess pore pressure generation due to fluid flow and/or liquefaction and/or strain softening of sensitive clay	Induced*	L'Heureux et al. (2012); Steiner et al. (2012); Vardiy et al. (2012); Vanneste et al. (2013, 2014, 2015)
24	Flemish Cap Slides	Offshore Canada, Flemish Cap, Flemish Pass	NO	N/A	Cannot be classified based on available data	Cannot be classified based on available data	Excess pore pressure generation due to fluid migration, or liquefaction of silt	Cannot be deduced from available data	Cameron et al. (2014)
25	Fram Slide	Offshore NW Svalbard, Fram Strait	NO	N/A	Cannot be classified based on available data	Cannot be classified based on available data	No information	Cannot be deduced from available data	Elger et al. (2015, 2017); Osti et al. (2017)
26	Gaviota Slide	Offshore California, Santa Barbara Basin	NO	N/A	Cannot be classified based on available data	Cannot be classified based on available data	No information	Cannot be deduced from available data	Edwards et al. (1995); Kluesner et al. (2020)
27	Gebra Slide	Offshore Trinity Peninsula, Antarctica, Bransfield Basin	NO	N/A	Cannot be classified based on	Cannot be classified based on available data	No information	Cannot be deduced from	Canals et al. (2004)

(continued on next page)

Table 1 (continued)

Slide name	Location	Available data		Classification				Selected references	
		Sediment cores	In-situ	Inferred failure plane lithology	Weak layer lithology	Potential failure mechanism	Weak layer type* (after Locat et al., 2014)		
28	Gloria Knolls Slide	Offshore NW Australia, Great Barrier Reef, Coral Sea	N/A	N/A	available data Cannot be classified based on available data	Lithological contrast (?)	No information	available data Cannot be deduced from available data	Puga-Bernabéu et al. (2017, 2019)
29	Goleta Slide	Offshore California Basin, Santa Barbara Basin	NO	N/A	Cannot be classified based on available data	Cannot be classified based on available data	No information	Cannot be deduced from available data	Fisher et al. (2005); Greene et al. (2006); Kluesner et al. (2020)
30	Gondola Slide	Offshore SW Italy, Adriatic Sea	NO	N/A	Cannot be classified based on available data	Clay layer* (?); contourite (?)	Excess pore pressure (?)	Cannot be deduced from available data	Minisini et al. (2006); Verdicio and Trincards (2008); Dalla Valle et al. (2015)
31	Grand Banks Slide (surficial failures (SF) and St. Pierre Slump (SPS))	Offshore Newfoundland, Canada, Laurentian Fan	OUT (SF), NO (SPS)	N/A	Sand-clay interface; turbidite	Sand-clay sequence; turbidite (?); contourite (?)	No information	Cannot be deduced from available data	Piper et al. (1988, 1999); Mosher and Piper (2007); Schulten (2019); Schulten et al. (2019a, 2019b)
32	Great Bahama Bank Failures	Offshore Bahamas, NW Great Bahama Bank	NO	N/A	Cannot be classified based on available data	Cannot be classified based on available data	No information	Cannot be deduced from available data	Principaud et al. (2015, 2018)
33	Hermosa Slide	Offshore Nicaragua, Pacific Ocean	IN	N/A	Ash layer	Ash-clay sequence	Excess pore pressure generation and further strength reduction due to particle rearrangement/breakage	Induced*	Harders et al. (2010)
34	Hinlopen (Yermak) Slide	Offshore northern Svalbard, Arctic Ocean	OUT	N/A	Contourite	Lithological contrast*; contourite* (?)	No information	Cannot be deduced from available data	Vanneste et al. (2006); Winkelmann et al. (2006, 2008); Winkelmann and Stein (2007)
35	Humboldt Slide	Offshore western US, Pacific Ocean	N/A	N/A	Cannot be classified based on available data	Cannot be classified based on available data	No information	Cannot be deduced from available data	Gardner et al. (1999)
36	Jan Mayen Slide	Offshore SW Jan Mayen Island, Norwegian-Greenland Sea	OUT	N/A	Ash layer (?)	Ash-clay sequence*	No information	Induced* (?)	Laberg et al. (2014)
37	Kitimat Slide	Offshore western Canada, Kitimat Delta	IN, OUT	N/A	Sand layer (?)	Sand layer (?) sand-clay sequence* (?)	No information	Cannot be deduced from available data	Stacey et al. (2018)
38	Licosa Slide	Offshore NW Italy, eastern Tyrrhenian Sea	IN, OUT	N/A	Ash layer	Ash layer; ash-clay sequence*	Excess pore pressure generation	Induced*	Trincardi et al. (2003); Sammartini et al. (2019)
39	Little Bahama Bank Failures	Offshore Bahamas, NW Little Bahama Bank	N/A	N/A	Cannot be classified based on available data	Cannot be classified based on available data	No information	Cannot be deduced from available data	Tournadour et al. (2015)
40	Lofoten Slides	Offshore Norway, Lofoten Basin, Norwegian Sea	IN, OUT	N/A	Silt-clay interface; contourite	Silt-clay sequence; contourite	Strain softening	Induced* (?)	Vanneste et al. (2012); Baeten et al. (2013, 2014)
41	Mauritania Slide	Offshore Mauritania, NW Africa, Atlantic Ocean	IN	N/A	Clay layer	Clay layer; contourite (?)	Excess pore pressure generation due to rapid sedimentation changes	Inherited* (?)	Antobreh and Krastel (2007); Henrich et al. (2008); Förster et al. (2010)
42	Molly Hole Slide	Offshore Svalbard, Fram Strait	N/A	N/A	Cannot be classified based on	Cannot be classified based	No information	Cannot be deduced from	Freire et al. (2014)

(continued on next page)

Table 1 (continued)

Slide name	Location	Available data		Classification				Selected references	
		Sediment cores	In-situ	Inferred failure plane lithology	Weak layer lithology	Potential failure mechanism	Weak layer type* (after Locat et al., 2014)		
43	Munson-Nygren-Retriever Slide	Offshore eastern US, Georges Bank, Atlantic Ocean	N/A	N/A	available data Cannot be classified based on available data	on available data Cannot be classified based on available data	No information	available data Cannot be deduced from available data	Chaytor et al. (2012)
44	Nankai Slide (MTDs)	Offshore SW Japan, southern Kumano Basin	OUT	N/A	Cannot be classified based on available data	Cannot be classified based on available data	No information	Cannot be deduced from available data	Expedition 333 Scientists (2011); Lackey et al. (2018)
45	Nice Airport Slide	Offshore Nice, southern France, Ligurian Sea	IN	IN	Clay layer	Clay layer; sand-clay sequence*	Excess pore pressure generation due to seepage from aquifer and further strength reduction due to strain softening	Induced*	Dan et al. (2007); Stegmann et al. (2011); Vanneste et al. (2014); Kopf et al. (2016)
46	North Aegean Slide	Offshore Greece, North Aegean Trough, North Aegean Sea	NO	N/A	Clay layer; sand-clay interface (?)	Sand-clay sequence (?)	No information	Cannot be deduced from available data	Lykousis et al. (2002)
47	Nyk Slide	Offshore Norway, Norwegian Sea	NO	N/A	Contourite (?)	Lithological contrast* (?); contourite* (?)	Excess pore pressure (?)	Cannot be deduced from available data	Lindberg et al. (2004)
48	Orkdalsfjorden Slide	Offshore Norway, Orkdalsfjorden	IN	N/A	Clay layer; sand-clay interface	Sand-clay sequence; turbidite (?)	Excess pore pressure generation due to groundwater pressure and strain softening behaviour of clays	Induced*	L'Heureux et al. (2014)
49	Pianosa Slump	Offshore western Italy, Corsica Trough, Northern Tyrrhenian Sea	IN, OUT	IN, OUT	Clay layer	Clay layer	Strength reduction due to strain softening	Induced*	Miramontes Garcia (2016); Miramontes et al. (2018)
50	Ranger Slide	Offshore Baja California, Mexico, northern Sebastian Vizcaino Bay	N/A	N/A	Cannot be classified based on available data	Cannot be classified based on available data	No information	Cannot be deduced from available data	Normark (1974, 1990)
51	Sahara Slide	Offshore NW Africa, Atlantic Ocean	NO	N/A	Cannot be classified based on available data	Lithological contrast* (?)	Excess pore pressure	Induced* (?)	Georgiopoulou et al. (2010); Li et al. (2017)
52	Sklinnadjupet Slide	Offshore Norway, Norwegian Sea	NO	N/A	Clay layer (?)	Diatom-ooze-clay sequence* (?)	Excess pore pressure	Induced* (?)	Rise et al. (2006, 2010)
53	Spitzbergen Fracture Zone Slide	Offshore NW Svalbard, Fram Strait	NO	N/A	Cannot be classified based on available data	Cannot be classified based on available data	No information	Cannot be deduced from available data	Osti et al. (2017)
54	Storegga Slide	Offshore Norway, Norwegian Sea	OUT	N/A	Clay layer; contourite	Clay layer (?); clay-clay sequence* (?); contourite (?)	Excess pore pressure generation due to rapid sedimentation and strain softening behaviour of clays	Inherited* (?)	Bugge et al. (1988); Haflidason et al. (2003, 2004, 2005); Canals et al. (2004); Bryn et al. (2005a); Kvalstad et al. (2005); Solheim et al. (2005)
55	Trænadjupet Slide	Offshore Norway, Lofoten Basin, Norwegian Sea	OUT	N/A	Clay layer; contourite	Clay layer; clay-clay sequence*; contourite	Excess pore pressure generation due to rapid sedimentation	Inherited* (?)	Laberg and Vorren (2000); Laberg et al. (2002, 2003)
56	Tuaheni Slide	Offshore Poverty Bay, eastern New Zealand's North Island, South Pacific Ocean	IN	N/A	Cannot be classified based on available data	Lithological contrast* (?)	Excess pore pressure related to gas hydrates	Inherited*	Kuhlmann et al. (2019); Luo et al. (2020)

(continued on next page)

Table 1 (continued)

Slide name	Location	Available data		Classification				Selected references	
		Sediment cores	In-situ	Inferred failure plane lithology	Weak layer lithology	Potential failure mechanism	Weak layer type* (after Locat et al., 2014)		
57	Twin Slides	Offshore SW Italy, Gela Basin, Sicily Channel	IN	N/A	Ash-clay interface	Ash-clay sequence	Excess pore pressure and further strength reduction due to particle rearrangement	Induced*	Kuhlmann et al. (2014, 2016, 2017)
58	Uruguay Slides	Offshore Uruguay, Atlantic Ocean	NO	N/A	Cannot be classified based on available data	Lithological contrast* (?); contourite	No information	Cannot be deduced from available data	Krassel et al. (2011); Henkel et al. (2011); Ai et al. (2014)
59	Vesterålen Slides	Offshore Norway, Norwegian Sea	OUT	IN, OUT	Clay layer	Sand-clay sequence* (?)	Excess pore pressure generation and strain softening	Induced*	Vanneste et al. (2012, 2014); L'Heureux et al. (2013); Vanneste et al. (2014); Stegmann et al. (2016)
60	Vieste Slide	Offshore eastern Italy, Adriatic Sea	NO	N/A	Cannot be classified based on available data	Cannot be classified based on available data	No information	Cannot be deduced from available data	Dalla Valle et al. (2015); Gamberi et al. (2019)
61	Villafranca Slide	Offshore Italy, Gioia Basin, Tyrrhenian Sea	NO	N/A	Cannot be classified based on available data	Cannot be classified based on available data	No information	Cannot be deduced from available data	Gamberi et al. (2011); Rovere et al. (2014)
62	Viper Slide	Offshore Australia, Great Barrier Reef, Coral Sea	N/A	N/A	Cannot be classified based on available data	Cannot be classified based on available data	No information	Cannot be deduced from available data	Webster et al. (2016); Puga-Bernabéu et al. (2019)
63	Western Levee Slide (Laurentian Fan)	Offshore eastern Canada, Scotian Slope, Atlantic Ocean	NO	N/A	Cannot be classified based on available data	Cannot be classified based on available data	No information	Induced* (?)	Mosher et al. (1994); Normandeau et al. (2019a, 2019b)
64	Yamba Slides	Offshore Yamba, eastern Australia, South Pacific Ocean	IN	N/A	Cannot be classified based on available data	Cannot be classified based on available data	No information	Cannot be deduced from available data	Hubble et al. (2019)

Hydroacoustic and geophysical mapping data were available for all selected case studies.

IN = sediment cores/in-situ measurements sampling the basal surface inside the slide area are available

NO = sediment cores/in-situ measurements are available, but did not sample the failure or glide plane

OUT = sediment cores/in-situ measurements sampling the failure plane equivalent sediments outside the slide area are available

N/A = no data available

(\*) = inferred by authors of this review

Based on the available data, we classified all case studies according to Locat et al. (2014). Please refer to Supplementary data A.1 for all details.

weak layers and promote failure relate to excess pore pressure generation and strain softening (Table 1); however, failure mechanisms were often deduced from geophysical data alone rather than from direct sampling. Although only 26 of the 64 selected case studies collected data from relevant sediment layers by means of in-situ measurements and sediment coring, 29 discussed potential failure mechanisms (Table 1).

The data further indicate that the weak layer classification of Locat et al. (2014) cannot be uniformly applied across all the case studies. The classification of Locat et al. (2014) considers the processes that may cause the formation of weak layers (e.g. excess pore pressure generation); however, limitations in the available data mean that identification of these processes, and thus a determination of whether weak layers are *inherited* or *induced*, is not always possible (Table 1). We therefore introduce a complementary classification that is based on the lithology of the weak layer, which can be more readily determined for the case studies (see Section 3 below), and can be used as the basis to interpret the processes that form and activate them. Potential failure mechanisms may then be deduced from those lithologies (Table 1). The classification

further allows specific weak layer types to be linked to different environments and assess their likely global distributions (Section 3.2).

### 3. Weak layer classification

The prerequisite for a robust lithological classification of weak layers is data from sediment cores and in-situ measurements that sampled the glide and/or failure planes of the submarine landslide, and ideally also sampled material in adjacent undisturbed sediment sequences. As discussed earlier (Section 2.1), such data were available for 26 of the 64 case studies; nevertheless, a total of 30 case studies discussed the nature of weak layers (Table 1). Therefore, weak layers are often characterised by relying on information of the study area, and geophysical data and short cores interpolated to the depth of interest, rather than direct measurements.

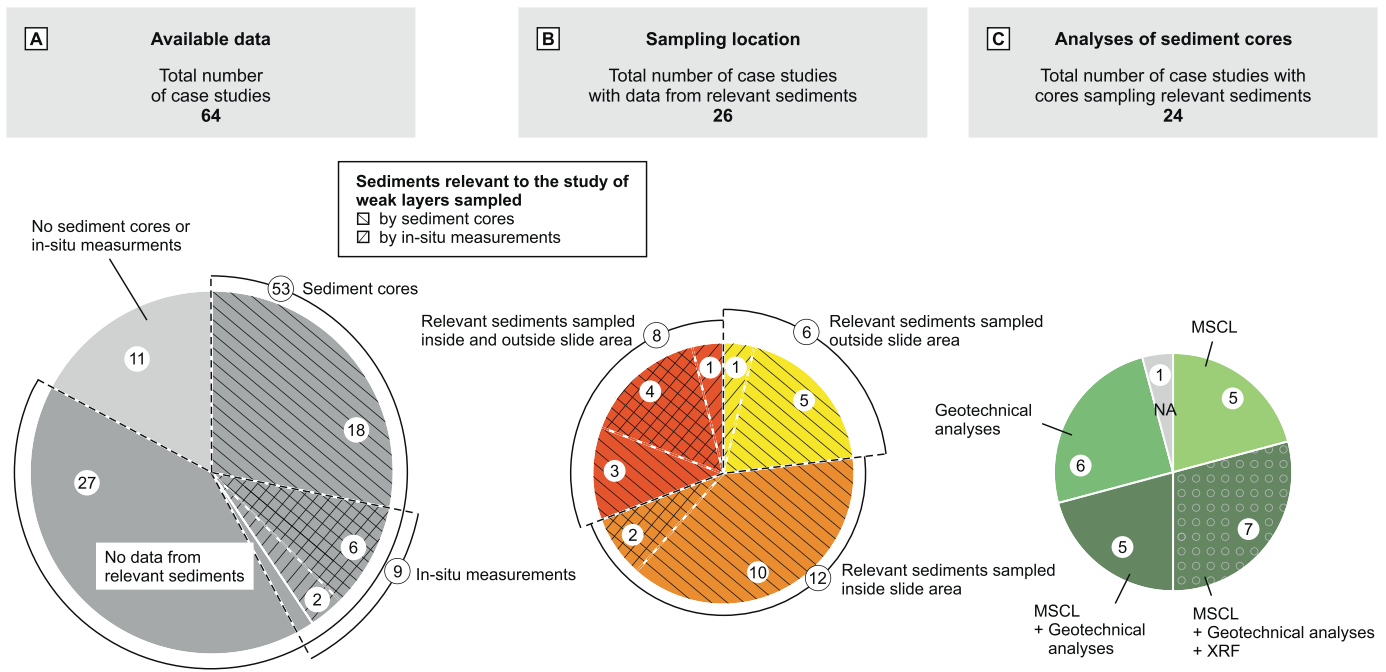


**Fig. 3.** Pie charts counting case studies A. without data from sediment cores or in-situ measurements – light grey, and with data from sediment cores and in-situ measurements – dark grey: no data from relevant sediments (i.e. basal surface of landslide, or failure plane equivalent sediments) – no pattern, cores sampling relevant sediments – left-tilted lines, in-situ measurements sampling relevant sediments – right-tilted lines; B. with sediment cores and in-situ measurements from relevant sediments: inside and outside the slide area – dark orange, inside the slide area – orange, outside the slide area – yellow; and C. with analyses on sediment cores that sampled relevant sediments: no information – grey, MSCL (multi-sensor core logging) – light green, geotechnical analyses (water content, undrained (fall cone and vane) shear strength tests, particle size distribution, Atterberg limits, oedometer, direct shear and/or triaxial tests) – green, MSCL and geotechnical analyses – dark green, MSCL, geotechnical analyses and XRF (X-ray fluorescence) – dark green with circles. Please refer to Supplementary data A.1 for all details. (For interpretation of the references to colour in this figure legend, the reader is referred to the web version of this article.)

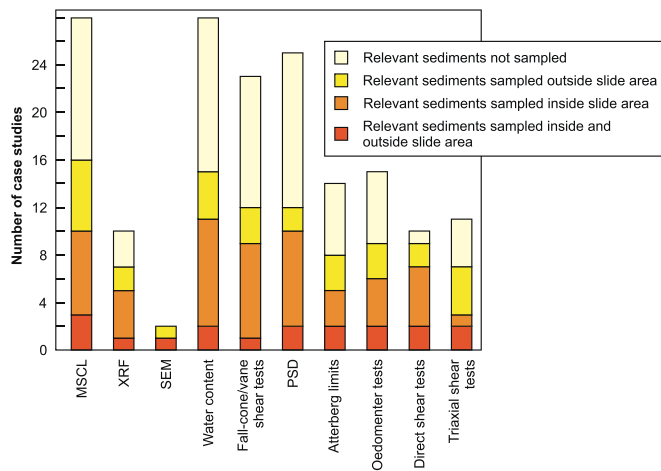


**Fig. 4.** Number of case studies that carried out further analyses on available sediment cores (for all details please refer to Supplementary data A.1). Colour scale illustrates the coring location: not sampling the relevant sediments – light yellow, sampling failure plane equivalent sediments outside – light orange, the basal surface inside – orange, or both, the basal surface inside and the failure plane equivalent sediments outside the slide area – dark orange. MSCL – multi-sensor core logging, XRF – X-ray fluorescence, SEM – scanning electron microscopy, PSD – particle size distribution. (For interpretation of the references to colour in this figure legend, the reader is referred to the web version of this article.)

### 3.1. A lithological approach

Here, we present a classification of weak layers based on lithology (Table 2) that includes: (1) siliciclastic, (2) volcanoclastic, and (3)

fossiliferous sediments. In siliciclastic sediments, weak layers can form in strain softening sediments (usually sensitive clay layers) or along sediment sequences, where permeability and/or strength contrasts promote failure. Volcanoclastic and fossiliferous weak layers are typically related to sediment sequences (e.g. ash-clay or diatom-clay) that may fail either due to strain softening of their weathered products or due to strength reduction and excess pore pressure generation as a result of liquefaction and particle breakage.

#### 3.1.1. Siliciclastic sediments

**3.1.1.1. Clay layers.** Clay layers have been invoked as weak layers because they can be prone to high compressibility and/or sensitivity (e.g. Sultan et al., 2004; L’Heureux et al., 2012), and were identified in three case studies (Table 1; Förster et al., 2010; Dalla Valle et al., 2015; Miramontes et al., 2018). Clays have unique mechanical and physico-chemical properties that can cause them to be mechanically weaker than other siliciclastic sediments. These unique properties are explained by the negative charge of clay minerals and their preferential attraction of positively charged ions (diffuse double layer (DDL) theory by Gouy-Chapman; Bolt, 1956). Reducing the ionic concentration or ionic valence will increase the spacing of the DDL and hence the sediment’s porosity and volume (Bolt, 1956). Therefore, not only the type of clay minerals (e.g. kaolinite versus montmorillonite), but also the dominant type and concentration of exchangeable cations, and pore water salt concentrations have great influence on the mechanical behaviour of clays (e.g. Moore, 1991).

Miramontes et al. (2018) suggested that the Pianosa Slump, on the eastern margin of the Corsica Trough initiated along a zeolitic clay layer. Zeolites are known for their cation exchange capabilities (Mumpton, 1999), and could attract more cations than the clay particles. Over time, this cation exchange results in a decrease of cation concentration around

**Table 2**  
Lithological classification of weak layers in submarine landslide studies.

Type	Description	Example	Selected references
<i>Siliciclastic sediments</i>			
Clay layers	Clay layers may have inherently lower shear strength (e.g. montmorillonite) or can face sudden shear strength reduction (e.g. sensitive clays) due to strain softening (i.e. particle re-arrangement)	e.g. Pianosa Slump, offshore western Italy, Northern Tyrrhenian Sea	Miramontes et al. (2018)
Sand-clay sequence	High-permeability sediments (i.e. sand or sandy layers) overlain by low-permeability sediments (i.e. clay layers) may favour the accumulation of excess pore pressure at the material interface, which may also cause strain softening behaviour of the clays	e.g. Finneidfjord Slide, coastal Norway, Norwegian Sea	L'Heureux et al. (2012)
Clay-clay sequence	High-water content clay (e.g. contourites) overlain by low-permeability sediments (i.e. clay) may promote excess pore pressure accumulation	e.g. Trænadjupet Slide, offshore Norway, Norwegian Sea	Laberg and Vorren (2000)
<i>Volcaniclastic sediments</i>			
Ash-clay sequence	Permeability interface between highly permeable ash layer versus overlying low-permeability clay layers may promote excess pore pressure generation; strength contrast may also cause strain softening within the overlying clay	e.g. Licosa Slide; offshore NW Italy, eastern Tyrrhenian Sea	Sammartini et al. (2019)
<i>Fossiliferous sediments</i>			
Diatom-clay sequence	Permeability interface between diatom ooze and overlying low-permeability clay layers may cause excess pore pressure generation along the diatom ooze layer or at the material interface; strain softening may occur in the overlying clay	e.g. Cap Blanc Slide, offshore NW Africa, Atlantic Ocean	Urlaub et al. (2018)

the clays and a weak sediment layer develops, due to the repulsive forces of the clay minerals (Miramontes et al., 2018). Another process that may lead to a decrease in cation concentration within weak layers is leaching. Fresh ground water percolating through marine sediments, such as those subaerially exposed during low sea level stands, leads to leaching of salt and consequent removal of ionic bonds between clay particles. Thus, leaching results in weakened sediments, termed sensitive clays, such as those found offshore Canada and Norway (e.g. Rosenqvist, 1966; Torrance, 1974; L'Heureux et al., 2011; L'Heureux et al., 2012; Vardy et al., 2012). Although failure likely initiated along the sensitive clay, the weak layers of these case studies have been classified as 'siliciclastic sediment sequence', as lateral fluid flow along permeable sand layers likely promoted strength reduction in the overlying clay layer (e.g. L'Heureux et al., 2012).

**3.1.1.2. Siliciclastic sediment sequences.** Siliciclastic sediment sequences have been inferred as weak layers in 16 case studies. Failure along lithological contrasts was hypothesised for another six case studies, albeit without any validation from sediment cores or in-situ geotechnical testing; hence the precise nature of these contrasts is unknown (Table 1). Such sediment sequences can be the result of various sedimentation regimes:

Contourites have often been inferred as potential weak layers of submarine landslides due to their inherent compositional and geotechnical properties (e.g. Lindberg et al., 2004; Bryn et al., 2005b). Although recent studies have shown that contourite geometry plays a critical role in localising slope failure (Miramontes et al., 2018), others have pointed towards rapid variations in physical and geotechnical properties within contourites as key factors to make them more susceptible to failure (Rashid et al., 2017). The sedimentology of contourites strongly depends on the availability of upstream sediments from different sources and variations in current speed (e.g. Faugères et al., 1993; Rashid et al., 2017). They usually consist of well sorted muddy or sandy sediments that are characterised by high water contents and compressibility, which may favour the generation of excess pore pressure (Laberg and Camerlenghi, 2008). In total, four case studies have been related to contouritic sediment sequences (Table 1). The weak layers of both, the Trænadjupet Slide and the Storegga Slide, offshore Norway are characterised by siliciclastic sediment sequences that resulted from variations in climate-controlled oceanographic conditions (e.g. Laberg et al., 2002; Berg et al., 2005). Rapid deposition of low-permeability glacio-marine sediments above high-water content, fine-grained hemipelagic and/or contouritic sediments likely caused the development of excess pore pressure, thereby increasing the failure potential along this layer (e.g. Laberg and Vorren, 2000; Laberg et al., 2002; Berg et al., 2005; Bryn

et al., 2005b; Kvalstad et al., 2005; Solheim et al., 2005). In addition to such permeability contrasts, strength contrasts between contouritic and surrounding sediments can influence the formation of failure planes and promote failure (e.g. Lofoten Slides, offshore Norway, Baeten et al., 2013, 2014; AFEN Slide, offshore northern UK, Wilson et al., 2004; Gatter et al., 2020). Although another six case studies, namely the Hinlopen and Nyk Slide offshore Norway, the Gondola Slide offshore Italy, the Mauritania Slide offshore NW Africa, the Uruguay Slides offshore Uruguay, and the St. Pierre Slump (Grand Banks Slide) offshore eastern Canada discussed contourites as potential weak layers, a verification was not possible due to lack of sample data (Table 1; Lindberg et al., 2004; Vanneste et al., 2006; Antobreh and Krastel, 2007; Winkelmann and Stein, 2007; Krastel et al., 2011; Dalla Valle et al., 2015; Schulten et al., 2019b).

Turbidites have been identified as weak layers in five case studies (Table 1). Slope failure of the Baiyun Slide, in the Pearl River Mouth Basin offshore China, was related to the migration of free gas from deeper strata into a permeable turbidite layer. This gas-charging likely caused the development of excess pore pressure along the interface between the higher-permeability and overlying low-permeability sediments (Li et al., 2014b; Sun et al., 2018). Similarly, gas-hydrate bearing sandy turbidites interbedded with hemipelagic muds were found beneath several MTDs (mass-transport deposits) in the Ulleung Basin (e.g. Riedel et al., 2012). Schulten (2019) found that weak layers of surficial failures in the Grand Banks area, offshore eastern Canada, correspond to permeability contrasts between sandy turbidites and clay-rich mud. In Norway, turbidites, which likely sourced from quick clay slides on land, have been identified as weak layers of several fjord slides (e.g. Brattøra Slide, L'Heureux et al., 2011; Finneidfjord Slide, L'Heureux et al., 2012; Orkdalsfjorden Slide, L'Heureux et al., 2014). The contrasting permeability between sand and clay sediments within the turbidites may have enabled sub-lateral fluid migration along the sand layers and the formation of artesian groundwater pressure. Excess pore pressure and strain softening of the weaker, sensitive clay likely caused failure along the clay layer (e.g. L'Heureux et al., 2012; Vardy et al., 2012).

Particular attention should be paid to sequences of coarse- and fine-grained sediments, particularly at river deltas. These sequences can form permeability contrasts and may create vertically confined aquifers that can host artesian groundwater pressures that extend offshore (e.g. Micallef et al., 2021). Such offshore aquifers have been observed in fjords, and also suggested to have been a significant factor in the 1979 Nice Airport Slide. A sandy gravel alluvial aquifer overlain by fine-grained sediments was identified as a weak layer for the Nice Airport Slide. Failure likely initiated within the sensitive clay layer which was

further weakened by leaching due to fluid flow in the underlying sand (e.g. Dan et al., 2007).

Lastly, weak layers have been associated with gas hydrate dissociation and free gas migration. Generation of excess pore pressure along the interface between methane-charged higher-permeability and overlying fine-grained, low-permeability sediments was suggested as potential preconditioning factor for repeated slope failure in the Eivissa Channel, Western Mediterranean Sea (Berndt et al., 2012; Lafuerza et al., 2012). Reduction in effective stress due to gas charging and alteration of sediment physical properties as a result of gas hydrate dissociation was also suggested for slope failure along the flank of Sackville Spur, offshore eastern Canada (Mosher et al., 2021). However, the link between free gas and shear strength reduction is still subject to debate (Kaminski et al., 2020).

### 3.1.2. Volcaniclastic sediment sequences

Ash layers have been suggested or identified as weak layers, affecting the formation of failure planes in four case studies (Table 1; Harders et al., 2010; Laberg et al., 2014; Kuhlmann et al., 2017; Sammartini et al., 2019). Based on their work on submarine landslides offshore Nicaragua, in particular on the Hermosa Slide, Harders et al. (2010) proposed that ash layers overlain by impermeable clay can act as weak layers. They proposed that the rearrangement and breakage of ash particles, e.g. due to seismic shaking, may cause a sudden volume reduction. This compaction within the ash layer promotes a rapid accumulation of pore fluid along the interface between the ash and the overlying clay. The transient pore pressure increase would thereby cause an abrupt reduction in shear strength at the interface, and focused shearing along the 'compacted' ash layer or within the overlying clay (Harders et al., 2010). Wiemer and Kopf (2017b) noted that hard-grained ash sands (low crushability) may actually increase the shear strength of the slope material due to the particles' roughness and angularity (Riley et al., 2003), favouring seismic strengthening (Fig. 5).

Soft-grained pumice, however, may be weak due to its high crushability and favour pore pressure build-up (Wiemer and Kopf, 2017b). A coarse-grained ash layer, composed of sub-angular pumice and glass shards, overlain by clayey sediments has been identified as potential failure plane of the Licosa Slide, offshore south-western Italy. The permeable ash likely enabled lateral fluid flow along the layer. Lateral fluid flow and/or seismic shaking could have caused excess pore pressure to develop, and together with particle breakage and rearrangement supposedly caused failure in the upper part of the ash layer or along the ash-clay interface (Sammartini et al., 2019). The same mechanism was suggested for the Twin Slides, offshore Sicily (Kuhlmann et al., 2016, 2017).

Another mechanism proposed to form weak layers within volcaniclastic sediments is strain softening of weathered ash, which constitutes mechanically weaker clay. This hypothesis was confirmed by shear experiments on ash samples at different alteration stages, which demonstrated a marked decrease in shear strength with increasing alteration (Wiemer and Kopf, 2015). It was noted, however, that this alteration is usually found below 800 m bsf, while submarine landslides are concentrated in the upper 400 m bsf (McAdoo et al., 2000; Hühnerbach et al., 2004). This could explain the lack of matching case studies.

### 3.1.3. Fossiliferous sediment sequences

Fossiliferous sediments have been proposed to affect submarine slope stability (e.g. Tanaka and Locat, 1999) and have been invoked as potential weak layers (e.g. foraminifera-rich layers; Sawyer and Hodelka, 2016, diatom-rich layers; Volpi et al., 2003; Urlaub et al., 2018). Urlaub et al. (2018) postulated that diatomaceous sediments overlain by impermeable clay layers likely acted as weak layer and promoted failure of the Cap Blanc Slide, offshore NW Africa. From a geotechnical point of view, even minor amounts of diatoms (about 10%) were found to fundamentally alter key physical properties, often in a complex manner (e.g. Tanaka and Locat, 1999; Shiwakoti et al., 2002;

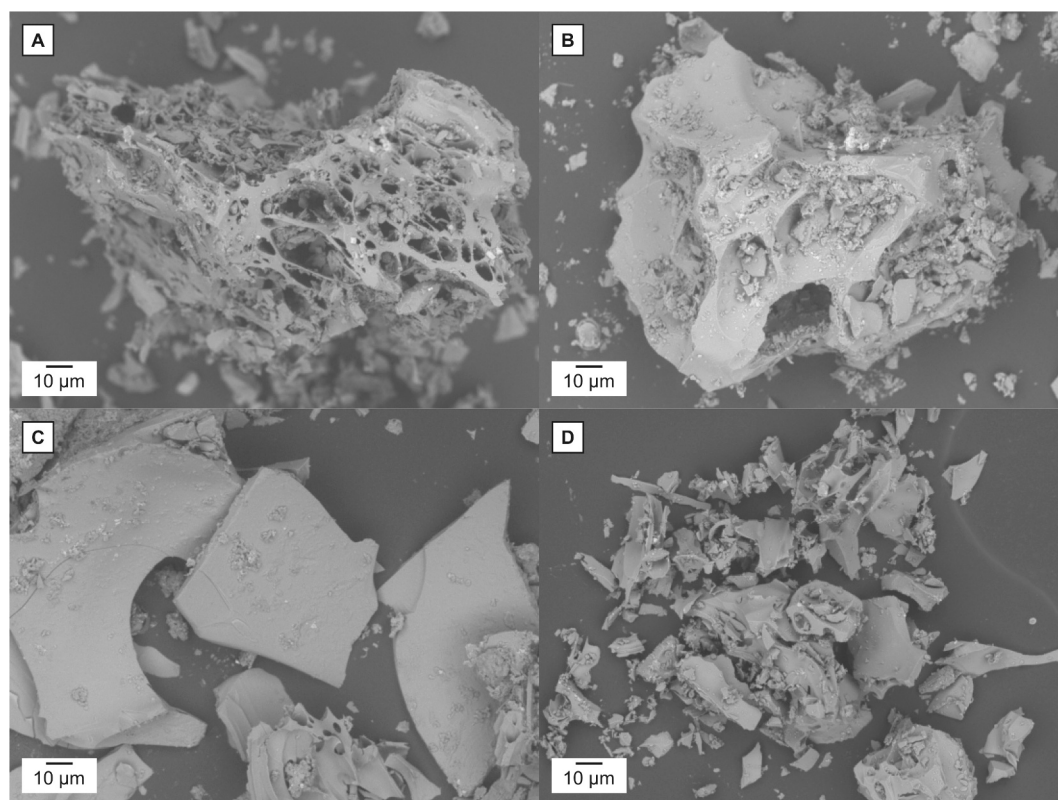


Fig. 5. Examples of (A) porous and (B) elongated, dense pumice, (C) mafic ash, and (D) cusped-dominated ash from the Hikurangi margin, New Zealand obtained from Scanning Electron Microscopy (SEM).

Volpi et al., 2003). Diatomaceous sediments have higher water content, porosity, permeability and compressibility; however, they also exhibit higher shear strength which may make them more resistant to static and cyclic loading compared to sediments that lack diatoms (Shiwakoti et al., 2002; Tanaka et al., 2003; Díaz-Rodríguez, 2011; Wiemer and Kopf, 2017a). It has to be noted though that geotechnical studies on diatoms have been performed mainly on disc-shaped (centric) diatom frustules (cells), and that the shear strength of diatomaceous sediments is strongly dependent on the shape of the diatom frustules (Fig. 6). High shear strength is attributed to disc-shaped (pennate) frustules, while tube-shapes exhibit higher compressibility and therefore, have a lower comparative shear strength (Rack et al., 1993).

Another important aspect of diatomaceous sediments is that their presence is also crucial as a source of pore fluid. Similar to ash particles, the crushing of diatoms and subsequent loss of sediment fabric can cause an increase in pore pressure and a significant loss of strength (Urlaub et al., 2015). The prerequisite for this mechanism to apply is the occurrence of a sealing layer, i.e. clay that prevents the pore fluid to dissipate (e.g. Urlaub et al., 2018, 2020). The most likely scenario for slope failure along a diatom-clay weak layer is probably particle breakage due to additional loading or liquefaction (e.g. seismic shaking) which causes both excess pore pressure generation and strain softening (Rodríguez-Ochoa et al., 2015).

Similar to diatomaceous sediments, foraminifera and nannofossils are also capable of storing large quantities of intraparticle fluid. When subject to moderate compressive stresses, foraminifera are susceptible to breakage and release intraparticle water, whereas nannofossils exhibit only minor fracturing (Demars, 1982). Beemer et al. (2019) showed that crushing strongly depends on the bio-morphology of the particles, with smaller void space and thicker walls in benthic examples exhibiting strength 15 times stronger than tested planktic examples. In addition, progressive dissolution of calcareous microfossils causes a decrease in the mean grain size, primarily by fragmentation of sand-sized foraminifera and corrosion, and further fragmentation of smaller carbonate particles, which results in a decrease in shear strength (Johnson et al., 1977). In contrast, Sawyer and Hodelka (2016) highlighted that a foraminifera-rich sediment layer likely contributed to the rapid arrested of a landslide in the Ursa Basin, northern Gulf of Mexico. This observation shows that intact foraminifera may actually have a slope strengthening effect.

### 3.2. Environments and global distribution

As sediment type can vary according to depositional environment (e.g. Dutkiewicz et al., 2015), it stands to reason that the different types of weak layer (which are linked to sediment lithology) may show an affinity to different geographic and physiographic regions. For example, weak layers attributed to contourites will be more common in higher

latitudes, or at oceanic gateways, where thermohaline circulation is pronounced (Rebesco et al., 2014). Weak layers related to sand layers will be more probable where episodic high energy sediment transport occurs, such as offshore from bedload-dominated river deltas or in areas affected by recurrent turbidity currents (e.g. Hart et al., 1992; Piper and Normark, 2009; Hizzett et al., 2018; Bailey et al., 2021). We now discuss some of the spatial controls on sediment lithology with a view to provide some general guidance on the environments and regions in which different weak layers may be anticipated; and hence where landslides that are linked to weak layers may be more likely. This section is not intended to be a fully comprehensive atlas of global ocean sediment variability, but instead to provide an overview of some of the key processes that may control the presence of weak layers and their anticipated spatial extents. A series of process-based models is presented that can be incorporated into future hazard assessments and that can, and should be, ground-truthed by future surveys and sampling campaigns.

#### 3.2.1. Siliciclastic weak layers

The collected data show that weak layers are predominantly related to siliciclastic sediment sequences and are found in various environmental settings worldwide (Fig. 7E, F). Despite sharing a common primary lithology, physical and geotechnical properties of these weak layers can vary greatly depending on the environmental setting (and therefore, the prevailing sedimentation regime). In addition, depending on the geographic and physiographic regimes, different prevailing failure mechanisms may influence the formation of weak layers. The following section outlines some of the many settings in which siliciclastic weak layers have been recognised.

**3.2.1.1. Glacial environments.** Submarine landslides are documented on many glaciated, or formerly glaciated, continental margins around the globe (e.g. Piper and McCall, 2003; Lee, 2009; Leynaud et al., 2009; Pope et al., 2018). These areas are often characterised by episodic high sedimentation rates and alternating deposition of various sediment types with diverse physical and geotechnical properties (e.g. Leynaud et al., 2009; Mosher, 2009; Baeten et al., 2014; Normandeau et al., 2019a; Schulten et al., 2019b). In the Storegga Slide area offshore Norway, for example, rapid burial of marine contouritic clays by thick deposits of glacial clay-rich sediments have been linked to the accumulation of excess pore pressure and shear strength degradation under seismic loading (Bryn et al., 2003, 2005a; Kvalstad et al., 2005). Similarly, alternating sequences of glacial sediments, meltwater plume deposits and contourites have been identified as potential weak layers for both, the Lofoten Slides offshore Norway and failures on the Storfjorden Trough-Mouth Fan, offshore Svalbard (e.g. Hjelstuen et al., 2007; Lucchi et al., 2012; Baeten et al., 2014). In addition, debris flow deposits and turbidites interbedded in glaciomarine deposits may also form permeability and strength contrasts, often over extensive areas (e.g. Piper and

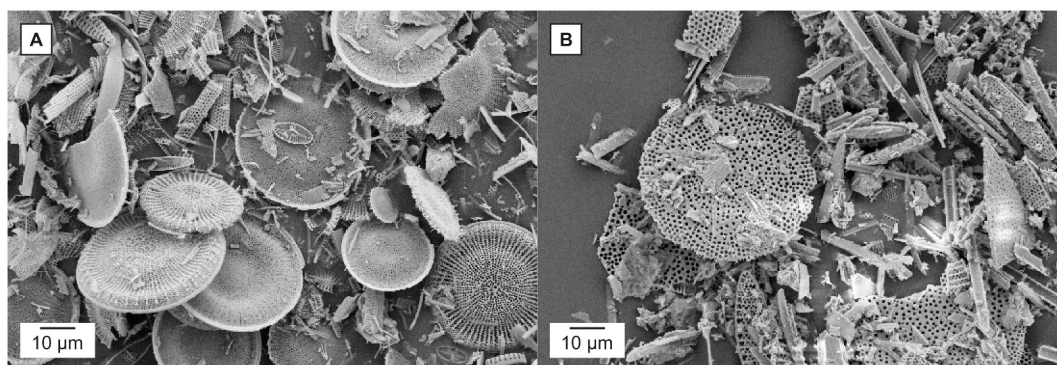
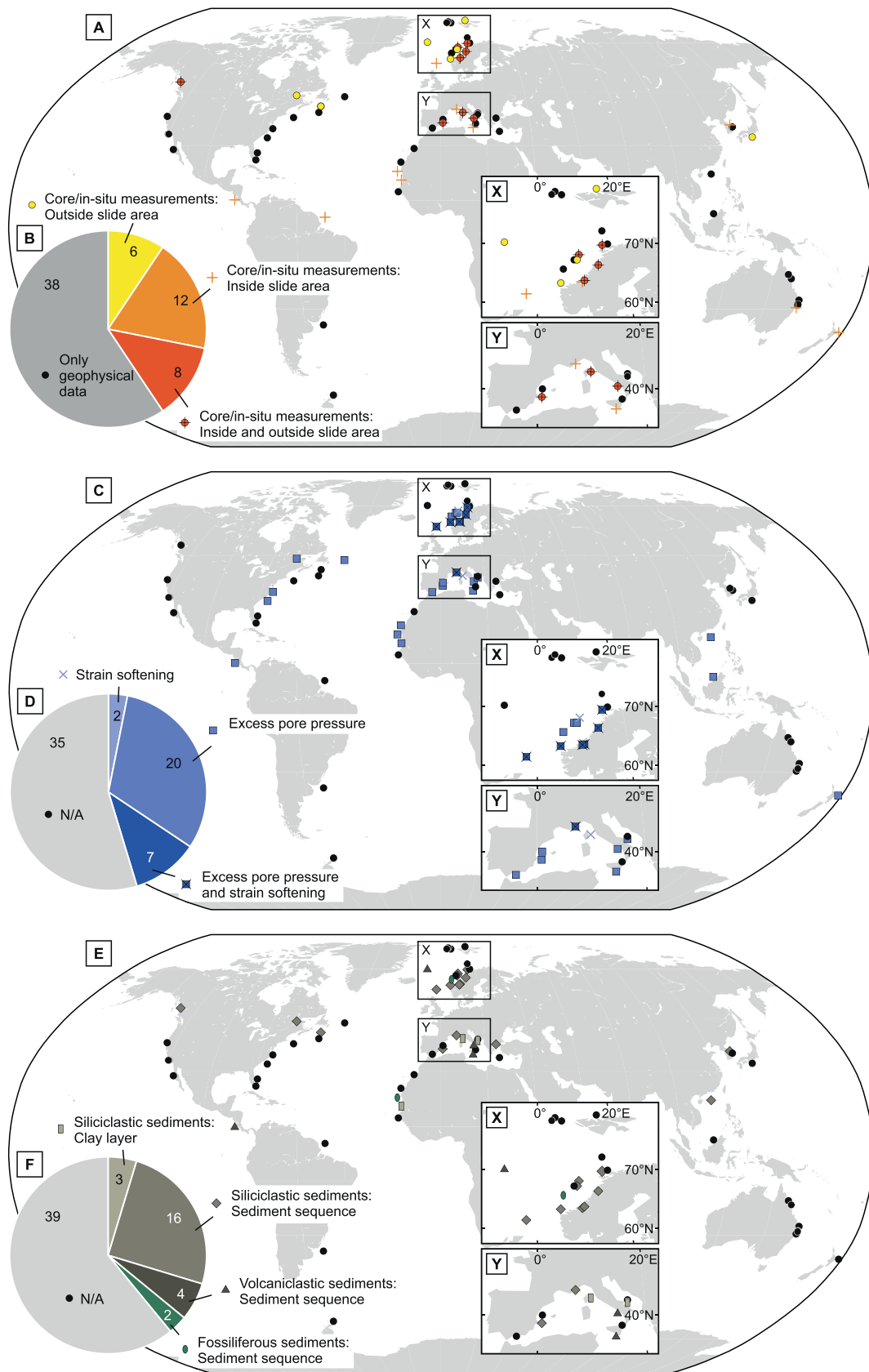


Fig. 6. Examples of (A) mainly centric diatoms from the Lower Saxony, Germany and (B) mainly pennate diatoms from the South Sandwich Trench, South Atlantic Ocean, obtained from Scanning Electron Microscopy (SEM; modified from Dziadek, 2014).



(caption on next page)

**Fig. 7.** Overview maps of the case studies used in this review (A, C, E). Subsets represent zoom-ins to case studies in the NE Atlantic (X) and the western Mediterranean (Y). Each point represents one submarine landslide or submarine landslide complex (exceptions are the Eastern Sea I and II, Lofoten and Vesterålen Slides for which several smaller, related slides are represented by only one point). Different symbols illustrate the data available for each landslide: A. orange cross – sediment cores/in-situ measurements sampling relevant sediments inside slide area, yellow circle – sediment cores/in-situ measurements sampling relevant sediments outside slide area, dark orange circle with cross – sediment cores/in-situ measurements sampling relevant sediments inside and outside slide area, and black circle – no sediment cores/in-situ measurements sampling relevant sediment are available. C. Symbols illustrate the inferred main failure mode of individual slides: blue cross – failure due to strain softening, blue square – failure due to excess pore pressure generation, blue square with cross – failure due to excess pore pressure generation and strain softening, and black circle – no information available. E. Weak layer types, classified based on their lithology: light brown rectangle – clay layers, brown diamonds – siliciclastic sediment sequence, dark green triangle – volcanoclastic sediment sequence, green ellipse – fossiliferous sediment sequence, and black circle – no information available. Pie charts counting case studies (B) with different datasets, (D) for each failure mode, and (F) for each type of weak layer. (For interpretation of the references to colour in this figure legend, the reader is referred to the web version of this article.)

McCall, 2003; Mosher et al., 2004; Schulten, 2019; Bellwald et al., 2020). Therefore, even landslide deposits themselves may induce the formation of weak layers. Mosher et al. (1994) showed that MTDs form a significant part of the Scotian Slope sedimentary column, offshore Canada, which results in strong variations in sediment physical properties, and failure even on very low slope angles.

These examples reveal a commonality that appears to effectively precondition glacial slopes to failure: Rapid changes in sedimentation rate and type (e.g. coarse- and fine-grained turbidites, plumites, and

glaciomarine sediments) resulting in the sequencing of sediment layers of varying physical and geotechnical properties. As glacial environments are prone to seismic shaking, gas hydrate dissolution and slope oversteepening (e.g. Mosher et al., 2004; Leynaud et al., 2009), these areas become particularly prone to submarine slope failure. In particular, these conditions may be expected along formerly glaciated continental margins (e.g. Gowan et al., 2021).

**3.2.1.2. Contouritic environments.** Although contourites are prominent

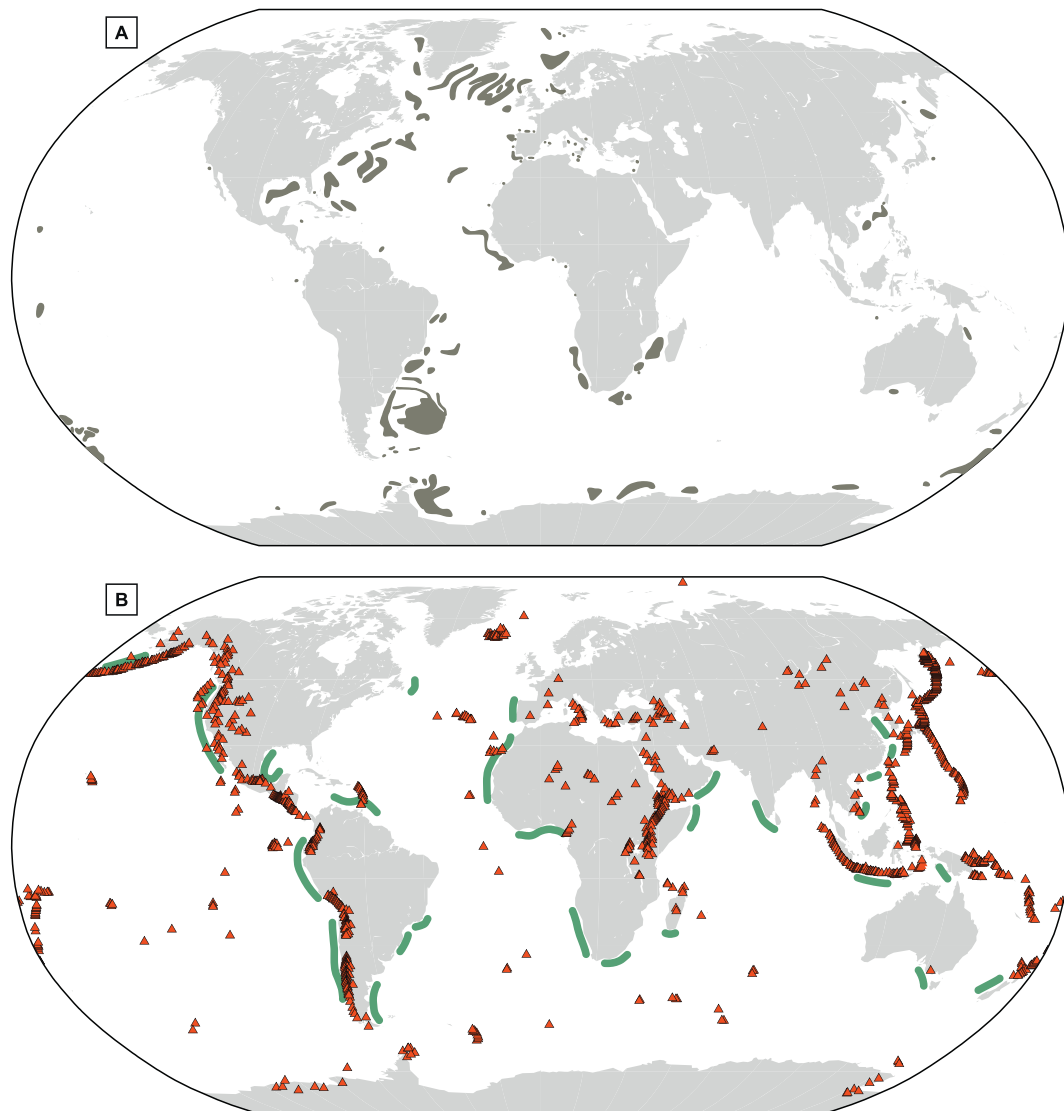


**Fig. 8.** World distribution of (A) contourite depositional systems (modified from Rebesco et al., 2014; Thran et al., 2018) and (B) volcanoes (red triangles; Global Volcanism Program, 2013) and upwelling regions (green; modified from Kämpf and Chapman, 2016). (For interpretation of the references to colour in this figure legend, the reader is referred to the web version of this article.)

features in glacial environments (e.g. offshore Norway or eastern Canada) they are not limited to these regions, and occur in multiple locations worldwide (Fig. 8A). Contourites are sediment deposits that form due to the interaction of bottom currents with the seafloor. As such, the sedimentology of contourites strongly depends on the type of the transported material (i.e. the source region), variations in current speed and seafloor morphology (e.g. Faugères et al., 1993). High-latitude contourites typically feature sediment properties that distinctively differ from glaciogenic sediments (e.g. Storegga Slide, Berg et al., 2005; Bryn et al., 2005b). In shallow waters, rapid variations in physical and geotechnical properties were also found within contourites (Rashid et al., 2017). Such distinct lithological contrasts, however, appear to generally be absent in middle- to low-latitude contourites (Miramontes et al., 2018). However, exceptions may occur, particularly at constricted oceanic gateways, where periodically high velocity bottom currents may be capable of transporting sand-sized sediment (e.g. Brackenridge et al., 2018; Fønnesu et al., 2020).

It therefore stands to reason that large, repeated slope failures in high-latitude contourites (e.g. AFEN Slide offshore UK, Wilson et al., 2003; Storegga Slide offshore Norway, Hafliðason et al., 2004; Bryn et al., 2005a; e.g. St. Pierre Slump (Grand Banks Slide) and slope failure along Sackville Spur offshore eastern Canada, Schulten et al., 2019b; Mosher et al., 2021) are preconditioned by lithological contrasts, i.e. weak layers, whereas the dominant preconditioning factor for slope failure in middle- to low-latitude contourites generally appears to be related to the resultant slope geometry (e.g. Pianosa Slump offshore Corsica Trough, Miramontes et al., 2018).

**3.2.1.3. Fjords.** The compiled data show that sand layers have another important function in the formation of submarine landslides. That is, they act as aquifers in near coastal environments (e.g. fjords – Brattøra, Finneidfjord and Orkdalsfjorden Slides, L'Heureux et al., 2011, L'Heureux et al., 2012, L'Heureux et al., 2014; or continental slope – Nice Airport Slide, Dan et al., 2007), and even on continental slopes (Mosher, 2009; Gustafson et al., 2019). Alternating layers of low- and high-permeability sediments can affect the groundwater flow and cause excess pore pressure generation, thereby promoting failure. Failure is typically associated with artesian groundwater pressure along the sand-clay interface and strain softening of the often inherently weaker, sensitive clays (e.g. L'Heureux et al., 2011; L'Heureux et al., 2012, 2014). Such sensitive clays (often related to onshore quick clay slide activity) are common in uplifted fjord valleys of Scandinavia, Canada and to a lesser extent in Alaska (e.g. Torrance, 1983). These sediments, with similar origin as those found in this study (e.g. Finneidfjord, L'Heureux et al., 2012; Steiner et al., 2012) could play a crucial role in the formation of submarine landslides in near-coastal areas. Although the landslide volumes in fjords are limited by the morphology of these environmental settings (e.g. Syvitski et al., 1987; Prandle, 2009), they can have major social-economic impact due to their near-coastal location.

**3.2.1.4. River deltas and fans.** River deltas and fans are characterised by spatial and temporal variations in sediment supply (e.g. Morehead et al., 2003; Ducassou et al., 2009). In general, sediment supply is controlled by the relative strength of hydraulic parameters such as river discharge, wave energy flux and tidal range (Orton and Reading, 1993).

The reasons for temporal variations in sediment discharge can be manifold, including varying water sources throughout the seasons (i.e. rain/monsoon versus snow melt), availability of easily mobilised channel sediments, alternating channel morphology (e.g. due to climate change), and variations in sediment supply from erosion (e.g. Morehead et al., 2003). Large amounts of sediment are delivered episodically to relatively localised areas on the continental margins, resulting in the accumulation of thick sediment deposits over relatively short periods of time. The alternation between coarse-grained sediments originating

from multiple stages of turbidite deposition and predominately fine-grained hemipelagic sediment deposition in quiescent periods may favour the formation of permeability contrasts within the stratigraphy of river deltas and fans. The rapid accumulation of under-consolidated sediments and alternating sediment sequences can lead to repeated, and often volumetrically large-scale slope failures (e.g. Mississippi River delta, Prior et al., 1979; Coleman, 1988).

A global study of 11,000 deltas shows that while river- and tide-dominated deltas only account for 21% of those worldwide, these two delta types are collectively responsible for 89% of the present day sediment flux to the ocean from rivers (Nienhuis et al., 2020). It is offshore from these system types that we anticipate to find areas of preferential deposition and weak layer formation. The statistically more common wave-dominated deltas are considered less likely candidate sites due to the limited fluxes of sediment (only 11% of the total riverine input) and reworking and mixing of sediment due to wave action. However, local exceptions are possible, e.g. in wave-dominated deltas that experience rare but sudden outbursts of sediment. One such example is the Gaoping River, Southern Taiwan, where normal river discharge can be dramatically exceeded due to heavy rainfall during the passage of tropical cyclones (sometimes reaching >20,000 m<sup>3</sup>/s; Carter et al., 2012). Sediment failures and resultant turbidity currents have been reported to occur days to weeks after the passage of tropical cyclones, rather than being coincident with them. This delay has been linked to the generation of excess pore pressures by rapid sediment loading and their inhibited dissipation due to permeability barriers in the sediment pile (Pope et al., 2017b).

**3.2.1.5. Canyon systems and deep-sea fans.** Similar to river deltas and fans, deep-sea fans are characterised by distinct variations in lithology that derive from variability in sediment supply and depositional processes. The Amazon Fan, for example, largely consists of coarse-grained MTDs and turbidites intercalated in thick muddy levee deposits (e.g. Piper et al., 1997; Maslin, 2009). In the Pearl River canyon, slope sediments vary between organic-rich fine-grained sediments that are interbedded with coarse-grained turbidites and fine-grained contourites and hemipelagic deposits (e.g. Wang et al., 2017; Sun et al., 2018). Numerous coarse- and fine-grained MTDs have been identified within the mud-rich levee deposits in the Mars-Ursa region, directly downip of the Mississippi River (e.g. Sawyer et al., 2007; Dugan, 2012), and in the Rosetta province, fed by the Nile Delta offshore Egypt, MTDs represent about 40% of the Pleistocene-Holocene sediment sequence (e.g. Garziglia et al., 2008).

In such environments, MTDs often play a crucial role in weak layer formation as they may alter fluid flow within a sediment sequence. Coarse-grained, high-permeability parts of MTDs will promote fluid flow, whereas fine-grained, densified MTD bases will act as buffers to vertical pore fluid migration, ultimately promoting slope failure (e.g. Dugan, 2012; Elger et al., 2018; Moernaut et al., 2020; Sun and Alves, 2020; Wu et al., 2021).

### 3.2.2. Volcaniclastic weak layers

The main mechanisms proposed to cause failure along volcaniclastic weak layers are particle rearrangement and breakage, and transient pore pressure generation (e.g. Harders et al., 2010). Pore pressure, however, will only accumulate if a sealing layer (i.e. low-permeability layer) prohibits pore pressure dissipation. Therefore, volcaniclastic weak layers have only been identified in the form of sediment sequences (e.g. Hermosa Slide, Harders et al., 2010; Licosa Slide, Sammartini et al., 2019).

The recognition of volcaniclastic sediments as weak layers, has potentially broad implications on submarine landslide hazard since many regions around the world contain abundant volcaniclastic material that may fail under certain conditions (e.g. Miramontes et al., 2018; Fig. 8B). Volcanic ash, in particular, can be transported over large areas,

tens to hundreds of kilometres from their source (e.g. Riley et al., 2003), enabling the formation of laterally extensive weak layers. Such weak layers may promote large-scale or repeated slope failures in proximal or distal areas of the volcanic source. Notice that although not included in this review, landslides on volcanic island slopes are common (e.g. Moore et al., 1989; Le Friant et al., 2019), and have to be carefully investigated due to their tsunamigenic potential (e.g. Silver et al., 2009; Watt et al., 2012; Le Friant et al., 2019; Barrett et al., 2020). In most cases, however, slope failures on volcanic islands include subaerial parts with their headwalls extending onshore (e.g. Hunt et al., 2011; Watt et al., 2012; León et al., 2020), which did not meet our criteria to be included in the presented landslide catalogue.

### 3.2.3. Fossiliferous weak layers

Similar to volcanoclastic sediments, particle rearrangement and breakage, and transient pore pressure generation are the main failure mechanisms related to fossiliferous weak layers (e.g. Urlaub et al., 2015). Urlaub et al. (2018) highlighted that diatom ooze layers overlain by clay likely acted as weak layers for the Cap Blanc Slide, offshore NW Africa, while diatom ooze layers overlain by coarser sediments did not show such a correlation. This shows that although high shear strength of diatom ooze would suggest a strengthening effect, their high compressibility may lead to a drastic volume reduction and transient pore pressure generation during burial.

Such fossiliferous weak layers may precondition large submarine landslides. For example, episodic upwelling results in the widespread deposition of diatomaceous ooze offshore NW Africa, forming laterally extensive weak layers on slopes that usually experience low sediment accumulations, promoting slope failure over large areal extents (e.g. Cap Blanc Slide; Urlaub et al., 2018). Diatom ooze-related weak layers may, therefore, be found in other upwelling regions, which occur in several other regions around the world (Fig. 8B).

Fossiliferous weak layers have also been identified in carbonate sediments, i.e. foraminifera and nannofossils. Foraminifera in particular are susceptible to breakage and release of intraparticle water when subject to moderate compressive stresses (Demars, 1982). The distribution of calcareous ooze is strongly depth-controlled. Large accumulations of well-preserved assemblages are found in shallow water depth above the lysocline, where sediment supply exceeds carbonate dissolution. Below the lysocline, the rate of carbonate dissolution drastically increases with water depth, until it equals carbonate supply at the calcite compensation depth, CCD (Berger, 1971; Berger and Johnson, 1976; Johnson et al., 1977). About one half of the global pelagic deep-sea floor is blanketed by calcareous ooze, dominated mainly by foraminifera and coccolithophores (e.g. Johnson et al., 1977; Dutkiewicz et al., 2015). On average, about 25% of initially produced planktic foraminifera settle on the seafloor (Beemer et al., 2019), accounting for about 32–80% of the total deep-marine calcite budget (Schiebel, 2002).

Large-scale failures of carbonate sediments were recognised on the northern and eastern flanks of the Ontong Java Plateau, on slopes less than 1° (Berger and Johnson, 1976; Mosher et al., 1993). Although the exact failure mechanism is unclear, it appears that carbonate dissolution played a crucial role (Berger and Johnson, 1976). Repeated slope failure has also been observed offshore carbonate platforms (e.g. Zampetti et al., 2004; ten Brink et al., 2006; Jo et al., 2015; Principaud et al., 2015; Tournadour et al., 2015; Etienne et al., 2021), which are found in many locations worldwide (e.g. Laugié et al., 2019). Failure planes of several landslides along the Great Bahama Bank, offshore Bahamas were linked to a distinct lithological interface between Early Pliocene nannofossil ooze/chalk and overlying Late Messinian bioclastic wackestones to packstones. Although the ultimate failure mechanism remains unclear, trapped aquifer horizons, diagenetic processes in the foraminiferal oozes, and textural and density contrasts between the mud-prone nannofossil chalk and the overlying dolomitic and low-Mg calcite may have contributed to a decrease in shear strength (Principaud et al., 2015). Study of slope failures in carbonate-dominated settings remains less

extensive than in siliciclastic regions. This bias has previously been recognised and it is clear that future studies are required to understand the complex depositional and early diagenetic conditions of such materials (e.g. ten Brink et al., 2006; Clare et al., 2019; Wu et al., 2021).

## 4. Limitations

### 4.1. Limitations of landslide catalogue

The data presented in this paper are compiled from 186 references and include information from 64 case studies, which were summarised in a new global landslide catalogue (Table 1). Although the selected case studies cover various environments worldwide, the catalogue is in parts highly incomplete. One limitation of the catalogue is the uneven coverage of seafloor settings. Submarine landslide investigations generally focus on larger events, those in areas of hydrocarbon exploration and development, and/or those in areas where landslides may threaten human life. In addition, failure planes and weak layers of submarine landslides are usually not the primary target of these investigation, and reliable data (i.e. sediment cores from the adjacent undisturbed sediment sequence) are therefore rare. Even if sediment cores are available, the inconsistency in analytical methods in weak layer research makes a comparison between individual case studies very difficult (Figs. 3 and 4).

Another limitation relates to information obtained from sediment cores that were recovered from inside the mobilised area of submarine landslides. During downslope movement material is often entrained at the base of the slide, as a result of basal erosion and thus remove some or all of the original weak layer (e.g. Gee et al., 2005; Badhani et al., 2020). Weak layer sediments may, therefore, be missing in sediment cores that are recovered from inside the slide area. The most reliable method to identify weak layers is the combination of sediment cores taken from inside and outside the slide area, provided the stratigraphy sampled outside the slide is equivalent to that which failed. As shown in the case of the Finneidfjord Slide, the comparison between such cores enables a very accurate delineation of the weak layer and allows to estimate potential erosion due to sliding (e.g. L'Heureux et al., 2012). Although this review focused on case studies with cores from inside the slide area, the results have shown that additional information, e.g. from sediment cores that recovered the undisturbed sediment sequence or numerical modelling, is needed to reliably identify the weak layer and the failure mechanism.

In recent years, there has been a great effort in investigating submarine landslide hazard potential and building landslide catalogues; however, these catalogues have largely concentrated on landslide morphology rather than geotechnical properties (e.g. Mediterranean Sea, Urgeles and Camerlenghi, 2013; Katz et al., 2015; León et al., 2020; North Atlantic, Hühnerbach et al., 2004; offshore Canada, Lintern et al., 2020; offshore Central America, Harders et al., 2011; offshore New Zealand, Watson et al., 2020; Nankai Trough, Lackey et al., 2020); and the geotechnical studies that exist tend to provide a bulk characterisation of sediment sequences, rather than the detailed, depth-resolved studies that are needed for weak layer research (e.g. Sawyer and DeVore, 2015). The landslide catalogue, even though too limited to be statistically robust and infer universal rules for weak layers, provides a useful step towards understanding the global controls on, and the role of, weak layers in submarine landslide formation. The catalogue has enabled us to recognise a relationship between weak layer lithology, environmental setting and ultimately failure mechanism. Building on this information will hopefully motivate future studies and efforts to target weak layers in future research.

### 4.2. Current limitations and challenges in weak layer research

The reliable investigation and characterisation of weak layers in a submarine landslide setting depends on their accurate identification,

their recovery during sediment coring and careful sampling, as well as the choice of analytical methods. In addition to inherent uncertainties of applied methods and acquired data, this task faces a multitude of challenges related to issues such as data coverage, spatial resolution, data correlation, and sampling bias, as well as sampling quality and quantity. In the following sub-sections, the main challenges and limitations encountered when attempting to identify failure planes and characterise weak layers are outlined, and some of the main reasons for these limitations are discussed.

#### 4.2.1. Identification of weak layers: The importance of spatial resolution and data migration

*Where is the failure plane located?* The answer to this seemingly simple question is a requisite for successful sampling and analysis of weak layers – and involves many challenges. The accuracy in the positional delineation of failure planes strongly depends on the resolution, precision and integration of datasets of different scales, namely acoustic imaging and geophysical borehole or core logging data.

A major challenge in this context is one of resolution: Weak layers often act on decimetre- to sub-decimetre-scales (e.g. L'Heureux et al., 2012; Sammartini et al., 2019; Gatter et al., 2020), but can be buried beneath tens to more than hundreds of metres of sediment and water. In order to identify and trace the spatial extent of failure planes and weak layers, we rely heavily on acoustic methods that require a compromise between penetration depth and vertical resolution. Both are inversely correlated and strongly depend on the deployed tools, as well as the type of sediment imaged (see Supplementary data A.2 for a summary of commonly deployed surveying tools). High-resolution sub-bottom profilers (e.g. Chirp-type systems), for example, may reach a vertical resolution of <0.05 m, but have a very limited penetration depth (<tens of metres), especially in thicker, sandy or over-consolidated sediments (e.g. Penrose et al., 2005). Such very-high-resolution datasets are therefore generally not suitable for investigating the failure planes and weak layers of large submarine landslides, as they fail to image the deeper sediment strata. Seismic reflection profiles, on the other hand, routinely reach penetration depths of hundreds of metres, but have a much lower vertical resolution (e.g. Judd and Hovland, 1992). Most of these datasets work on a metre-scale, a magnitude below that of weak layers, and thus may fail to accurately image thin weak layers, causing errors in their depth estimates or may entirely fail to image them (e.g. Widess, 1982). In addition, the presence of gaseous sediments may mask the reflection from underlying layers as they scatter acoustic energy, effectively limiting the penetration depth (e.g. Judd and Hovland, 1992; Fleischer et al., 2001). This may result in a significant vertical error in failure plane delineation when using acoustic imaging alone.

A further challenge is that of depth conversion: Since acoustic imaging is a function of the travel-time of the emitted signal, this time-based measurement needs to be converted to depth. Robust velocity models are needed for an accurate time-depth conversion that require additional information on the velocity of acoustic signals within both the water and sedimentary strata. This information is usually obtained from physical property measurements of recovered core material. Such measurements, however, may introduce several uncertainties, for example due to poor core recovery, sediment compression and expansion, or poor quality core logging (e.g. Weaver and Schultheiss, 1990; Jutzeler et al., 2014). Ideally, information derived from near-continuous in-situ borehole logging is used to overcome these uncertainties (e.g. Riedel et al., 2020). In-situ logs of chemical and physical properties may be used to extrapolate lithological information in sections of poor core recovery (e.g. Brewer et al., 1998; Major et al., 1998), and could be integrated relatively easily into IODP or seafloor drill rig (e.g. MeBo; Freudenthal and Wefer, 2007, 2013) campaigns by deploying logging tools after core recovery into the newly-drilled boreholes. Finally, to ensure positional accuracy in borehole logging and coring, a positional navigation tool should be placed on the wire above the coring device, and tiltmeters can be deployed to ensure vertical coring and to enable

subsequent corrections in positional accuracy.

#### 4.2.2. Sampling of weak layers: Accessibility and recovery challenges

Many studies rely solely upon remote geophysical data for submarine landslide investigation (Figs. 3 and 7) and, even if sediment cores are acquired, they typically do not sample relevant sediment horizons, which may lie tens to hundreds of metres below the seafloor (e.g. Talling et al., 2014; Fig. 3). Such cores also tend to focus on the characterisation of the landslide deposits or excavated glide planes within the slide area, rather than targeting sediments from adjacent undisturbed slopes. Targeting the undisturbed sediments of the adjacent slopes, including those stratigraphically-equivalent to the failure plane, however, is necessary in order to identify and characterise the material along which the landslide initiated.

**4.2.2.1. Sediment cores.** A wide range of sediment coring devices exist (Table A.2.1), each with advantages and disadvantages (e.g. Georgiopoulou, 2018). Although long cores are usually desirable, not all research vessels can support long and heavy coring devices whose operation is costly, both financially and time-wise. Sample material from such cores is often scarce for any given stratigraphic horizon within a sampled profile. Due to costly operations, the number of cores is limited (often not exceeding one) for each coring site and core diameters are relatively small (5.7–6.3 cm, e.g. Freudenthal and Wefer, 2007). These problems can be overcome with shorter gravity or piston cores. Such cores have the main advantage of being relatively cost-effective, and are relatively easy to handle, allowing for multiple deployments at the same site. They may also allow the recovery of large diameter ( $\geq 10$  cm) sediment cores, which are favourable for further geotechnical laboratory analyses. These cores, however, have very limited penetration depths (e.g. Georgiopoulou, 2018) and relevant deeper sediment horizons are seldom sampled. Furthermore, in the case of gas-bearing sediments, other coring devices, such as a pressure corer, are required in order to prevent substantial sediment disruption due to gas expansion upon core recovery (e.g. Paull and Ussler III, 2001; Holland et al., 2019). It is therefore critical to choose the appropriate coring technique(s) for individual study sites based on site-specific conditions (e.g. Weaver and Schultheiss, 1990; Georgiopoulou, 2018).

Another challenge is that of sediment recovery (e.g. Jutzeler et al., 2014). Thick, under-consolidated sandy layers are especially difficult to sample, because the loose material is easily washed out of the core barrels during recovery (e.g. Tuaheni Slide offshore New Zealand; Huhn, 2016; Pecher et al., 2018). In contrast, even very thin ash layers may be extremely hard to penetrate with conventional coring techniques because their particles interlock if pushed together during coring, thereby increasing the layer's strength exceedingly (e.g. offshore Montserrat; Huhn et al., 2019).

**4.2.2.2. In-situ measurements.** Although our capacity to obtain in-situ measurements has greatly improved over the last couple of decades, the devices are still seldom deployed for weak layer investigation (Fig. 3, Table 1). Similar to coring devices, in-situ measurement tools have to compromise between penetration depth and cost-effectiveness (Table A.2.1). Cone penetration testing with pore pressure measurement (CPTu) is the primary geotechnical tool to acquire continuous in-situ geotechnical data (Lunne et al., 1997). Dynamic CPTu (e.g. MARUM Free-Fall Cone Penetrometer with Pore pressure; Stegmann et al., 2006) is relatively cost-effective and can be easily deployed, but usually has a limited penetration depth. Higher penetration depths can be achieved with static CPTu (e.g. IFREMER Penfeld seabed rig or MARUM Geotechnical Offshore Seabed Tool (GOST); Meunier et al., 2004; Sultan et al., 2010; Jorat et al., 2014; Steiner et al., 2014). Static CPTu systems differ from dynamic CPTu instruments, in that they are pushed at constant penetration rates into the sediment (e.g. Steiner et al., 2014), which allows them to achieve greater penetration depths and also

penetrate resistant sediments, such as ash layers. These systems, however, require larger research vessels for deployment, and depending on the sediments encountered may be very time-consuming.

Sediment cores and in-situ measurements that sample relevant sediments, in particular the undisturbed sediment sequence outside the slide area, are rare (Fig. 3, Table 1). Despite continuously emerging tools in marine technology, sampling techniques and in-situ monitoring still generally lag behind the technological advances in geophysical data acquisition (e.g. Clare et al., 2017). The lack of adequate sampling devices constrains our efforts to effectively sample weak layers of submarine landslides. Direct measurement of parameters such as in-situ pore pressure, are time consuming, and are not always feasible due to weather constraints on offshore operations and the expense of ship time. Monitoring of pore pressure variations is also possible, but has been performed in only a limited manner due to logistical complications (Strout and Tjelta, 2005; Flemings et al., 2008; Dugan and Sheahan, 2012). Such monitoring typically requires connection to power and data transfer (e.g. via a seafloor cabled observatory network) which limits the sites that can be studied in detail.

The successful sampling (and investigation) of weak layers requires new technologies, e.g. further development of seafloor drill rigs. Seafloor drill rigs are lowered onto the seafloor from multi-purpose research vessels and retrieve sediment cores by remote control from the ship. They have the potential to bridge the gap between relatively cost-effective, but short, conventional coring devices, such as gravity, piston, or vibra-corer that can sample dense or weakly cemented strata, and the use of expensive drill ships (Freudenthal and Wefer, 2013). They have the advantage that once they are deployed on the seafloor, they can collect a number of sediment cores in a relatively time-effective way, and also enable further borehole logging and in-situ testing (e.g. Spagnoli et al., 2015; Huhn et al., 2019).

Due to difficulties in sampling the failure planes of large submarine landslides that may be buried hundreds of metres below the seafloor (e.g. Hafidason et al., 2004; Georgiopolou et al., 2010), targeting smaller landslides may prove to be more successful. The investigation of smaller submarine landslides has shown good results (e.g. Strozzyk et al., 2010a; Berndt et al., 2012; Lafuerza et al., 2012; Baeten et al., 2014; Gatter et al., 2020), as they allow for the deployment of more cost-effective coring devices, which can be used to obtain a number of cores from the slide area and the undisturbed sedimentary sequence. An alternative is to focus our efforts on landslides in lakes, which are also smaller in size and more readily accessible (e.g. Stegmann and Kopf, 2007; Van Daele et al., 2017; Moernaut et al., 2020; Stegmann and Kopf, 2007). Several previous studies suggest that morphometry and other characteristics may be similar between cohesive landslides across many orders of magnitude (e.g. Micallef et al., 2008; Moernaut and De Batist, 2011; Urgeles and Camerlenghi, 2013; Casas et al., 2016; Clare et al., 2017), allowing the extrapolation of information from small to larger landslides. Hence, it may be sensible to focus on smaller-scale landslides until deeper sampling is viable.

#### 4.2.3. Characterisation of weak layers: A problem of sample quality and quantity

To understand weak layers, it is not enough to know where within the slope's stratigraphy they are located, we also need to characterise them in terms of their sedimentological and geochemical composition, as well as their physical and geotechnical properties. This requires the sampling of weak layers in their undisturbed form, i.e. from the undisturbed adjacent slope.

Visual, descriptive sedimentological and non-destructive MSCL logging data are usually available for sediment cores, but further geotechnical characterisation is often scarce (Fig. 4). Advanced geotechnical tests usually require a large amount of undisturbed sediment. Apart from the limited availability of sample material, obtaining high-quality samples is also challenging (i.e. with little deformation due to the recovery and sampling procedures) for such testing (Clayton et al.,

1998). Despite the enormous value of deep ocean drilling programmes such as IODP for geological purposes, the samples collected within these programmes are often highly disturbed and, therefore, cannot be used for high-quality geotechnical tests (Vanneste et al., 2014). Although geotechnical properties, such as shear strength and pore pressure estimates, can also be obtained from in-situ measurements, such instruments are not often deployed (Fig. 3, Table 1) and usually have a limited penetration depth. In addition, CPTu-based investigation of sediments does not allow for a compositional classification of the tested sediments, which requires sediment cores or borehole records (e.g. Yin et al., 2021).

Some weak layers, e.g. volcanoclastic, may require additional geochemical analyses. Such sediments can be difficult to identify visually, but have characteristic geochemical signals in XRF-core logging data (e.g. Cassidy et al., 2014). Fossiliferous sediment on the other hand, may require high-resolution visual analyses (e.g. SEM images).

While geophysical data have become more readily available, there is a general scarcity of sedimentological and geotechnical data. Nevertheless, high-quality laboratory tests (e.g. shear strength or permeability) and in-situ geotechnical data are crucial for recognising and evaluating weak layers. In order to overcome limitations inherent to individual analysis methods, the integration of datasets is imperative. The combination of various methods (e.g. geotechnical characterisation from in-situ measurements and from core samples) enables to reduce uncertainties and to fill gaps (e.g. missing data points) in individual datasets.

## 5. Conclusion and outlook

Based on a new global submarine landslide catalogue that comprises 64 case studies, we reviewed the current state of knowledge of weak layers and their controls on submarine landslide formation. The review revealed that it is not always possible to infer whether weak layers are *inherited* or *induced* (sensu Locat et al., 2014) (Table 1), as this inference relies heavily upon the availability of specific information regarding the physical and geotechnical properties of the sediment. We therefore introduce an additional, complementary classification of weak layers that is based on their lithology (Table 2). Such an approach has the advantage of enabling the recognition of potential weak layer-forming sediments from sediment cores or in-situ measurements taken from the unfailed slopes. The combination of such a lithological-based classification with a failure mechanism-based scheme (e.g. Locat et al., 2014) may further allow relating weak layer lithologies to specific failure mechanisms, and thereby appears key for a robust weak layer investigation. A further benefit of the approach is that it allows the correlation of different types of weak layers (which are linked to sediment lithology) to distinct geographic regions and physiographic settings. These settings include contourite or turbidite systems that can create siliciclastic sediment sequences, areas of high productivity where biogenic sediments may dominate, or regions that experience repeated ash deposition from proximal or distal volcanic sources (Fig. 8). Successful identification of weak layers and further relation to specific failure mechanisms will significantly advance the assessment of submarine landslide hazard potential and will inform future risk assessment strategies.

The data show that the sequencing of specific sediment layers, such as sand-clay, ash-clay or diatom-clay, is key to the formation of weak layers. In total, 22 of the 64 case studies were related to distinct sediment sequences, while three submarine landslides were related to weak clay layers (Fig. 7E, F). In addition, failure along lithological contrasts was inferred for another six case studies. These submarine landslides, however, could not be classified properly, because the published data were insufficient. Failure mechanisms were often deduced from geophysical data alone rather than from direct sampling. In total, excess pore pressure was invoked as the main failure mechanism in 20 of the 64 case studies. Another seven case studies linked slope failure to a

combination of excess pore pressure and strain softening, while failure due to strain softening alone was referenced in two case studies (Fig. 7C, D).

The investigation and characterisation of weak layers and their mechanisms in a submarine landslide setting relies on their accurate identification, their recovery during sediment coring and correlation to geophysical records, and careful sampling and analysis. It further requires the sampling of weak layers in their undisturbed form, i.e. from the undisturbed adjacent slope. Sediment cores and in-situ measurements that sample relevant sediments, in particular the undisturbed sediment sequence outside the slide area, however, are rare (Fig. 7A, B).

Despite the increase in knowledge regarding submarine landslides over the past few decades (Fig. 2), our understanding of their failure planes and weak layers is still limited. Some of the most important aspects that should be considered for future weak layer investigations are outlined below:

- **Targeted research:** There is a clear need for research tailored towards failure plane and weak layer-focused investigations. The identification and characterisation of failure planes and weak layers are usually not the primary aim of current sampling campaigns; hence, the applied methods (e.g. coring techniques) are often not suitable to sample failure planes and failure plane equivalent samples outside the slide area.
- **Pre-site surveys:** A key criterion for successful weak layer investigations is a pre-sampling survey. The data is used to identify and locate the failure plane of submarine landslides and are also essential to identify suitable coring locations. Surveys need to be designed to consider the potential trade-offs between penetration depth and vertical resolution required to image and identify the depth zone that includes the failure plane and/or weak layer.
- **Sample collection:** One of the main limitations in weak layer characterisation is the limited amount of suitable material obtained from sediment cores for further geotechnical analyses. To ensure enough material is available, a number of cores (at least two) should be taken from each coring site, dedicating one entire core to further geotechnical (and potentially also geochemical) analyses.
- **Consistent workflow:** In order to overcome coverage and data limitations in the future, we suggest that there is value in capturing information in peer-reviewed and grey literature sources, as well as that held but not published by offshore industries. A standardised workflow (such as has been developed for characterisation of landslide morphometry; Clare et al., 2019) will allow for a more robust comparison between individual weak layer studies and settings (example provided in Supplementary data A.3). Such a workflow should ideally include detailed visual as well as non-destructive core logging techniques (e.g. MSCL, XRF, and potentially also Computed Tomography (CT) imaging), a sampling plan targeting the weak layer sediments (e.g. combination of standard and advanced geotechnical testing and high-resolution micro-CT imaging), and finally, integrate results into numerical models in order to characterise the weak layer and identify the failure mechanism.

#### Declaration of Competing Interest

The authors declare that they have no known competing financial interests or personal relationships that could have appeared to influence the work reported in this paper.

#### Acknowledgments

S. Kutterolf is gratefully thanked for providing the SEM images of volcanic material from the Integrated Ocean Drilling Program (IODP) Expedition 375. Constructive reviews by M. Urlaub and two anonymous reviewers significantly improved the paper. This work was supported by the European Union's Horizon 2020 research and innovation

programme under the Marie Skłodowska-Curie grant agreement No. 721403.

#### Appendix A. Supplementary data

Supplementary data to this article can be found online at <https://doi.org/10.1016/j.earscirev.2021.103845>.

#### References

- Ai, F., Strasser, M., Preu, B., Hanebuth, T.J.J., Krastel, S., Kopf, A., 2014. New constraints on oceanographic vs. seismic control on submarine landslide initiation: a geotechnical approach off Uruguay and northern Argentina. *Geo-Mar. Lett.* 34, 399–417. <https://doi.org/10.1007/s00367-014-0373-3>.
- Antobreh, A., Krastel, S., 2007. Mauritania slide complex: morphology, seismic characterisation and processes of formation. *Int. J. Earth Sci.* 96, 451–472.
- Badhani, S., Cattaneo, A., Dennielou, B., Leroux, E., Colin, F., Thomas, Y., Jouet, G., Rabineau, M., Droz, L., 2020. Morphology of retrogressive failures in the Eastern Rhone interfluvium during the last glacial maximum (Gulf of Lions, Western Mediterranean). *Geomorphology* 351, 106894. <https://doi.org/10.1016/j.geomorph.2019.106894>.
- Baeten, N.J., Laberg, J.S., Forwick, M., Vorren, T.O., Vanneste, M., Forsberg, C.F., Kvalstad, T.J., Ivanov, M., 2013. Morphology and origin of smaller-scale mass movements on the continental slope off northern Norway. *Geomorphology* 187, 122–134. <https://doi.org/10.1016/j.geomorph.2013.01.008>.
- Baeten, N.J., Laberg, J.S., Vanneste, M., Forsberg, C.F., Kvalstad, T.J., Forwick, M., Vorren, T.O., Hafliadason, H., 2014. Origin of shallow submarine mass movements and their glide planes - Sedimentological and geotechnical analyses from the continental slope off northern Norway. *J. Geophys. Res. Earth Surf.* 119, 2335–2360. <https://doi.org/10.1002/2013JF003068>.
- Bailey, L.P., Clare, M.A., Rosenberger, K.J., Cartigny, M.J., Talling, P.J., Paull, C.K., Gwiazda, R., Parsons, D.R., Simmons, S.M., Xu, J., Haigh, I.D., Maier, K.L., McGann, M., Lundsten, E., Monterey CCE Team, 2021. Preconditioning by sediment accumulation can produce powerful turbidity currents without major external triggers. *Earth Planet. Sci. Lett.* 562, 116845. <https://doi.org/10.1016/j.epsl.2021.116845>.
- Barrett, R., Lebas, E., Ramalho, R., Klauke, I., Kutterolf, S., Klügel, A., Lindhorst, K., Goss, F., Krastel, S., 2020. Revisiting the tsunamigenic volcanic flank collapse of Fogo Island in the Cape Verdes, offshore West Africa. *Geol. Soc. Lond., Spec. Publ.* 500, 13–26. <https://doi.org/10.1144/SP500-2019-187>.
- Beemer, R.D., Sadekov, A., Lebec, U., Shaw, J., Bandini-Maeder, A., Cassidy, M.J., 2019. Impact of Biology on Particle Crushing in Offshore Calcareous Sediments. Eighth International Conference on Case Histories in Geotechnical Engineering, March 24–27, 2019, Philadelphia, Pennsylvania. <https://doi.org/10.1061/9780784482124.065>.
- Bellwald, B., Planke, S., Becker, L.W.M., Myklebust, R., 2020. Meltwater sediment transport as the dominating process in mid-latitude trough mouth fan formation. *Nat. Commun.* 11 (1), 1–10.
- Berg, K., Solheim, A., Bryn, P., 2005. The Pleistocene to recent geological development of the Ormen Lange area. *Mar. Pet. Geol.* 22, 45–56. <https://doi.org/10.1016/j.marpetgeo.2004.10.009>.
- Berger, W.H., 1971. Sedimentation of planktonic foraminifera. *Mar. Geol.* 11 (5), 325–358. [https://doi.org/10.1016/0025-3227\(71\)90035-1](https://doi.org/10.1016/0025-3227(71)90035-1).
- Berger, W.H., Johnson, T.C., 1976. Deep-Sea carbonates: dissolution and mass wasting on ontong-Java Plateau. *Science* 192, 785–787. <https://doi.org/10.1126/science.192.4241.785>.
- Berndt, C., Costa, S., Canals, M., Camerlenghi, A., de Mol, B., Saunders, M., 2012. Repeated slope failure linked to fluid migration: the Ana submarine landslide complex, Eivissa Channel, Western Mediterranean Sea. *Earth Planet. Sci. Lett.* 319–320, 65–74. <https://doi.org/10.1016/j.epsl.2011.11.045>.
- Bolt, G.H., 1956. Physio-chemical analysis of the compressibility of pure clays. *Géotechnique* 6 (2), 86–93. <https://doi.org/10.1680/geot.1956.6.2.86>.
- Brackenkridge, R.E., Stow, D.A., Hernández-Molina, F.J., Jones, C., Mena, A., Alejo, I., Ducassou, E., Llave, E., Ercilla, G., Nombela, M.A., Perez-Arlucea, M., 2018. Textural characteristics and facies of sand-rich contourite depositional systems. *Sedimentology* 65 (7), 2223–2252. <https://doi.org/10.1111/sed.12463>.
- Brewer, T.S., Harvey, P.K., Lovell, M.A., Haggas, S., Williamson, G., Pezard, P., 1998. Ocean floor volcanism: constraints from the integration of core and downhole logging measurements. In: Harvey, P.K., Lovell, M.A. (Eds.), *Core-Log Integration*, Geological Society, London, Special Publications, 136, pp. 341–362. <https://doi.org/10.1144/GSL.SP.1998.136.01.28>.
- Bryn, P., Solheim, A., Berg, K., Lien, R., Forsberg, C.F., Hafliadason, H., Ottesen, D., Rise, L., 2003. The Storegga slide complex; repeated large scale sliding in response to climatic cyclicity. In: Locat, J., Mienert, J., Boisvert, L. (Eds.), *Submarine Mass Movements and their Consequences, Advances in Natural and Technological Hazards Research*, 19. Springer, Dordrecht, The Netherlands, pp. 215–222.
- Bryn, P., Berg, K., Forsberg, C.F., Solheim, A., Kvalstad, T.J., 2005a. Explaining the Storegga slide. *Mar. Pet. Geol.* 22, 11–19. <https://doi.org/10.1016/j.marpetgeo.2004.12.003>.
- Bryn, P., Berg, K., Stoker, M.S., Hafliadason, H., Solheim, A., 2005b. Contourites and their relevance for mass wasting along the Mid-Norwegian margin. *Mar. Pet. Geol.* 22, 85–96. <https://doi.org/10.1016/j.marpetgeo.2004.10.012>.

- Bugge, T., Belderson, R.H., Kenyon, N.H., 1988. The Storegga Slide. *Philos. Trans. R. Soc.* 325, 357–388.
- Cameron, G.D.M., Piper, D.J.W., MacKillop, K., 2014. Sediment failures in northern Flemish Pass. *Geol. Surv. Canada Open File* 7566, 141. <https://doi.org/10.4095/293680>.
- Canals, M., Lastras, G., Urgeles, R., Casamor, J.L., Mienert, J., Cattaneo, A., De Batist, M., Hafidason, H., Imbo, Y., Laberg, J.S., Locat, J., Long, D., Longva, O., Masson, D.G., Sultan, N., Trincardi, F., Bryn, P., 2004. Slope failure dynamics and impacts from seafloor and shallow sub-seafloor geophysical data: case studies from the COSTA project. *Mar. Geol.* 213, 9–72. <https://doi.org/10.1016/j.margeo.2004.10.001>.
- Carter, L., Milliman, J.D., Talling, P.J., Gavey, R., Wynn, R.B., 2012. Near-synchronous and delayed initiation of long run-out submarine sediment flows from a record-breaking river flood, offshore Taiwan. *Geophys. Res. Lett.* 39 (12), L12603 <https://doi.org/10.1029/2012GL051172>.
- Carter, L., Gavey, R., Talling, P.J., Liu, J.T., 2014. Insights into submarine geohazards from breaks in subsea telecommunication cables. *Oceanography* 27 (2), 58–67. <https://doi.org/10.5670/oceanog.2014.40>.
- Casas, D., Ercilla, G., Yenes, M., Estrada, F., Alonso, B., García, M., Somoza, L., 2011. The Baraza Slide: model and dynamics. *Mar. Geophys. Res.* 32, 245–256.
- Casas, D., Chiocci, F., Casalbore, D., Ercilla, G., De Urbina, J.O., 2016. Magnitude-frequency distribution of submarine landslides in the Gioia Basin (southern Tyrrhenian Sea). *Geo-Mar. Lett.* 36 (6), 405–414.
- Cassidy, M., Watt, S.F., Palmer, M.R., Trofimovs, J., Symons, W., MacLachlan, S.E., Stinton, A.J., 2014. Construction of volcanic records from marine sediment cores: a review and case study (Montserrat, West Indies). *Earth Sci. Rev.* 138, 137–155. <https://doi.org/10.1016/j.earscirev.2014.08.008>.
- Cauchon-Voyer, G., Locat, J., St-Onge, G., 2008. Late-Quaternary morpho-sedimentology and submarine mass movements of the Betsiamites area, lower St. Lawrence Estuary, Quebec, Canada. *Mar. Geol.* 251, 233–252. <https://doi.org/10.1016/j.margeo.2008.03.003>.
- Cauchon-Voyer, G., Locat, J., Leroueil, S., St-Onge, G., Demers, D., 2011. Large-scale subaerial and submarine Holocene and recent mass movements in the Betsiamites area, Quebec, Canada. *Eng. Geol.* 121, 28–45. <https://doi.org/10.1016/j.engeo.2011.04.011>.
- Cauchon-Voyer, G., Locat, J., St-Onge, G., Leroueil, S., Lajoussesse, P., 2012. Development and potential triggering mechanisms for a large Holocene landslide in the lower St. Lawrence Estuary. In: Yamada, Y., Kawamura, K., Ikehara, K., Ogawa, Y., Urgeles, R., Mosher, D., Chaytor, J., Strasser, M. (Eds.), *Submarine Mass Movements and their Consequences, Advances in Natural and Technological Hazards Research*, 31. Springer Science+Business Media B.V., Dordrecht, pp. 67–76.
- Chaytor, J.D., Twichell, D.C., ten Brink, U.S., 2012. A reevaluation of the Munson-Nygren-retriever submarine landslide complex, Georges Bank lower Slope, Western North Atlantic. In: Yamada, Y., Kawamura, K., Ikehara, K., Ogawa, Y., Urgeles, R., Mosher, D., Chaytor, J., Strasser, M. (Eds.), *Submarine Mass Movements and their Consequences, Advances in Natural and Technological Hazards Research*, 31. Springer Science+Business Media B.V., Dordrecht, pp. 135–145.
- Clare, M.A., Vardy, M.E., Cartigny, M.J.B., Talling, P.J., Himsforth, M.D., Dix, J.K., Harris, J.M., Whitehouse, R.J.S., Belal, M., 2017. Direct monitoring of active geohazards: emerging geophysical tools for deep-water assessments. *Near Surf. Geophys.* 15, 427–444. <https://doi.org/10.3997/1873-0604.2017033>.
- Clare, M., Chaytor, J., Dabson, O., Gamboa, D., Georgiopolou, A., Eady, H., Hunt, J., Jackson, C., Katz, O., Krastel, S., León, R., 2019. A consistent global approach for the morphometric characterization of subaqueous landslides. *Geol. Soc. Lond., Spec. Publ.* 477 (1), 455–477. <https://doi.org/10.1144/SP477.15>.
- Clarke, S., Hubble, T., Webster, J., Airey, D., De Carli, E., Ferraz, C., Reimer, P., Boyd, R., Keene, J., Shipboard party S512/2008, 2016. Sedimentology, structure and age estimate of five continental slope submarine landslides, eastern Australia. *Aust. J. Earth Sci.* 63 (5), 631–652. <https://doi.org/10.1080/08120099.2016.1225600>.
- Clayton, C.R.L., Siddique, A., Hopper, R.J., 1998. Effects of sampler design on tube sampling disturbance—numerical and analytical investigations. *Géotechnique* 48 (6), 847–867. <https://doi.org/10.1680/geot.1998.48.6.847>.
- Coleman, J.M., 1988. Dynamic changes and processes in the Mississippi River delta. *Geol. Soc. Am. Bull.* 100, 999–1015. [https://doi.org/10.1130/0016-7606\(1988\)100<0999:DCAPIT>2.3.CO;2](https://doi.org/10.1130/0016-7606(1988)100<0999:DCAPIT>2.3.CO;2).
- Cukur, D., Kim, S.P., Kong, G.S., Bahk, J.J., Horozal, S., Um, I.K., Lee, G.S., Chang, T.S., Ha, H.J., Völker, D., Kim, J.K., 2016. Geophysical evidence and inferred triggering factors of submarine landslides on the western continental margin of the Ulleung Basin, East Sea. *Geo-Mar. Lett.* 36, 425–444. <https://doi.org/10.1007/s00367-016-0463-5>.
- Cukur, D., Um, I.K., Chun, J.H., Lee, G.S., Kim, S.R., Bahk, J.J., Urgeles, R., Horozal, S., 2020. Factors leading to slope failure on a sediment-starved margin: the southwestern continental margin of the East Sea, Korea. *Mar. Geol.* 428, 106282. <https://doi.org/10.1016/j.margeo.2020.106282>.
- Dalla Valle, G., Gamberi, F., Fogliini, F., Trincardi, F., 2015. The Gondola slide: a mass transport complex controlled by margin topography (South-Western Adriatic margin, Mediterranean Sea). *Mar. Geol.* 336, 97–113. <https://doi.org/10.1016/j.margeo.2015.05.001>.
- Dan, G., Sultan, N., Savoye, B., 2007. The 1979 Nice harbour catastrophe revisited: Trigger mechanism inferred from geotechnical measurements and numerical modelling. *Mar. Geol.* 245 (1–4), 40–64. <https://doi.org/10.1016/j.margeo.2007.06.011>.
- Demars, K., 1982. Unique engineering properties and compression behavior of Deep-Sea calcareous sediments. In: Demars, K., Chaney, R. (Eds.), *Geotechnical Properties, Behavior, and Performance of Calcareous Soils*, pp. 97–112. <https://doi.org/10.1520/STP28912S>.
- Díaz-Rodríguez, J.A., 2011. Diatomaceous soils: monotonic behaviour. In: *International Symposium on Deformation Characteristics of Geomaterials*, Seoul, Korea, September 1–3, 2011.
- Ducassou, E., Migeon, S., Mulder, T., Murat, A., Capotondi, L., Bernasconi, M., Mascle, J., 2009. Evolution of the Nile deep-sea turbidite system during the late Quaternary: influence of climate change on fan sedimentation. *Sedimentology* 56, 2061–2090. <https://doi.org/10.1111/j.1365-3091.2009.01070.x>.
- Dugan, B., 2012. Petrophysical and consolidation behavior of mass transport deposits from the northern Gulf of Mexico, IODP Expedition 308. *Mar. Geol.* 315–318, 98–107. <https://doi.org/10.1016/j.margeo.2012.05.001>.
- Dugan, B., Sheahan, T.C., 2012. Offshore sediment overpressures of passive margins: mechanisms, measurement, and models. *Rev. Geophys.* 50, RG3001.
- Dutkiewicz, A., Müller, R.D., O'Callaghan, S., Jónsson, H., 2015. Census of seafloor sediments in the world's ocean. *Geology* 43 (9), 795–798. <https://doi.org/10.1130/G36883.1>.
- Dziadek, R., 2014. *Drained and Undrained Shear Strength Characteristics of Reconstituted Bio-Siliceous Sediments*, University of Bremen - FB5 Geowissenschaften. University of Bremen, Bremen.
- Edwards, B.D., Lee, H.J., Field, M.E., 1995. Mudflow generated by retrogressive slope failure, Santa Barbara Basin, California continental borderland. *J. Sediment. Res.* A65 (1), 57–68. <https://doi.org/10.1306/D4268022-2B26-11D7-8648000102C1865D>.
- Elger, J., Berndt, C., Krastel, S., Piper, D.J.W., Gross, F., Spielhagen, R.F., Meyer, S., 2015. The Fram Slide off Svalbard: a submarine landslide on a low-sedimentation-rate glacial continental margin. *J. Geol. Soc.* 172, 153–156. <https://doi.org/10.1144/jgs2014-055>.
- Elger, J., Berndt, C., Krastel, S., Piper, D.J.W., Gross, F., Geissler, W.H., 2017. Chronology of the Fram Slide complex offshore NW Svalbard and its implications for local and regional slope stability. *Mar. Geol.* 393, 141–155. <https://doi.org/10.1016/j.margeo.2016.11.003>.
- Elger, J., Berndt, C., Rüpke, L., Krastel, S., Gross, F., Geissler, W.H., 2018. Submarine slope failures due to pipe structure formation. *Nat. Commun.* 9 (1), 1–6.
- Etienne, S., Le Roy, P., Tournadour, E., Roest, W.R., Jorry, S., Collot, J., Partiat, M., Largeau, M.A., Roger, J., Clerc, C., Dechnick, B., Sanborn, K.L., Lepareur, F., Horowitz, J., Webster, J.M., Gaillot, A., 2021. Large-scale margin collapse along a partly drowned, isolated carbonate platform (Lansdowne Bank, SW Pacific Ocean). *Mar. Geol.* 436, 106477. <https://doi.org/10.1016/j.margeo.2021.106477>.
- Evans, D., Harrison, Z., Shannon, P.M., Laberg, J.S., Nielsen, T., Ayers, S., Holmes, R., Hout, R.J., Lindberg, B., Hafidason, H., Long, D., Kuijpers, A., Andersen, E.S., Bryn, P., 2005. Palaeoslides and other mass failures of Pliocene to Pleistocene age along the Atlantic continental margin of NW Europe. *Mar. Pet. Geol.* 22, 1131–1148. <https://doi.org/10.1016/j.marpetgeo.2005.01.010>.
- Expedition 333 Scientists, 2011. *NanTroSEIZE Stage 2: Subduction Inputs 2 and Heat Flow*. IODP Preliminary Report, 333. <https://doi.org/10.2204/iodp.pr.333.2011>.
- Faugères, J.C., Mézerais, M.L., Stow, D.A.V., 1993. Contourite drift types and their distribution in the North and South Atlantic Ocean basin. *Sediment. Geol.* 82, 189–203. [https://doi.org/10.1016/0037-0738\(93\)90121-K](https://doi.org/10.1016/0037-0738(93)90121-K).
- Fisher, M.A., Normark, W.R., Greene, H.G., Lee, H.J., Sliter, R.W., 2005. Geology and tsunamiic potential of submarine landslides in Santa Barbara Channel, Southern California. *Mar. Geol.* 224, 1–22. <https://doi.org/10.1016/j.margeo.2005.07.012>.
- Fleischer, P., Orsi, T.H., Richardson, M.D., Anderson, A.L., 2001. *Geo-Mar. Lett.* 21, 103–122.
- Flemings, P.B., Long, H., Dugan, B., Germaine, J., John, C.M., Behrmann, J.H., Sawyer, D., IODP Expedition 308 Scientists, 2008. *Pressure penetrometers document high overpressure near the seafloor where multiple submarine landslides have occurred on the continental slope, offshore Louisiana, Gulf of Mexico*. *Earth Planet. Sci. Lett.* 269, 309–325. <https://doi.org/10.1016/j.epsl.2007.12.005>.
- Fonnesu, M., Palermo, D., Galbiati, M., Marchesini, M., Bonamini, E., Bendias, D., 2020. A new world-class deep-water play-type deposited by the syndepositional interaction of turbidity flow and bottom currents: the giant Eocene Coral Field in northern Mozambique. *Mar. Pet. Geol.* 111, 179–201. <https://doi.org/10.1016/j.marpetgeo.2019.07.047>.
- Förster, A., Ellis, R.G., Henrich, R., Krastel, S., Kopf, A.J., 2010. Geotechnical characterization and strain analyses of sediment in the Mauritania Slide complex, NW-Africa. *Mar. Pet. Geol.* 27, 1175–1189. <https://doi.org/10.1016/j.marpetgeo.2010.02.013>.
- Freire, F., Gyllencreutz, R., Jafri, R.U., Jakobsson, M., 2014. Acoustic evidence of a submarine slide in the deepest part of the Arctic, the Molloy Hole. *Geo-Mar. Lett.* 34, 315–325. <https://doi.org/10.1007/s00367-014-0371-5>.
- Freudenthal, T., Wefer, G., 2007. *Scientific drilling with the sea floor drill rig MeBo*. *Sci. Drill.* 5, 63–66.
- Freudenthal, T., Wefer, G., 2013. *Drilling cores on the sea floor with the remote-controlled sea floor drilling rig MeBo*. In: *Geoscientific Instrumentation Methods and Data Systems*, 2, pp. 329–337.
- Gamberi, F., Rovere, M., Marani, M., 2011. Mass-transport complex evolution in a tectonically active margin (Gioia Basin, Southeastern Tyrrhenian Sea). *Mar. Geol.* 279, 98–110. <https://doi.org/10.1016/j.margeo.2010.10.015>.
- Gamberi, F., Dalla Valle, G., Fogliini, F., Rovere, M., Trincardi, F., 2019. Submarine landslides on the seafloor: hints on subaqueous mass-transport processes from the Italian continental margins (Adriatic and Tyrrhenian Seas, Offshore Italy). In: Ogata, K., Festa, A., Pini, G.A. (Eds.), *Submarine Landslides: Subaqueous Mass Transport Deposits from Outcrops to Seismic Profiles*, Geophysical Monograph, 246, pp. 339–356. <https://doi.org/10.1002/9781119500513.ch20>.
- Gardner, J.V., Prior, D.B., Field, M.E., 1999. The Humboldt Slide - a large shear-dominated retrogressive slope failure. *Mar. Geol.* 154, 323–338. [https://doi.org/10.1016/S0025-3227\(98\)00121-2](https://doi.org/10.1016/S0025-3227(98)00121-2).

- Garziglia, S., Migeon, S., Ducassou, E., Loncke, L., Mascle, J., 2008. Mass-transport deposits on the Rosetta province (NW Nile deep-sea turbidite system, Egyptian margin): Characteristics, distribution, and potential causal processes. *Mar. Geol.* 250, 180–198. <https://doi.org/10.1016/j.margeo.2008.01.016>.
- Gatter, R., Clare, M.A., Hunt, J.E., Watts, M., Madhusudhan, B.N., Talling, P.J., Huhn, K., 2020. A multi-disciplinary investigation of the AFEN Slide: the relationship between contourites and submarine landslides. *Geol. Soc. Lond., Spec. Publ.* 500, 173–193. <https://doi.org/10.1144/SP500-2019-184>.
- Gee, M.J.R., Gawthorpe, R.L., Friedmann, J.S., 2005. Giant striations at the base of a submarine landslide. *Mar. Geol.* 214, 287–294. <https://doi.org/10.1016/j.margeo.2004.09.003>.
- Gee, M.J.R., Uy, H.S., Warren, J., Morley, C.K., Lambiase, J.J., 2007. The Brunei slide: a giant submarine landslide on the North West Borneo margin revealed by 3D seismic data. *Mar. Geol.* 246, 9–23. <https://doi.org/10.1016/j.margeo.2007.07.009>.
- Georgiopolou, A., 2018. Seafloor sediment and rock sampling. In: Micallef, A., Krastel, S., Savini, A. (Eds.), *Submarine Geomorphology*. Springer Nature, Cham Switzerland, pp. 75–92.
- Georgiopolou, A., Masson, D.G., Wynn, R.B., Krastel, S., 2010. Sahara Slide: Age, initiation, and processes of a giant submarine slide. *Geochem. Geophys. Geosyst.* 11 (7), Q07014. <https://doi.org/10.1029/2010GC003066>.
- Global Volcanism Program, 2013. In: Venzke, E. (Ed.), *Volcanoes of the World*, v. 4.9.4 (17 Mar 2021). Smithsonian Institution. <https://doi.org/10.5479/si.GVP.VOTW4-2013>. Downloaded 27 Mar 2021.
- Gowan, E.J., Zhang, X., Khosravi, S., Rovere, A., Stocchi, P., Hughes, A.L.C., Gyllencreutz, R., Mangerud, J., Svendsen, J.I., Lohmann, G., 2021. A new global ice sheet reconstruction for the past 80 000 years. *Nat. Commun.* 12, 119. <https://doi.org/10.1038/s41467-021-21469-w>.
- Greene, H.G., Murai, L.Y., Watts, P., Maher, N.A., Fisher, M.A., Paull, C.E., Eichhubl, P., 2006. Submarine landslides in the Santa Barbara channel as potential tsunami sources. *Nat. Hazards Earth Syst. Sci.* 6, 63–88. <https://doi.org/10.5194/nhess-6-63-2006>.
- Gustafson, C., Key, K., Evans, R.L., 2019. Aquifer systems extending far offshore on the U. S. Atlantic margin. *Sci. Rep.* 9, 8709. <https://doi.org/10.1038/s41598-019-44611-7>.
- Hafliðason, H., Sejrup, H.P., Berstad, I.M., Nygård, A., Richter, T., Bryn, P., Lien, R., Berg, K., 2003. A weak layer feature on the Northern Storegga slide escarpment. In: Mienert, J., Weaver, P. (Eds.), *European Margin Sediment Dynamics, Side-Scan Sonar and Seismic Images*. Springer-Verlag, Berlin, Heidelberg, pp. 55–62.
- Hafliðason, H., Sejrup, H.P., Nygård, A., Mienert, J., Bryn, P., Lien, R., Forsberg, C.F., Berg, K., Masson, D., 2004. The Storegga slide: architecture, geometry and slide development. *Mar. Geol.* 213, 201–234. <https://doi.org/10.1016/j.margeo.2004.10.007>.
- Hafliðason, H., Lien, R., Sejrup, H.P., Forsberg, C.F., Bryn, P., 2005. The dating morphology of the Storegga Slide. *Mar. Pet. Geol.* 22, 123–136. <https://doi.org/10.1016/j.marpetgeo.2004.10.008>.
- Hampton, M.A., Lee, H.J., Locat, J., 1996. Submarine landslides. *Rev. Geophys.* 34, 35–59. <https://doi.org/10.1029/95RG03287>.
- Harbitz, C.B., Løvholt, F., Bungum, H., 2014. Submarine landslide tsunamis: how extreme and how likely? *Nat. Hazards* 72, 1341–1374.
- Harders, R., Kutterolf, S., Hensen, C., Moerz, T., Brueckmann, W., 2010. Tephra layers: A controlling factor on submarine translational sliding? *Geochem. Geophys. Geosyst.* 11 (5), Q05S23. <https://doi.org/10.1029/2009GC002844>.
- Harders, R., Ranero, C.R., Weinrebe, W., Behrmann, J.H., 2011. Submarine slope failure along the convergent continental margin of the Middle America Trench. *Geochem. Geophys. Geosyst.* 12 (6), Q05S32. <https://doi.org/10.1029/2010GC003401>.
- Hart, B.S., Prior, D.B., Barrie, J.V., Currie, R., Luternauer, J.L., 1992. A river mouth submarine channel and failure complex, Fraser Delta, Canada. *Sediment. Geol.* 81 (1–2), 73–87. [https://doi.org/10.1016/0037-0738\(92\)90057-X](https://doi.org/10.1016/0037-0738(92)90057-X).
- Henkel, S., Strasser, M., Schwenk, T., Hanebuth, T.J.J., Hüsener, J., Winkelmann, D., Tomasini, J., Krastel, S., Kasten, S., 2011. An interdisciplinary investigation of a recent submarine mass transport deposit at the continental margin off Uruguay. *Geochem. Geophys. Geosyst.* 12 (8), Q08009. <https://doi.org/10.1029/2011GC003669>.
- Henrich, R., Hanebuth, T.J.J., Krastel, S., Neubert, N., Wynn, R.B., 2008. Architecture and sediment dynamics of the Mauritania Slide complex. *Mar. Pet. Geol.* 25, 17–33. <https://doi.org/10.1016/j.marpetgeo.2007.05.008>.
- Hill, J.C., Brothers, D.S., Craig, B.K., ten Brink, U.S., Chaytor, J.D., Flores, C.H., 2017. Geologic controls on submarine slope failure along the central U.S. Atlantic margin: Insights from the Currituck Slide complex. *Mar. Geol.* 385, 114–130. <https://doi.org/10.1016/j.margeo.2016.10.007>.
- Hizzett, J.L., Hughes Clarke, J.E., Sumner, E.J., Cartigny, M.J.B., Talling, P.J., Clare, M. A., 2018. Which triggers produce the most erosive, frequent, and longest runout turbidity currents on deltas? *Geophys. Res. Lett.* 45 (2), 855–863. <https://doi.org/10.1002/2017GL075751>.
- Hjelstuen, B.O., Eldholm, O., Faleide, J.I., 2007. Recurrent Pleistocene mega-failures on the SW Barents Sea margin. *Earth Planet. Sci. Lett.* 258 (3–4), 605–618. <https://doi.org/10.1016/j.epsl.2007.04.025>.
- Holland, M.E., Schultheiss, P.J., Roberts, J.A., 2019. Gas hydrate saturation and morphology from analysis of pressure cores acquired in the Bay of Bengal during expedition NGHP-02, offshore India. *Mar. Pet. Geol.* 108, 407–423. <https://doi.org/10.1016/j.marpetgeo.2018.07.018>.
- Horozal, S., Bahk, J.J., Lee, S.H., Cukur, D., Urgeles, R., Kim, G.Y., Kim, S.P., Ryu, B.J., Kim, J.H., 2019. Mass-wasting processes along the margins of the Ulleung Basin, East Sea: insights from multichannel seismic reflection and multibeam echosounder data. In: Lintern, D.G., et al. (Eds.), *Subaqueous Mass Movements and their Consequences: Assessing Geohazards, Environmental Implications and Economic Significance of Subaqueous Landslides*, 477. Geological Society, London, Special Publications, pp. 107–119. <https://doi.org/10.1144/SP477.18>.
- Hsu, S.K., Tsai, C.H., Ku, C.Y., Sibuet, J.C., 2009. Flow of turbidity currents as evidenced by failure of submarine telecommunication cables. In: Chiozzi, F.L., Ridenti, D., Casalbore, D., Bosman, A. (Eds.), *International Conference on Seafloor Mapping for Geohazard Assessment, Extended Abstract, Rendiconti Online, Società Geologica Italiana*, 7, pp. 167–171.
- Hubble, T., Yeung, S., Clarke, S., Baxter, A., De Blasio, F., 2019. Submarine landslides offshore Yamba, NSW, Australia: an analysis of their timing, downslope motion and possible causes. In: Lintern, D.G., Mosher, D.C., Moscardelli, L.G., Bobrowsky, P.T., Campbell, C., Chaytor, J., Clague, J., Georgiopolou, A., Lajeunesse, P., Normandeau, A., Piper, D., Scherwath, M., Stacey, C., Turmel, D. (Eds.), *Subaqueous Mass Movements and their Consequences: Assessing Geohazards, Environmental Implications and Economic Significance of Subaqueous Landslides*, 477. Geological Society, London, Special Publications, pp. 207–222. <https://doi.org/10.1144/SP477.11>.
- Huhn, K., 2016. Cruise Report/Fahrtbericht SO247 – SlamZ: Slide Activity on the Hikurangi Margin, New Zealand, Wellington (NZ): 27.03.2016–Auckland (NZ): 27.04.2016. MARUM, Center for Marine Environmental Sciences, Bremen, Germany. [https://doi.org/10.2312/cr\\_so247](https://doi.org/10.2312/cr_so247).
- Huhn, K., Freudenthal, T., Gatter, R., Hilgenfeldt, C., Hönekopp, L., Hornbach, M., Kühn, M., Kuhlmann, J., Kutterolf, S., Meyer-Schack, B., Pallapies, K., Rapp, S.K., Sievers, C., Watt, S., Stelzner, M., 2019. FS METEOR M154-2 Cruise Report “Sector Collapse Kinematics and Tsunami Implications – SEKT”, Point-à-Pitre - Point-à-Pitre, April 29 - May 23 2019, Reports from MARUM and Department of Geosciences, University of Bremen, p. 82.
- Huhn, K., Arroyo, M., Cattaneo, A., Clare, M.A., Gràcia, E., Harbitz, C.B., Krastel, S., Kopf, A., Løvholt, F., Rovere, M., Strasser, M., Talling, P.J., Urgeles, R., 2020. Modern submarine landslide complexes. In: Ogata, K., Festa, A., Pini, G.A. (Eds.), *Submarine Landslides: Subaqueous Mass Transport Deposits from Outcrops to Seismic Profiles*. Geophysical Monograph Series, 246. American Geophysical Union and John Wiley & Sons, Inc., Washington, pp. 183–200. <https://doi.org/10.1002/9781119500513.ch12>.
- Hühnerbach, V., Masson, D.G., Partners of COAST-Project, 2004. Landslides in the North Atlantic and its adjacent seas: an analysis of their morphology, setting and behaviour. *Mar. Geol.* 213, 343–362. <https://doi.org/10.1016/j.margeo.2004.10.013>.
- Hunt, J.E., Wynn, R.B., Masson, D.G., Talling, P.J., Teagle, D.A.H., 2011. Sedimentological and geochemical evidence for multistage failure of volcanic island landslides: A case study from Icod landslide on north Tenerife, Canary Islands. *Geochem. Geophys. Geosyst.* 12 (12), Q12007. <https://doi.org/10.1029/2011GC003740>.
- Jo, A., Eberli, G.P., Grasmueck, M., 2015. Margin collapse and slope failure along southwestern Great Bahama Bank. *Sediment. Geol.* 317, 43–52. <https://doi.org/10.1016/j.sedgeo.2014.09.004>.
- Johnson, T.C., Hamilton, E.L., Berger, W.H., 1977. Physical properties of calcareous ooze: Control by dissolution at depth. *Mar. Geol.* 24 (4), 259–277. [https://doi.org/10.1016/0025-3227\(77\)90071-8](https://doi.org/10.1016/0025-3227(77)90071-8).
- Jorat, M.E., Mörz, T., Schunn, W., Kreiter, S., 2014. Geotechnical Offshore Seabed Tool (GOST): A new cone penetrometer. In: *Third International Symposium on Cone Penetration Testing*, Las Vegas, Nevada, USA, 12–14 May 2014.
- Judd, A.G., Hovland, M., 1992. The evidence of shallow gas in marine sediments. *Cont. Shelf Res.* 12 (10), 1081–1095.
- Jutzeler, M., White, J.D.L., Talling, P.J., McCanta, M., Morgan, S., Le Friant, A., Ishizuka, O., 2014. Coring disturbances in IODP piston cores with implications for offshore record of volcanic events and the Missoula megafloods. *Geochem. Geophys. Geosyst.* 15, 3572–3590. <https://doi.org/10.1002/2014GC005447>.
- Kaminski, P., Urlaub, M., Grabe, J., Berndt, C., 2020. Geomechanical behaviour of gassy soils and implications for submarine slope stability: a literature analysis. In: Georgiopolou, A.A.L.A., Benetti, S., Chaytor, J.D., Clare, M.A., Gamboa, D., Haughton, P.D.W., Moernaut, J., Mountjoy, J.J. (Eds.), *Subaqueous Mass Movements and their Consequences: Advances in Process Understanding, Monitoring and Hazard Assessments*, 500. Geological Society, London, Special Publications, pp. 277–288. <https://doi.org/10.1144/SP500-2019-149>.
- Kämpf, J., Chapman, P., 2016. *Upwelling Systems of the World: A Scientific Journey to the Most Productive Marine Ecosystems*. Springer International Publishing, Switzerland, p. 47.
- Katz, O., Reuven, E., Aharonov, E., 2015. Submarine landslides and fault scarps along the eastern Mediterranean Israeli continental-slope. *Mar. Geol.* 369, 100–115. <https://doi.org/10.1016/j.margeo.2015.08.006>.
- Kluesner, J.W., Brothers, D.S., Wright, A.L., Johnson, S.Y., 2020. Structural controls on slope failure within the Western Santa Barbara channel based on 2-D and 3-D seismic imaging. *Geochem. Geophys. Geosyst.* 21. <https://doi.org/10.1029/2020GC009055> e2020GC009055.
- Kokusho, T., 1999. Water film in liquefied sand and its effect on lateral spread. *J. Geotech. Geoenviron.* 125, 817–826. [https://doi.org/10.1061/\(ASCE\)1090-0241\(1999\)125:10\(817\)](https://doi.org/10.1061/(ASCE)1090-0241(1999)125:10(817)).
- Kokusho, T., Kojima, T., 2002. Mechanism for postliquefaction water film generation in layered sand. *J. Geotech. Geoenviron.* 128, 129–137. [https://doi.org/10.1061/\(ASCE\)1090-0241\(2002\)128:2\(129\)](https://doi.org/10.1061/(ASCE)1090-0241(2002)128:2(129)).
- Kopf, A.J., Stegmann, S., Garziglia, S., Henry, P., Dennielou, B., Haas, S., Weber, K.C., 2016. Soft sediment deformation in the shallow submarine slope off Nice (France) as a result of a variably charged Pliocene aquifer and mass wasting processes. *Sediment. Geol.* 344, 290–309. <https://doi.org/10.1016/j.sedgeo.2016.05.014>.
- Korup, O., 2012. Earth’s portfolio of extreme sediment transport events. *Earth Sci. Rev.* 112, 115–125. <https://doi.org/10.1016/j.earscirev.2012.02.006>.

- Korup, O., Clague, J.J., Hermanns, R.L., Hewitt, K., Strom, A.L., Weidinger, J.T., 2007. Giant landslides, topography, and erosion. *Earth Planet. Sci. Lett.* 261, 578–589. <https://doi.org/10.1016/j.epsl.2007.07.025>.
- Krastel, S., Wefer, G., Hanebuth, T.J.J., Antobreh, A.A., Freudenthal, T., Pretz, B., Schwenk, T., Strasser, M., Violante, R., Winkelmann, D., 2011. M78/3 shipboard scientific party, 2011. Sediment dynamics and geohazards off Uruguay and the de la Plata River region (northern Argentina and Uruguay). *Geo-Mar. Lett.* 31, 271–283. <https://doi.org/10.1007/s00367-011-0232-4>.
- Krastel, S., Wynn, R.B., Feldens, P., Schürer, A., Böttner, C., Stevenson, C., Cartigny, J.B., Hühnerbach, V., Unverricht, D., 2016. Flow behaviour of a giant landslide and debris flow entering Agadir Canyon, NW Africa. In: Lamarche, G., Mountjoy, J., Bull, S., Hubble, T., Krastel, S., Lane, E., Micallef, A., Moscardelli, L., Mueller, C., Pecher, I., Woelz, S. (Eds.), *Submarine Mass Movements and Their Consequences, Advances in Natural and Technological Hazards Research*, 41. Springer International Publishing Switzerland, Cham, pp. 145–154.
- Krastel, S., Urlaub, M., Georgiopolou, A., Wynn, R.B., Schwenk, T., Stevenson, C., Feldens, P., 2019. Mass wasting along the NW African continental margin. In: Lintern, D.G., Mosher, D.C., Moscardelli, L.G., Bobrowsky, P.T., Campbell, C., Chaytor, J.D., Clague, J.J., Georgiopolou, A., Lajeunesse, P., Normandeau, A., Piper, D.J.W., Scherwath, M., Stacey, C., Turmel, D. (Eds.), *Subaqueous Mass Movements and their Consequences: Assessing Geohazards, Environmental Implications and Economic Significance of Subaqueous Landslides*, 477. Geological Society, London, Special Publications, pp. 151–167. <https://doi.org/10.1144/SP477.36>.
- Kuhlmann, J., Asiola, A., Strasser, M., Trincardi, F., Huhn, K., 2014. Integrated stratigraphic and morphological investigation of the twin slide complex offshore Southern Sicily. In: Krastel, S., Behrmann, J.H., Völker, D., Stipp, M., Berndt, C., Urgeles, R., Chaytor, J., Huhn, K., Strasser, M., Harbitz, C.B. (Eds.), *Submarine Mass Movements and their Consequences, Advances in Natural and Technological Hazards Research*, 37. Springer International Publishing Switzerland, Cham, pp. 583–594.
- Kuhlmann, J., Huhn, K., Ikari, M., 2016. Do embedded volcanoclastic layers serve as potential Glide Planes: an integrated analysis from the Gela Basin offshore Southern Sicily. In: Lamarche, G., Mountjoy, J., Bull, S., Hubble, T., Krastel, S., Lane, E., Micallef, A., Moscardelli, L., Mueller, C., Pecher, I., Woelz, S. (Eds.), *Submarine Mass Movements and their Consequences, Advances in Natural and Technological Hazards Research*, 41. Springer International Publishing Switzerland, Cham, pp. 273–280.
- Kuhlmann, J., Asiola, A., Trincardi, F., Klügel, A., Huhn, K., 2017. Landslide frequency and failure mechanisms at NE Gela Basin (Strait of Sicily). *J. Geophys. Res. Earth Surf.* 122, 2223–2243. <https://doi.org/10.1002/2017JF004251>.
- Kuhlmann, J., Orpin, A.R., Mountjoy, J.J., Crutchley, G.J., Henrys, S., Lunenburg, R., Huhn, K., 2019. Seismic and lithofacies characterization of a gravity core transect down the submarine Tuaheni Landslide Complex, NE New Zealand. In: Lintern, D.G., Mosher, D.C., Moscardelli, L.G., Bobrowsky, P.T., Campbell, C., Chaytor, J.D., Clague, J.J., Georgiopolou, A., Lajeunesse, P., Normandeau, A., Piper, D.J.W., Scherwath, M., Stacey, C., Turmel, D. (Eds.), *Subaqueous Mass Movements and their Consequences: Assessing Geohazards, Environmental Implications and Economic Significance of Subaqueous Landslides*, 477. Geological Society, London, Special Publications, pp. 479–495. <https://doi.org/10.1144/SP477.37>.
- Kvalstad, T.J., Andresen, L., Forsberg, C.F., Berg, K., Bryn, P., Wangen, M., 2005. The Storegga slide: evaluation of triggering sources and slide mechanics. *Mar. Pet. Geol.* 22, 245–256. <https://doi.org/10.1016/j.marpetgeo.2004.10.019>.
- Laberg, J.S., Camerlenghi, A., 2008. Chapter 25 the significance of contourites for submarine slope stability. *Dev. Sedimentol.* 60, 537–556. [https://doi.org/10.1016/S0070-4571\(08\)10025-5](https://doi.org/10.1016/S0070-4571(08)10025-5).
- Laberg, J.S., Vorren, T.O., 1993. A late Pleistocene submarine slide on the Bear Island Trough Mouth Fan. *Geo-Mar. Lett.* 13, 227–234.
- Laberg, J.S., Vorren, T.O., 2000. The Trænadjupet Slide, offshore Norway - morphology, evacuation and triggering mechanisms. *Mar. Geol.* 171, 95–114. [https://doi.org/10.1016/S0025-3227\(00\)00112-2](https://doi.org/10.1016/S0025-3227(00)00112-2).
- Laberg, J.S., Vorren, T.O., Dowdeswell, J.A., Kenyon, N.H., Taylor, J., 2000. The Andøya slide and the Andøya canyon, north-eastern Norwegian-Greenland Sea. *Mar. Geol.* 162, 259–275. [https://doi.org/10.1016/S0025-3227\(99\)00087-0](https://doi.org/10.1016/S0025-3227(99)00087-0).
- Laberg, J.S., Vorren, T.O., Mienert, J., Evans, D., Lindberg, B., Ottesen, D., Kenyon, N.H., Henriksen, S., 2002. Late Quaternary paleoenvironment and chronology in the Trænadjupet Slide area offshore Norway. *Mar. Geol.* 188, 35–60. [https://doi.org/10.1016/S0025-3227\(02\)00274-8](https://doi.org/10.1016/S0025-3227(02)00274-8).
- Laberg, J.S., Vorren, T.O., Mienert, J., Hafliðason, H., Bryn, P., Lien, R., 2003. Preconditions leading to the Holocene Trænadjupet Slide offshore Norway. In: Locat, J., Mienert, J. (Eds.), *Submarine Mass Movements and their Consequences, Natural and Technological Hazards Research*, 19. Springer Science+Business Media, Dordrecht, pp. 247–254.
- Laberg, J.S., Kawamura, K., Amundsen, H., Baeten, N., Forwick, M., Rynningen, T.A., Vorren, T.O., 2014. A submarine landslide complex affecting the Jan Mayen Ridge, Norwegian-Greenland Sea: slide-scar morphology and processes of sediment evacuation. *Geo-Mar. Lett.* 34, 51–58.
- Lackey, J., Moore, G., Strasser, M., 2018. Three-dimensional mapping and kinematic characterization of mass transport deposits along the outer Kumano Basin and Nankei accretionary wedge, Southwest Japan. *Progress Earth Planet. Sci.* 5, 65. <https://doi.org/10.1186/s40645-018-0223-4>.
- Lackey, J.K., Regalla, C.A., Moore, G.F., 2020. Tectonic influences on trench slope basin development via structural restoration along the outer Nankai accretionary prism, Southwestern Japan. *Geochem. Geophys. Geosyst.* 21 <https://doi.org/10.1029/2020GC009038> e2020GC009038.
- Lafuerza, S., Sultan, N., Canals, M., Lastras, G., Cattaneo, A., Frigola, J., Costa, S., Berndt, C., 2012. Failure mechanisms of Ana Slide from geotechnical evidence, Eivissa Channel, Western Mediterranean Sea. *Mar. Geol.* 307–310, 1–21. <https://doi.org/10.1016/j.margeo.2012.02.010>.
- Lastras, G., Canals, M., Urgeles, R., De Batist, M., Calafat, A.M., Casamor, J.L., 2004. Characterisation of the recent BIG'95 debris flow deposit on the Ebro margin, Western Mediterranean Sea, after a variety of seismic reflection data. *Mar. Geol.* 213, 235–255. <https://doi.org/10.1016/j.margeo.2004.10.008>.
- Lastras, G., Canals, M., Amblas, D., Frigola, J., Urgeles, R., Calafat, A.M., Acosta, J., 2007. Slope instability along the northeastern Iberian and Balearic continental margins. *Geol. Acta* 5, 35–47.
- Laugié, M., Michel, J., Pohl, A., Poli, E., Borgomano, J., 2019. Global distribution of modern shallow-water marine carbonate factories: a spatial model based on environmental parameters. *Sci. Rep.* 9, 16433. <https://doi.org/10.1038/s41598-019-52821-2>.
- Le Friant, A., Lebas, E., Brunet, M., Lafuerza, S., Hornbach, M., Coussens, M., Watt, S., Cassidy, M., Talling, P.J., IODP 340 Expedition Ship Party, 2019. Submarine landslides around Volcanic Island: a review of what can be learned from the lesser antilles arc. In: Ogata, K., Festa, A., Pini, G.A. (Eds.), *Submarine Landslides: Subaqueous Mass Transport Deposits from Outcrops to Seismic Profiles. Geophysical Monograph Series*, 246. American Geophysical Union and John Wiley & Sons, Inc, Washington, pp. 277–297.
- Lee, H.J., 2009. Timing of occurrence of large submarine landslides on the Atlantic Ocean margin. *Mar. Geol.* 264 (1–2), 53–64. <https://doi.org/10.1016/j.margeo.2008.09.009>.
- Lee, H.J., Locat, J., Desgagnés, P., Parsons, J.D., McAdoo, B.G., Orange, D.L., Puig, P., Wong, F.L., Dartnell, P., Boulanger, E., 2007. Submarine mass movements on continental margins. In: Nittrouer, C.A., Austin, J.A., Field, M.E., Kravitz, J.H., Syvitski, J.P.M., Wiberg, P.L. (Eds.), *Continental Margin Sedimentation: From Sediment Transport to Sequence Stratigraphy*. Blackwell Publishing Ltd, Oxford, UK, pp. 213–274. <https://doi.org/10.1002/9781444304398.ch5>.
- León, R., Urgeles, R., Pérez-López, R., Payo, E., Vázquez-Izquierdo, A., Giménez-Moreno, C.J., Casas, D., 2020. Geological and tectonic controls on morphometrics of submarine landslides of the Spanish margins. In: Georgiopolou, A., Amy, L.A., Benetti, S., Chaytor, J.D., Clare, M.A., Gamboa, D., Houghton, P.D.W., Moernaut, J., Mountjoy, J.J. (Eds.), *Subaqueous Mass Movements and their Consequences: Advances in Process Understanding, Monitoring and Hazards Assessment*, 500. Geological Society, London, Special Publication, pp. 495–513. <https://doi.org/10.1144/SP500-2019-153>.
- Lewis, K.B., 1971. Slumping on a continental slope inclined at 1°–4°. *Sedimentology* 16, 97–110. <https://doi.org/10.1111/j.1365-3091.1971.tb00221.x>.
- Leynaud, D., Sultan, N., Mienert, J., 2007. The role of sedimentation rate and permeability in the slope stability of the formerly glaciated Norwegian continental margin: the Storegga slide model. *Landslides* 4, 297–309.
- Leynaud, D., Mienert, J., Vanneste, M., 2009. Submarine mass movements on glaciated and non-glaciated European continental margins: a review of triggering mechanisms and preconditions to failure. *Mar. Pet. Geol.* 26, 618–632. <https://doi.org/10.1016/j.marpetgeo.2008.02.008>.
- L'Heureux, J.S., Hansen, L., Longva, O., Emdal, A., Grande, L.O., 2010. A multidisciplinary study of submarine landslides at the Nidelva fjord delta, Central Norway - Implications for geohazard assessment. *Nor. J. Geol.* 90, 1–20.
- L'Heureux, J.S., Glimsdal, S., Longva, O., Hansen, L., Harbitz, C.B., 2011. The 1888 shoreline landslide and tsunami in Trondheimsfjorden, Central Norway. *Mar. Geophys. Res.* 32, 313–329. <https://doi.org/10.1007/s11001-010-9103-z>.
- L'Heureux, J.S., Longva, O., Steiner, A., Hansen, L., Vardy, M.E., Vanneste, M., Hafliðason, H., Brendryen, J., Kvalstad, T.J., Forsberg, C.F., Chand, S., Kopf, A., 2012. Identification of weak layers and their role for the stability of slopes at Finneidfjord, Northern Norway. In: Yamada, Y., Kawamura, K., Ikehara, K., Ogawa, Y., Urgeles, R., Mosher, D., Chaytor, J., Strasser, M. (Eds.), *Submarine Mass Movements and their Consequences, Advances in Natural and Technological Hazards Research*, 31. Springer Science+Business Media B.V, Dordrecht, pp. 321–330.
- L'Heureux, J.S., Vanneste, M., Rise, L., Brendryen, J., Forsberg, C.F., Nadim, F., Longva, O., Chand, S., Kvalstad, T.J., Hafliðason, H., 2013. Stability, mobility and failure mechanism for landslides at the upper continental slope off Vesterålen, Norway. *Mar. Geol.* 346, 192–207. <https://doi.org/10.1016/j.margeo.2013.09.009>.
- L'Heureux, J.S., Longva, O., Hansen, L., Vanneste, M., 2014. The 1930 landslide in Orkdalsfjorden: morphology and failure mechanism. In: Krastel, S., Behrmann, J.H., Völker, D., Stipp, M., Berndt, C., Urgeles, R., Chaytor, J., Huhn, K., Strasser, M., Harbitz, C.B. (Eds.), *Submarine Mass Movements and their Consequences, Advances in Natural and Technological Hazards Research*, 37. Springer International Publishing Switzerland, Cham, pp. 239–247.
- Li, W., Wu, S., Völker, D., Zhao, F., Mi, L., Kopf, A., 2014a. Morphology, seismic characterization and sediment dynamics of the Baiyun Slide complex on the northern South China Sea margin. *J. Geol. Soc. Lond.* 171, 865–877. <https://doi.org/10.1144/jgs2014-034>.
- Li, W., Wu, S., Wang, X., Zhao, F., Wang, D., Mi, L., Li, Q., 2014b. Baiyun slide and its relation to fluid migration in the Northern Slope of Southern China Sea. In: Krastel, S., Behrmann, J.H., Völker, D., Stipp, M., Berndt, C., Urgeles, R., Chaytor, J., Huhn, K., Strasser, M., Harbitz, C.B. (Eds.), *Submarine Mass Movements and their Consequences, Advances in Natural and Technological Hazards Research*, 37. Springer International Publishing Switzerland, Cham, pp. 105–115.
- Li, W., Alves, T.M., Urlaub, M., Georgiopolou, A., Klauke, L., Wynn, R.B., Gross, F., Meyer, M., Replschläger, J., Berndt, C., Krastel, S., 2017. Morphology, age and sediment dynamics of the upper headwall of the Sahara Slide complex, Northwest Africa: evidence for a large late Holocene failure. *Mar. Geol.* 393, 109–123. <https://doi.org/10.1016/j.margeo.2016.11.013>.

- Li, W., Krastel, S., Alves, T.M., Urlaub, M., Mehringer, L., Schürer, A., Feldens, P., Gross, F., Stevenson, C.J., Wynn, R.B., 2018. The Agadir Slide offshore NW Africa: Morphology, emplacement dynamics, and potential contribution to the Moroccan Turbidite System. *Earth Planet. Sci. Lett.* 498, 436–449. <https://doi.org/10.1016/j.epsl.2018.07.005>.
- Lindberg, B., Laberg, J.S., Vorren, T.O., 2004. The Nyk Slide - morphology, progression, and age of a partly buried submarine slide offshore northern Norway. *Mar. Geol.* 213, 277–289. <https://doi.org/10.1016/j.margeo.2004.10.010>.
- Lintern, D.G., Rutherford, J., Hill, P.R., Campbell, C., Normandeau, A., 2020. Towards a national-scale assessment of the subaqueous mass movement hazard in Canada. In: Georgiopoulou, A.A.L.A., Benetti, S., Chaytor, J.D., Clare, M.A., Gamboa, D., Houghton, P.D.W., Moernaut, J., Mountjoy, J.J. (Eds.), *Subaqueous Mass Movements and their Consequences: Advances in Process Understanding, Monitoring and Hazard Assessments*, 500. Geological Society, London, Special Publications, pp. 97–113. <https://doi.org/10.1144/SP500-2019-206>.
- Locat, J., Lee, H.J., 2002. Submarine landslides: advances and challenges. *Can. Geotech. J.* 39, 193–212. <https://doi.org/10.1139/t01-089>.
- Locat, J., Leroueil, S., Locat, A., Lee, H., 2014. Weak layers: their definition and classification from a geotechnical perspective. In: Krastel, S., Behrmann, J.H., Völker, D., Stipp, M., Berndt, C., Urgeles, R., Chaytor, J., Huhn, K., Strasser, M., Harbitz, C.B. (Eds.), *Submarine Mass Movements and their Consequences, Advances in Natural and Technological Hazards Research*, 37. Springer International Publishing Switzerland, Cham, pp. 3–12.
- Løvholt, F., Schulten, I., Mosher, D.C., Harbitz, C., Krastel, S., 2019. Modeling of the 1929 Grand Banks slump and landslide tsunami. In: Lintern, D.G., Mosher, D.C., Moscardelli, L.G., Bobrowsky, P.T., Campbell, C., Chaytor, J.D., Clague, J.J., Georgiopoulou, A., Lajeunesse, P., Normandeau, A., Piper, D.J.W., Scherwath, M., Stacey, C., Turmel, D. (Eds.), *Subaqueous Mass Movements and their Consequences: Assessing Geohazards, Environmental Implications and Economic Significance of Subaqueous Landslides*, 477. Geological Society, London, Special Publications, pp. 315–331. <https://doi.org/10.1144/SP477-28>.
- Lucchi, R.G., Pedrosa, M.T., Camerlenghi, A., Urgeles, R., De Mol, B., Rebesco, M., 2012. Recent submarine landslides on the continental slope of Storfjorden and Kveithola Trough-Mouth fans (North West Barents Sea). In: Yamada, Y., Kawamura, K., Ikehara, K., Ogawa, Y., Urgeles, R., Mosher, D., Chaytor, J., Strasser, M. (Eds.), *Submarine Mass Movements and their Consequences, Advances in Natural and Technological Hazards Research*, 31. Springer, Dordrecht, The Netherlands, pp. 735–745.
- Lunne, T., Robertson, P.K., Powell, J.J.M., 1997. *Cone Penetration Testing in Geotechnical Practice*. Blackie Academic & Professional, London, p. 312.
- Luo, M., Torres, M.E., Kasten, S., Mountjoy, J.J., 2020. Constraining the age and evolution of the Tuaheni Landslide Complex, Hikurangi Margin, New Zealand, using pore-water geochemistry and numerical modelling. *Geophys. Res. Lett.* 47 <https://doi.org/10.1029/2020GL087243> e2020GL087243.
- Lykousis, V., Roussakis, G., Alexandri, M., Pavlakis, P., Papouli, I., 2002. Sliding and regional slope stability in active margins: North Aegean Trough (Mediterranean). *Mar. Geol.* 186, 281–298. [https://doi.org/10.1016/S0025-3227\(02\)00269-4](https://doi.org/10.1016/S0025-3227(02)00269-4).
- Madhusudhan, B.N., Clare, M.A., Clayton, C.R.I., Hunt, J.E., 2017. Geotechnical profiling of deep-ocean sediments at the AFEN submarine slide complex. *Q. J. Eng. Geol. Hydrogeol.* 50, 148–157. <https://doi.org/10.1144/qjgeh2016-057>.
- Major, C.O., Pirmez, C., Goldberg, D., Leg 166 Scientific Party, 1998. High-resolution core-log integration techniques: examples from the Ocean Drilling Program. In: Harvey, P.K., Lovell, M.A. (Eds.), *Core-Log Integration*, 136. Geological Society, London, Special Publications, pp. 285–295. <https://doi.org/10.1144/GSL.SP.1998.136.01.24>.
- Maslin, M.A., 2009. Review of the timing and causes of the Amazon-Fan mass transport and avulsion deposits during the latest Pleistocene. In: Kneller, B., Martinsen, O.J., McCaffrey, B. (Eds.), *External Controls on Deep-Water Depositional Systems*. SEPM Society for Sedimentary Geology, Special Publication, 92, pp. 133–144. <https://doi.org/10.2110/sepm.sp.092.133>.
- Maslin, M., Vilela, C., Mikkelsen, N., Grootes, P., 2005. Causes of catastrophic sediment failures of the Amazon Fan. *Quat. Sci. Rev.* 24, 2180–2193. <https://doi.org/10.1016/j.quascirev.2005.01.016>.
- Masson, D.G., Harbitz, C.B., Wynn, R.B., Pedersen, G., Løvholt, F., 2006. Submarine landslides: processes, triggers and hazard prediction. *Philos. Trans. R. Soc.* 364, 2009–2039. <https://doi.org/10.1098/rsta.2006.1810>.
- Masson, D.G., Wynn, R.B., Talling, P.J., 2010. Large landslides on passive continental margins: processes, hypotheses and outstanding questions. In: Mosher, D.C., Shipp, R.C., Moscardelli, L., Chaytor, J.D., Baxter, C.D.P., Lee, H.J., Urgeles, R. (Eds.), *Submarine Mass Movements and their Consequences, Advances in Natural and Technological Hazards Research*, 28. Springer Science+Business Media B.V., Dordrecht, pp. 153–166.
- McAdoo, B.G., Pratson, L.F., Orange, D.L., 2000. Submarine landslide geomorphology, US continental slope. *Mar. Geol.* 169, 103–136. [https://doi.org/10.1016/S0025-3227\(00\)00050-5](https://doi.org/10.1016/S0025-3227(00)00050-5).
- Meunier, J., Sultan, N., Jegou, P., Harmegnies, F., 2004. First tests of Penfeld: a new seabed penetrometer. Proceedings of Fourteenth International Society of Offshore and Polar Engineering Conference, Toulon, France, 23–28 May 2004.
- Meyer, M., Geersen, J., Krastel, S., Schwenk, T., Winkelmann, D., 2012. Dakar slide offshore Senegal, NW-Africa: Interaction of stacked giant mass-wasting events and canyon evolution. In: Yamada, Y., Kawamura, K., Ikehara, K., Ogawa, Y., Urgeles, R., Mosher, D., Chaytor, J., Strasser, M. (Eds.), *Submarine Mass Movements and their Consequences, Advances in Natural and Technological Hazards Research*, 31. Springer Science+Business Media B.V., Dordrecht, pp. 177–188.
- Micallef, A., Berndt, C., Masson, D.G., Stow, D.A., 2008. Scale invariant characteristics of the Storegga Slide and implications for large-scale submarine mass movements. *Mar. Geol.* 247 (1–2), 46–60. <https://doi.org/10.1016/j.margeo.2007.08.003>.
- Micallef, A., Person, M., Berndt, C., Bertoni, C., Cohen, D., Dugan, B., Evans, R., Haroon, A., Hensen, C., Jegen, M., Key, K., Kooi, H., Liebetrau, V., Lofi, J., Mailloux, B.J., Martin-Nagle, R., Michael, H.A., Müller, T., Schmidt, M., Schwalenberg, K., Trembath-Reichert, E., Weymer, B., Zhang, Y., Thomas, A.T., 2021. Offshore freshened groundwater in continental margins. *Rev. Geophys.* 58 <https://doi.org/10.1029/2020RG000706> e2020RG000706.
- Minisini, D., Trincardi, F., Asioli, A., 2006. Evidence of slope instability in the Southwestern Adriatic margin. *Nat. Hazards Earth Syst. Sci.* 6, 1–20. <https://doi.org/10.5194/nhess-6-1-2006>.
- Miramontes Garcia, E., 2016. *Glissements Sous-Marins en Mer Tyrrhénienne Septentrionale et Relations Avec Les Dépôts Contouritaires et Turbiditaires: Morphologie, Stratigraphie, Géotechnique et Modélisation*. PhD Thesis. Université de Bretagne Occidentale, IFREMER, Unité Géosciences Marines, Laboratoire Aléas géologiques et Dynamique sédimentaire, p. 210.
- Miramontes, E., Sultan, N., Garziglia, S., Jouet, G., Pelleter, E., Cattaneo, A., 2018. Altered volcanic deposits as basal failure evidence of submarine landslides. *Geology* 46 (7), 663–666. <https://doi.org/10.1130/G40268.1>.
- Moernaut, J., De Batist, M., 2011. Frontal emplacement and mobility of sublacustrine landslides: results from morphometric and seismostratigraphic analysis. *Mar. Geol.* 285, 29–45. <https://doi.org/10.1016/j.margeo.2011.05.001>.
- Moernaut, J., Wiemer, G., Kopf, A., Strasser, M., 2020. Evaluating the sealing potential of young and thin mass-transport deposits: Lake Villarrica, Chile. In: Georgiopoulou, A., Amy, L.A., Benetti, S., Chaytor, J.D., Clare, M.A., Gamboa, D., Houghton, P.D.W., Moernaut, J., Mountjoy, J.J. (Eds.), *Subaqueous Mass Movements and their Consequences: Advances in Process Understanding, Monitoring and Hazard Assessment*, 500. Geological Society, London, Special Publication, pp. 129–146. <https://doi.org/10.1144/SP500-2019-155>.
- Mollison, K.C., Power, H.E., Clarke, S.L., Baxter, A.T., Lane, E.M., Hubble, T.C.T., 2020. The sedimentology and tsunamigenic potential of the Byron submarine landslide off New South Wales, Australia. *Geol. Soc. Lond., Spec. Publ.* 500, 27–40. <https://doi.org/10.1144/SP500-2019-160>.
- Moore, R., 1991. The chemical and mineralogical controls upon the residual strength of pure and natural clays. *Géotechnique* 41 (1), 35–47. <https://doi.org/10.1680/geot.1991.41.1.35>.
- Moore, J.G., Clague, D.A., Holcomb, R.T., Lipman, P.W., Normark, W.R., Torresan, M.E., 1989. Prodigious submarine landslides on the Hawaiian Ridge. *J. Geophys. Res.* 94 (B12), 17,465–17,484. <https://doi.org/10.1029/JB094B12p17465>.
- Morehead, M.D., Syvitski, J.P., Hutton, E.W.H., Peckham, S.D., 2003. Modeling the temporal variability in the flux of sediment from ungauged river basins. *Glob. Planet. Chang.* 39, 95–110. [https://doi.org/10.1016/S0921-8181\(03\)00019-5](https://doi.org/10.1016/S0921-8181(03)00019-5).
- Morgenstern, N.R., 1967. *Submarine slumping and the initiation of turbidity currents*. In: Richards, A.F. (Ed.), *Marine Geotechnique*, 189–220. University of Illinois Press, Urbana, Ill.
- Mosher, D.C., 2009. International year of planet Earth 7. Oceans: submarine landslides and consequent Tsunami in Canada. *Geosci. Can.* 36 (4), 179–190. [https://id.erudit.org/iderudit/geocan36\\_4ser04](https://id.erudit.org/iderudit/geocan36_4ser04).
- Mosher, D.C., Piper, D.J.W., 2007. Analysis of multibeam seafloor imagery of the Laurentian Fan and the 1929 Grand Banks landslide area. In: Lykousis, V., Sakellariou, D., Locat, J. (Eds.), *Submarine Mass Movements and their Consequences, Advances in Natural and Technological Hazards Research*, 27. Springer, Dordrecht, pp. 77–88.
- Mosher, D.C., Mayer, L.A., Shipley, T.H., Winterer, E.L., Hagen, R.A., Marsters, J.C., Bassinot, F., Layle, M., 1993. Seismic stratigraphy of the Ontong Java Plateau. *Proceedings of the ocean drilling program*. *Sci. Res.* 130, 33–49.
- Mosher, D.C., Moran, K., Hiscott, R.N., 1994. Late quaternary sediment, sediment mass flow processes and slope stability on the Scotian Slope, Canada. *Sedimentology* 41, 1039–1061. <https://doi.org/10.1111/j.1365-3091.1994.tb01439.x>.
- Mosher, D.C., Piper, D.J.W., Campbell, C., Jenner, K.A., 2004. Near-surface geology and sediment-failure geohazards of the central Scotian Slope. *AAPG Bull.* 88 (60), 703–723. <https://doi.org/10.1306/01260403084>.
- Mosher, D.C., Hawken, J.E., Campbell, C.C., 2021. Gas hydrates and submarine sediment mass failure: A case study from Sackville Spur, offshore Newfoundland. In: Mienert, J., Berndt, C., Trehu, A., Camerlenghi, A., Liu, S.S. (Eds.), *The World Atlas of Submarine Gas Hydrates in Continental Margins*. Springer (in press).
- Mulder, T., Cochonat, P., 1996. Classification of offshore mass movements. *J. Sediment. Res.* 66, 43–57. <https://doi.org/10.1306/D42682AC-2B26-11D7-8648000102C1865D>.
- Mumpton, F.A., 1999. La roca magica: Uses of zeolites in agriculture and industry. *Proc. Natl. Acad. Sci. U. S. A.* 96 (7), 3463–3470. <https://doi.org/10.1073/pnas.96.7.3463>.
- Murawski, H., Meyer, W., 2010. *Geologisches Wörterbuch*, 12. Auflage, pp. 220. Spektrum Akademischer Verlag, Heidelberg, Germany.
- Nienhuis, J.H., Ashton, A.D., Edmonds, D.A., Hoitink, A.J.F., Kettner, A.J., Rowland, J.C., Törnqvist, T.E., 2020. Global-scale human impact on delta morphology has led to net land area gain. *Nature* 577, 514–518. <https://doi.org/10.1038/s41586-019-1905-9>.
- Normandeau, A., Campbell, D.C., Piper, D.J.W., Jenner, K.A., 2019a. Are submarine landslides an underestimated hazard on the western North Atlantic passive margin? *Geology* 47, 848–852. <https://doi.org/10.1130/G46201.1>.
- Normandeau, A., Campbell, D.C., Piper, D.J.W., Jenner, K.A., 2019b. New evidence for a major late Quaternary submarine landslide on the external western levee of Laurentian Fan. In: Lintern, D.G., Mosher, D.C., Moscardelli, L.G., Bobrowski, P.T., Campbell, C., Chaytor, J.D., Clague, J.J., Georgiopoulou, A., Lajeunesse, P.,

- Normandeau, A., Piper, D.J.W., Scherwath, M., Stacey, C., Turmel, D. (Eds.), *Subaqueous Mass Movements*, 477. Geological Society, London, Special Publications, pp. 377–387. <https://doi.org/10.1144/SP477.14>.
- Normark, W.R., 1974. Ranger submarine slide, Northern Sebastian Vizcaino Bay, Baja California, Mexico. *Geol. Soc. Am. Bull.* 85, 781–784. [https://doi.org/10.1130/0016-7606\(1974\)85<781:RSSNSV>2.0.CO;2](https://doi.org/10.1130/0016-7606(1974)85<781:RSSNSV>2.0.CO;2).
- Normark, W.R., 1990. Return to ranger submarine slide, Baja California, Mexico. *Geo-Mar. Lett.* 10, 81–91.
- O'Leary, D.W., 1991. Structure and morphology of submarine slab slides: Clues to origin and behaviour. *Mar. Geotechnol.* 10 (1–2), 53–69. <https://doi.org/10.1080/10641199109379882>.
- Orton, G.J., Reading, H.G., 1993. Variability of deltaic processes in terms of sediment supply, with particular emphasis or grain size. *Sedimentology* 40, 475–512. <https://doi.org/10.1111/j.1365-3091.1993.tb01347.x>.
- Osti, G., Franek, P., Forwick, M., Laberg, J.S., 2017. Controlling factors for slope instability in a seismically active region: the NW-Svalbard continental margin. *Mar. Geol.* 390, 131–146. <https://doi.org/10.1016/j.margeo.2017.06.005>.
- Paull, C.K., Ussler III, W., 2001. History and significance of gas sampling during DSDP and ODP drilling associated with gas hydrates. In: Paull, C.K., Dillon, W.P. (Eds.), *Natural Gas Hydrates: Occurrence, Distribution, and Detection*, Geophysical Monograph, vol. 124. American Geophysical Union, Washington DC, USA, pp. 53–65.
- Paull, C.K., Buelow, W.J., Ussler III, W., Borowski, W.S., 1996. Increased continental-margin slumping frequency during sea-level lowstands above gas hydrate-bearing sediments. *Geology* 24, 143–146. [https://doi.org/10.1130/0091-7613\(1996\)024<0143:ICMSFD>2.3.CO;2](https://doi.org/10.1130/0091-7613(1996)024<0143:ICMSFD>2.3.CO;2).
- Pecher, I.A., Barnes, P.M., Levay, L.J., Expedition 372 Scientists, 2018. Expedition 372 Preliminary Report: Creeping Gas Hydrate Slides and Hikurangi LWD, 26.11.2017–04.01.2018. <https://doi.org/10.14379/iopd.pr.372.2018>.
- Penrose, J.D., Siwabessy, P.J.W., Gavrilov, A., Parnum, I., Hamilton, L.J., Bickers, A., Brooke, B., Ryan, D.A., Kennedy, P., 2005. Acoustic Techniques for Seabed Classification. Cooperative Research Centre for Coastal Zone Estuary and Waterway Management, Technical Report, 32, p. 130.
- Piper, D.J.W., McCall, C., 2003. A synthesis of the distribution of submarine mass movements on the Eastern Canadian margin. In: Locat, J., Mienert, J., Boisvert, L. (Eds.), *Submarine Mass Movements and their Consequences, Advances in Natural and Technological Hazards Research*, 19. Springer, Dordrecht, The Netherlands, pp. 291–298.
- Piper, D.J., Normark, W.R., 2009. Processes that initiate turbidity currents and their influence on turbidites: a marine geology perspective. *J. Sediment. Res.* 79 (6), 347–362. <https://doi.org/10.2110/jsr.2009.046>.
- Piper, D.J.W., Shor, A.N., Clarke, J.E.H., 1988. The 1929 “Grand Banks” earthquake, slump, and turbidity current. *Geol. Soc. Am. Spec. Pap.* 229, 77–92. <https://doi.org/10.1130/SPE229-p77>.
- Piper, D.J.W., Pirmez, C., Manley, P.L., Long, D., Flood, R.D., Normark, W.R., Showers, B., 1997. 6. Mass-transport deposits of the Amazon Fan. In: Flood, R.D., Piper, D.J.W., Klaus, A., Peterson, L.C. (Eds.), *Proceedings of the Ocean Drilling Program, Scientific Results*, 155, pp. 109–146.
- Piper, D.J.W., Cochonot, P., Morrison, M.L., 1999. The sequence of events around the epicentre of the 1929 Grand Banks earthquake: initiation of debris flows and turbidity current inferred from sidescan sonar. *Sedimentology* 46, 79–97. <https://doi.org/10.1046/j.1365-3091.1999.00204.x>.
- Pope, E.L., Talling, P.J., Carter, L., 2017a. Which earthquakes trigger damaging submarine mass movements: Insights from a global record of submarine cable breaks? *Mar. Geol.* 384 (1), 131–146. <https://doi.org/10.1016/j.margeo.2016.01.009>.
- Pope, E.L., Talling, P.J., Carter, L., Clare, M.A., Hunt, J.E., 2017b. Damaging sediment density flows triggered by tropical cyclones. *Earth Planet. Sci. Lett.* 458, 161–169. <https://doi.org/10.1016/j.epsl.2016.10.046>.
- Pope, E.L., Talling, P.J., Ó Cofaigh, C., 2018. The relationship between ice sheets and submarine mass movements in the Nordic Seas during the Quaternary. *Earth Sci. Rev.* 178, 208–256. <https://doi.org/10.1016/j.earscirev.2018.01.007>.
- Prandle, D., 2009. *Estuaries. Dynamics, Mixing, Sedimentation and Morphology*. Cambridge University Press, New York, US, p. 248.
- Principaud, M., Mulder, T., Gillet, H., Borgomano, J., 2015. Large-scale carbonate submarine mass-wasting along the northwestern slope of the Great Bahama Bank (Bahamas): Morphology, architecture, and mechanisms. *Sediment. Geol.* 317, 27–42. <https://doi.org/10.1016/j.sedgeo.2014.10.008>.
- Principaud, M., Mulder, T., Hanquiez, V., Ducassou, E., Eberli, G.P., Chabaud, L., Borgomano, J., 2018. Recent morphology and sedimentary processes along the western slope of Great Bahama Bank (Bahamas). *Sedimentology* 65, 2088–2116. <https://doi.org/10.1111/sed.12458>.
- Prior, D.B., Coleman, J.M., Garrison, L.E., 1979. Digitally acquired undistorted side-scan sonar images of submarine landslides, Mississippi River delta. *Geology* 7, 423–425. [https://doi.org/10.1130/0091-7613\(1979\)7<423:DAUSSI>2.0.CO;2](https://doi.org/10.1130/0091-7613(1979)7<423:DAUSSI>2.0.CO;2).
- Prior, D.B., Doyle, E.H., Neurauter, T., 1986. The currutuck slide, Mid-Atlantic continental slope - revisited. *Mar. Geol.* 73, 25–45. [https://doi.org/10.1016/0025-3227\(86\)90109-X](https://doi.org/10.1016/0025-3227(86)90109-X).
- Puga-Bernabéu, A., Beaman, R.J., Webster, J.M., Thomas, A.L., Jacobsen, G., 2017. Gloria knolls slide: a prominent submarine landslide complex on the Great Barrier Reef margin of North-Eastern Australia. *Mar. Geol.* 385, 68–83. <https://doi.org/10.1016/j.margeo.2016.12.008>.
- Puga-Bernabéu, A., Webster, J.M., Beaman, R.J., Thran, A., López-Cabrera, J., Hineostroza, G., Daniell, J., 2019. Submarine landslide along the mixed siliciclastic-carbonate margin of the Great Barrier Reef (Offshore Australia). In: Ogata, K., Festa, A., Pini, G.A. (Eds.), *Submarine Landslides: Subaqueous Mass Transport Deposits from Outcrops to Seismic Profiles*. Geophysical Monograph Series, vol. 246, pp. 313–338. <https://doi.org/10.1002/9781119500513.ch19>.
- Rack, F.R., Bryant, W.R., Julson, A.P., 1993. Microfabric and physical properties of deep-sea high latitude carbonate oozes. In: Rezak, R., Lavoie, D.L. (Eds.), *Carbonate Microfabrics*. Springer-Verlag, New York, pp. 129–147.
- Rashid, H., MacKillop, K., Sherwin, J., Piper, D.J.W., Marche, B., Vermooten, M., 2017. Slope instability on a shallow contourite-dominated continental margin, southeastern Grand Banks, eastern Canada. *Mar. Geol.* 393, 203–215. <https://doi.org/10.1016/j.margeo.2017.01.001>.
- Rebesco, M., Hernández-Molina, F.J., Van Rooij, D., Wählin, A., 2014. Contourites and associated sediments controlled by deep-water circulation processes: State-of-the-art and future considerations. *Mar. Geol.* 352, 111–154. <https://doi.org/10.1016/j.margeo.2014.03.011>.
- Riedel, M., Bahk, J.J., Scholz, N.A., Ryu, B.J., Yoo, D.G., Kim, W., Kim, G.Y., 2012. Mass-transport deposits and gas hydrate occurrences in the Ulleung Basin, East Sea - Part 2: Gas hydrate content and fracture-induced anisotropy. *Marine and Petroleum Geology* 35, 75–90. <https://doi.org/10.1016/j.margeo.2012.03.005>.
- Riedel, M., Freundenthal, T., Bergenthal, M., Haecckel, M., Wallmann, K., Spangenberg, E., Bialas, J., Bohrmann, G., 2020. Physical properties and core-log seismic integration from drilling at the Danube deep-sea fan, Black Sea. *Mar. Pet. Geol.* 114, 104192. <https://doi.org/10.1016/j.margeo.2019.104192>.
- Riley, C.M., Rose, W.I., Bluth, G.J.S., 2003. Quantitative shape measurements of distal volcanic ash. *J. Geophys. Res.* 108 (B10), 2504. <https://doi.org/10.1029/2001JB000818>.
- Rise, L., Ottesen, D., Longva, O., Solheim, A., Andersen, E.S., Ayers, S., 2006. The Skinnadjupet slide and its relation to the Elsterian glaciation on the mid-Norwegian margin. *Mar. Pet. Geol.* 23, 569–583. <https://doi.org/10.1016/j.margeo.2006.05.005>.
- Rise, L., Chand, S., Hjelstuen, B.O., Hafliðason, H., Bøe, R., 2010. Late Cenozoic geological development of the south Vøring margin, mid-Norway. *Mar. Pet. Geol.* 27, 1789–1803. <https://doi.org/10.1016/j.margeo.2010.09.001>.
- Rodríguez-Ochoa, R., Nadim, F., Hicks, M.A., 2015. Influence of weak layers on seismic stability of submarine slopes. *Mar. Pet. Geol.* 65, 247–268. <https://doi.org/10.1016/j.margeo.2015.04.007>.
- Rosenqvist, I.T.H., 1966. Norwegian research into the properties of quick clay – a review. *Eng. Geol.* 1 (6), 445–450. [https://doi.org/10.1016/0013-7952\(66\)90020-2](https://doi.org/10.1016/0013-7952(66)90020-2).
- Rovere, M., Gamberi, F., Mercorella, A., Leidi, E., 2014. Geomorphometry of a submarine mass-transport complex and relationships with active faults in a rapidly uplifting margin (Gioia Basin, NE Sicily margin). *Mar. Geol.* 356, 31–43. <https://doi.org/10.1016/j.margeo.2013.06.003>.
- Ruffman, A., Hann, V., 2006. The Newfoundland Tsunami of November 18, 1929: an examination of the twenty-eight deaths of the “South Coast Disaster”. *Newfoundland Labrador Stud.* 21, 1719–1726.
- Sammartini, M., Camerlenghi, A., Budillon, F., Insinga, D.D., Zugar, F., Conforti, A., Iori, M., Romeo, R., Tonielli, R., 2019. Open-slope, translational submarine landslide in a tectonically active volcanic continental margin (Licosa submarine landslide, southern Tyrrhenian Sea). In: Lintern, D.G., Mosher, D.C., Moscardelli, L.G., Bobrowsky, P.T., Campbell, C., Chaytor, J.D., Clague, J.J., Georgiopolou, A., Lajeunesse, P., Normandeau, A., Piper, D.J.W., Scherwath, M., Stacey, C., Turmel, D. (Eds.), *Subaqueous Mass Movements and their Consequences: Assessing Geohazards, Environmental Implications and Economic Significance of Subaqueous Landslides*, 477. Geological Society, London, Special Publication, pp. 133–150. <https://doi.org/10.1144/SP477.34>.
- Sawyer, D.E., DeVore, J.R., 2015. Elevated shear strength of sediments on active margins: evidence for seismic strengthening. *Geophys. Res. Lett.* 42, 10,216–10,221. <https://doi.org/10.1002/2015GL066603>.
- Sawyer, D.E., Hodelka, B., 2016. Tiny fossils, big impact: the role of foraminifera-enriched condensed section in arresting the movement of a large retrogressive submarine landslide in the Gulf of Mexico. In: Lamarche, G., Mountjoy, J., Bull, S., Hubble, T., Krastel, S., Lane, E., Micallef, A., Moscardelli, L., Mueller, C., Pecher, I., Woelz, S. (Eds.), *Submarine Mass Movements and their Consequences, Advances in Natural and Technological Hazards Research*, 41. Springer International Publishing Switzerland, Cham, pp. 479–486.
- Sawyer, D.E., Flemings, P.B., Shipp, R.C., Winkler, C.D., 2007. Seismic geomorphology, lithology, and evolution of the late Pleistocene Mars-Ursa turbidite region, Mississippi Canyon area, northern Gulf of Mexico. *AAPG Bull.* 91 (2), 215–234.
- Schiebel, R., 2002. Planktonic foraminiferal sedimentation and the marine calcite budget. *Global Biochem. Cycles* 16 (4), 1065. <https://doi.org/10.1029/2001GB001459>.
- Schmuck, E.A., Paull, C.K., 1993. Evidence for gas accumulation associated with diapirism and gas hydrates at the head of the Cape Fear Slide. *Geo-Mar. Lett.* 13, 145–152.
- Schulten, I., 2019. *Slumps, Slides and Debris Flows of the St. Pierre Slope: a Reanalysis of Slope Instability Due to the 1929 Grand Banks Earthquake*. PhD Thesis. Dalhousie University, Halifax, Nova Scotia (213 pp).
- Schulten, I., Mosher, D.C., Krastel, S., Piper, D.J.W., Kienast, M., 2019a. Surficial sediment failures due to the 1929 Grand Banks Earthquake, St Pierre Slope. In: Lintern, D.G., Mosher, D.C., Moscardelli, L.G., Bobrowsky, P.T., Campbell, C., Chaytor, J.D., Clague, J.J., Georgiopolou, A., Lajeunesse, P., Normandeau, A., Piper, D.J.W., Scherwath, M., Stacey, C., Turmel, D. (Eds.), *Submarine Mass Movements and their Consequences: Assessing Geohazards, Environmental Implications and Economic Significance of Subaqueous Landslide*, 477. Geological Society, London, Special Publications, pp. 583–596. <https://doi.org/10.1144/SP477.25>.
- Schulten, I., Mosher, D.C., Piper, D.J.W., Krastel, S., 2019b. A massive slump on the St. Pierre slope, a new perspective on the 1929 grand banks submarine landslide.

- J. Geophys. Res. Solid Earth 124, 7538–7561. <https://doi.org/10.1029/2018JB017066>.
- Shiwakoti, D.R., Tanaka, H., Tanaka, M., Locat, J., 2002. Influences of diatom microfossils on engineering properties of soils. *Soils Found.* 42 (3), 1–17. <https://doi.org/10.3208/sandf.42.3.1>.
- Silver, E., Day, S., Ward, S., Hoffmann, G., Llanes, P., Driscoll, N., Appelgate, B., Saunders, S., 2009. Volcano collapse and tsunami generation in the Bismarck Volcanic Arc, Papua New Guinea. *J. Volcanol. Geotherm. Res.* 186, 210–222. <https://doi.org/10.1016/j.jvolgeores.2009.06.013>.
- Solheim, A., Berg, K., Forsberg, C.F., Bryn, P., 2005. The Storegga Slide complex: repetitive large scale sliding with similar cause and development. *Mar. Pet. Geol.* 22, 97–107. <https://doi.org/10.1016/j.marpetgeo.2004.10.013>.
- Spagnoli, G., Finkenzeller, S., Freudenthal, T., Hoekstra, T., Woollard, W., Storteboom, O., van den Berg, A.P., Weixler, L., 2015. First deployment of the underwater drill rig MeBo200 in the North Sea and its application for the geotechnical exploration. In: *Proceedings of the SPE Offshore Europe Conference & Exhibition in Aberdeen, Scotland, UK, 8–11 May 2015*.
- Stacey, C.D., Lintern, D.G., Enkin, R.J., 2018. Multifaceted re-analysis of the enigmatic Kitimat slide complex, Canada. *Sediment. Geol.* 369, 46–59. <https://doi.org/10.1016/j.sedgeo.2018.01.006>.
- Stegmann, S., Kopf, A., 2007. Marine deep-water free-fall CPT measurements for landslide characterisation off Crete, Greece (eastern Mediterranean Sea), Part 1: A new 4000m cone penetrometer. In: Lykousis, V., Sakellariou, D., Locat, J. (Eds.), *Submarine Mass Movements and their Consequences, Advances in Natural and Technological Hazards Research*, 27. Springer, Dordrecht, The Netherlands, pp. 171–177.
- Stegmann, S., Mörz, T., Kopf, A., 2006. Initial results of a new Free Fall-Cone Penetrometer (FF-CPT) for geotechnical in situ characterisation of soft marine sediments. *Nor. J. Geol.* 86, 199–208.
- Stegmann, S., Sultan, N., Kopf, A., Apprioual, R., Pelleau, P., 2011. Hydrogeology and its effects on slope stability along the coastal aquifer of Nice, France. *Mar. Geol.* 280, 168–181. <https://doi.org/10.1016/j.margeo.2010.12.009>.
- Stegmann, S., Kreiter, S., L'Heureux, J.S., Vanneste, M., Völker, D., Baeten, N.J., Knudsen, S., Rise, L., Longva, O., Brendryen, J., Hafliðason, H., Chand, S., Mörz, T., Kopf, A., 2016. First results of the geotechnical in situ investigation for soil characterization along the upper slope off Vesterålen: Northern Norway. In: Lamarche, G., Mountjoy, J., Bull, S., Hubble, T., Krastel, S., Lane, E., Micallef, A., Moscardelli, L., Mueller, C., Pecher, I., Woelz, S. (Eds.), *Submarine Mass Movements and their Consequences, Advances in Natural and Technological Hazards Research*, 41. Springer International Publishing Switzerland, Cham, pp. 211–219.
- Steiner, A., L'Heureux, J.S., Kopf, A., Vanneste, M., Longva, O., Lange, M., Hafliðason, H., 2012. An in-situ free-fall piezocene penetrometer for characterizing soft and sensitive clays at finnedfjord (Northern Norway). In: Yamada, Y., Kawamura, K., Ikehara, K., Ogawa, Y., Urgeles, R., Mosher, D., Chaytor, J., Strasser, M. (Eds.), *Submarine Mass Movements and their Consequences, Advances in Natural and Technological Hazards Research*, 31. Springer Science+Business Media B.V., Dordrecht, pp. 99–109.
- Steiner, A., Kopf, A., L'Heureux, J.S., Kreiter, S., Stegmann, S., Hafliðason, H., Moerz, T., 2014. In situ dynamic piezocene penetrometer tests in natural clayey soils – a reappraisal of strain-rate corrections. *Can. Geotech. J.* 51, 272–288.
- Strout, J.M., Tjelta, T.I., 2005. In situ pore pressures: what is their significance and how can they be reliably measured? *Mar. Pet. Geol.* 22, 275–285. <https://doi.org/10.1016/j.marpetgeo.2004.10.024>.
- Strozyk, F., Strasser, M., Förster, A., Kopf, A., Huhn, K., 2010a. Slope failure repetition in active margin environments: Constraints from submarine landslides in the Hellenic fore arc, eastern Mediterranean. *J. Geophys. Res.* 115, B08103 <https://doi.org/10.1029/2009JB006841>.
- Strozyk, F., Strasser, M., Krastel, S., Meyer, M., Huhn, K., 2010b. Reconstruction of retreating mass wasting in response to progressive slope steepening of the northeastern Cretan margin, eastern Mediterranean. *Mar. Geol.* 271, 44–54. <https://doi.org/10.1016/j.margeo.2010.01.008>.
- Sultan, N., Cochonot, P., Canals, M., Cattaneo, A., Dennielou, B., Hafliðason, H., Laberg, J.S., Long, D., Mienert, J., Trincardi, F., Urgeles, R., Vorren, T.O., Wilson, C., 2004. Triggering mechanisms of slope instability processes and sediment failures on continental margins: a geotechnical approach. *Mar. Geol.* 213, 291–321. <https://doi.org/10.1016/j.margeo.2004.10.011>.
- Sultan, N., Savoye, B., Jouet, G., Leynaud, D., Cochonot, P., Henry, P., Stegmann, S., Kopf, A., 2010. Investigation of a possible submarine landslide at the Var delta front (Nice continental slope, Southeast France). *Can. Geotech. J.* 47, 486–496.
- Sun, Q., Alves, T., 2020. Petrophysics of fine-grained mass-transport deposits: a critical review. *J. Asian Earth Sci.* 192, 104291. <https://doi.org/10.1016/j.jseas.2020.104291>.
- Sun, Q., Xie, X., Piper, D.J.W., Wu, J., Wu, S., 2017. Three dimensional seismic anatomy of multi-stage mass transport deposits in the Pearl River Mouth Basin, northern China Sea: their ages and kinematics. *Mar. Geol.* 393, 93–108. <https://doi.org/10.1016/j.margeo.2017.05.005>.
- Sun, Q., Cartwright, J., Xie, X., Lu, X., Yuan, S., Chen, C., 2018. Reconstruction of repeated Quaternary slope failures in the northern South China Sea. *Mar. Geol.* 401, 17–35. <https://doi.org/10.1016/j.margeo.2018.04.009>.
- Syvitski, J.P.M., Burrell, D.C., Skei, J.M., 1987. *Fjords*. Springer-Verlag, New York, US, p. 215.
- Talling, P.J., 2014. On the triggers, resulting flow types and frequencies of subaqueous sediment density flows in different settings. *Mar. Geol.* 352, 155–182. <https://doi.org/10.1016/j.margeo.2014.02.006>.
- Talling, P.J., Wynn, R.B., Masson, D.G., Frenz, M., Cronin, B.T., Schiebel, R., Akhmetzhanov, A.M., Dallmeier-Tiessen, S., Benetti, S., Weaver, P.P.E., Georgiopoulou, A., Zühlsdorff, C., Amy, L.A., 2007. Onset of submarine debris flow deposition far from original giant landslide. *Nature* 450, 541–544.
- Talling, P.J., Clare, M., Urlaub, M., Pope, E., Hunt, J.E., Watt, S.F.L., 2014. Large submarine landslides on continental slopes: Geohazards, methane release, and climate change. *Oceanography* 27 (2), 32–45. <https://doi.org/10.5670/oceanog.2014.38>.
- Tanaka, H., Locat, J., 1999. A microstructural investigation of Osaka Bay clay: the impact of microfossils on its mechanical behaviour. *Can. Geotech. J.* 36, 493–508. <https://doi.org/10.1139/t99-009>.
- Tanaka, M., Tanaka, H., Kamei, T., Hayashi, S., 2003. Effects of diatom microfossil contents on engineering properties of soils. In: *Proceedings of the Thirteenth International Offshore and Polar Engineering Conference, Honolulu, Hawaii, USA, May 25–30, 2003*.
- Tappin, D.R., Watts, P., McMurtry, G.M., Lafoy, Y., Matsumoto, T., 2001. The Sissano, Papua New Guinea tsunami of July 1998 – offshore evidence on the source mechanism. *Mar. Geol.* 175 (1–4), 1–23. [https://doi.org/10.1016/S0025-3227\(01\)00131-1](https://doi.org/10.1016/S0025-3227(01)00131-1).
- ten Brink, U.S., Geist, E.L., Andrews, B.D., 2006. Size distribution of submarine landslides and its implication to tsunami hazard in Puerto Rico. *Geophys. Res. Lett.* 33 (11), L11307 <https://doi.org/10.1029/2006GL026125>.
- ten Brink, U.S., Lee, H.J., Geist, E.L., Twitchell, D., 2009. Assessment of tsunami hazard to the U.S. East Coast using relationships between submarine landslides and earthquakes. *Mar. Geol.* 264 (1–2), 65–73. <https://doi.org/10.1016/j.margeo.2008.05.011>.
- Thakur, V., L'Heureux, J.S., Locat, A., 2017. Landslides in sensitive clays. In: *Advances in Natural and Technological Hazards Research*, 46. Springer, Cham, Switzerland, p. 593.
- Thomas, S., Hooper, J., Clare, M., 2010. Constraining geohazards to the past: impact assessment of submarine mass movements on seabed developments. In: Mosher, D. C., Shipp, C., Moscardelli, L., Chaytor, J., Baxter, C., Lee, H., Urgeles, R. (Eds.), *Submarine Mass Movements and their Consequences, Advances in Natural and Technological Hazards Research*, 28. Springer Science+Business Media B.V., Dordrecht, pp. 387–398.
- Thran, A.C., Dutkiewicz, A., Spence, P., Müller, R.D., 2018. Controls on the global distribution of contourite drifts: Insights from an eddy-resolving ocean model. *Earth Planet. Sci. Lett.* 489, 228–240. <https://doi.org/10.1016/j.epsl.2018.02.044>.
- Torrance, J.K., 1974. A laboratory investigation of the effect of leaching on the compressibility and shear strength of Norwegian marine clays. *Géotechnique* 24 (2), 155–173. <https://doi.org/10.1680/geot.1974.24.2.155>.
- Torrance, J.K., 1983. Towards a general model of quick clay development. *Sedimentology* 30, 547–555. <https://doi.org/10.1111/j.1365-3091.1983.tb00692.x>.
- Tournadour, E., Mulder, T., Borgomano, J., Hanquiez, V., Ducassou, E., Gillet, H., 2015. Origin and architecture of a Mass Transport complex on the northwest slope of Little Bahama Bank (Bahamas): Relations between off-bank transport, bottom current sedimentation and submarine landslides. *Sediment. Geol.* 317, 9–26. <https://doi.org/10.1016/j.sedgeo.2014.10.003>.
- Trincardi, F., Cattaneo, A., Correggiari, A., Mongardi, S., Breda, A., Asioli, A., 2003. Submarine slides during relative sea level rise: two examples from the Eastern Tyrrhenian margin. In: Locat, J., Mienert, J. (Eds.), *Submarine Mass Movements and their Consequences, Advances in Natural and Technological Hazards Research*, 19. Springer Science+Business Media, Dordrecht, pp. 469–478.
- Turner, A.K., Schuster, R.L., 1996. *Landslides. Investigation and Mitigation. Special Report 247*, pp. 671. National Academy of Sciences, United States of America.
- Urgeles, R., Camerlenghi, A., 2013. Submarine landslides of the Mediterranean Sea: Trigger mechanisms, dynamics, and frequency-magnitude distribution. *J. Geophys. Res. Earth Surf.* 118 (4), 2600–2618. <https://doi.org/10.1002/2013JF002720>.
- Urgeles, R., Lastras, G., Canals, M., Willmott, V., Moreno, A., Casas, D., Baraza, J., Berné, S., 2003. The BIG'95 debris flow and adjacent unfailed sediments in the NW Mediterranean Sea: Geotechnical-sedimentological properties, and dating. In: Locat, J., Mienert, J. (Eds.), *Submarine Mass Movements and their Consequences, Advances in Natural and Technological Hazards Research*, 19. Springer Science+Business Media, Dordrecht, pp. 479–487.
- Urgeles, R., Laynaud, D., Lastras, G., Canals, M., Mienert, J., 2006. Back-analysis and failure mechanisms of a large submarine slide on the Ebro slope, NW Mediterranean. *Mar. Geol.* 226, 185–206. <https://doi.org/10.1016/j.margeo.2005.10.004>.
- Urlaub, M., Talling, P.J., Zervos, A., Masson, D., 2015. What causes large submarine landslides on low gradient (<2°) continental slopes with slow (~0.15 m/kyr) sediment accumulation? *J. Geophys. Res. Solid Earth* 120, 6722–6739. <https://doi.org/10.1002/2015JB012347>.
- Urlaub, M., Geersen, J., Krastel, S., Schwenk, T., 2018. Diatom ooze: crucial for the generation of submarine mega-slides? *Geology* 46 (4), 331–334. <https://doi.org/10.1130/G39892.1>.
- Urlaub, M., Krastel, S., Schwenk, T., 2020. Submarine landslides in an upwelling system: climatically controlled preconditioning of the cap blank slide complex (Offshore NW Africa). In: Ogata, K., Festa, A., Pini, G.A. (Eds.), *Submarine Landslides: Subaqueous Mass Transport Deposits from Outcrops to Seismic Profiles*, Geophysical Monograph, 246, pp. 299–311. <https://doi.org/10.1029/1978JL119500513.ch18>.
- Van Daele, M., Meyer, I., Moernaut, J., De Decker, S., Verschuren, D., De Batist, M., 2017. A revised classification and terminology for stacked and amalgamated turbidites in environments dominated by (hem)pelagic sedimentation. *Sediment. Geol.* 357, 72–82. <https://doi.org/10.1016/j.sedgeo.2017.06.007>.
- Vanneste, M., Mienert, J., Büinz, S., 2006. The Hinlopen Slide: a giant, submarine slope failure on the northern Svalbard margin, Arctic Ocean. *Earth Planet. Sci. Lett.* 245, 373–388. <https://doi.org/10.1016/j.epsl.2006.02.045>.
- Vanneste, M., L'Heureux, J.S., Baeten, N., Brendryen, J., Vardy, M.E., Steiner, A., Forsberg, C.F., Kvalstad, T.J., Laberg, J.S., Chand, S., Longva, O., Rise, L.,

- Hafliðason, H., Hjelstuen, B.O., Forwick, M., Morgan, E., Lecomte, I., Kopf, A., Vorren, T.O., Reichel, T., 2012. Shallow landslides and their dynamics in coastal and deepwater environments, Norway. In: Yamada, Y., Kawamura, K., Ikehara, K., Ogawa, Y., Urgeles, R., Mosher, D., Chaytor, J., Strasser, M. (Eds.), *Submarine Mass Movements and their Consequences*, Advances in Natural and Technological Hazards Research, 31. Springer Science+Business Media B.V, Dordrecht, pp. 29–41.
- Vanneste, M., Longva, O., L'Heureux, J.S., Vardy, M.E., Morgan, E., Forsberg, C.F., Kvalstad, T.J., Strout, J.M., Brendryen, J., Hafliðason, H., Lecomte, I., Steiner, A., Kopf, A., Mörz, T., Kreiter, S., 2013. Finneidfjord, a field laboratory for integrated submarine slope stability assessments and characterization of landslide-prone sediments: a review. In: *Offshore Technology Conference, OTC 130TC-P-686-OTC*, Houston, Texas, USA.
- Vanneste, M., Sultan, N., Garziglia, S., Forsberg, C.F., L'Heureux, J.S., 2014. Seafloor instabilities and sediment deformation processes: the need for integrated, multi-disciplinary investigations. *Mar. Geol.* 352, 183–214. <https://doi.org/10.1016/j.margeo.2014.01.005>.
- Vanneste, M., Forsberg, C.F., Knudsen, S., Kvalstad, T.J., L'Heureux, J.S., Lunee, T., Vardy, M.E., Chand, S., Longva, O., Morgan, E., Kopf, A., Mörz, T., Steiner, A., Brendryen, J., Hafliðason, H., 2015. Integration of very-high-resolution seismic and CPTU data from a coastal area affected by shallow landsliding - the Finneidfjord natural laboratory. In: *Frontiers in Offshore Geotechnics III, Chapter 137*, International Symposium on Frontiers in Offshore Geotechnics, Oslo, Norway.
- Vardy, M.E., L'Heureux, J.S., Vanneste, M., Longva, O., Steiner, A., Forsberg, C.F., Hafliðason, H., Brendryen, J., 2012. Multidisciplinary investigation of a shallow near-shore landslide, Finneidfjord, Norway. *Near Surf. Geophys.* 10, 267–277. <https://doi.org/10.3997/1873-2012022>.
- Verdicchio, G., Trincardi, F., 2008. Mediterranean shelf-edge muddy contourites: examples from the Gela and south Adriatic basin. *Geo-Mar. Lett.* 28, 137–151.
- Volpi, V., Camerlenghi, A., Hillenbrand, C.D., Rebescio, M., Ivaldi, R., 2003. Effects of biogenic silica on sediment compaction and slope stability on the Pacific margin of the Antarctic Peninsula. *Basin Res.* 15, 339–363. <https://doi.org/10.1046/j.1365-2117.2003.00210.x>.
- Wang, X., Wang, Y., He, M., Chen, W., Zhuo, H., Gao, S., Wang, M., Zhou, J., 2017. Genesis and evolution of the mass transport deposits in the middle segment of the Pearl River canyon, South China Sea: Insights from 3D seismic data. *Mar. Pet. Geol.* 88, 555–574. <https://doi.org/10.1016/j.marpetgeo.2017.08.036>.
- Watson, S.J., Mountjoy, J.J., Crutchley, G.J., 2020. Tectonic and geomorphic controls on the distribution of submarine landslides across active and passive margins, eastern New Zealand. In: Georgiopolou, A.A.L.A., Benetti, S., Chaytor, J.D., Clare, M.A., Gamboa, D., Haughton, P.D.W., Moernaut, J., Mountjoy, J.J. (Eds.), *Subaqueous Mass Movements and their Consequences: Advances in Process Understanding, Monitoring and Hazard Assessments*, 500. Geological Society, London, Special Publications, pp. 477–494. <https://doi.org/10.1144/SP500-2019-165>.
- Watt, S.F.L., Talling, P.J., Vardy, M.E., Heller, V., Hühnerbach, V., Urlaub, M., Sarkar, S., Masson, D.G., Henstock, T.J., Minshull, T.A., Paulatto, M., Le Friant, A., Berndt, C., Crutchley, G.J., Karstens, J., Stinton, A.J., Maeno, F., 2012. Combinations of volcanic-flank and seafloor-sediment failure offshore Montserrat, and their implications for tsunami generation. *Earth Planet. Sci. Lett.* 319–320, 228–240. <https://doi.org/10.1016/j.epsl.2011.11.032>.
- Watts, A.B., Masson, D.G., 1995. A giant landslide on the north flank of Tenerife, Canary Islands. *J. Geophys. Res.* 100 (B12), 21,487–24,498. <https://doi.org/10.1029/95JB02630>.
- Weaver, P.P.E., Schultheiss, P.J., 1990. Current methods for obtaining, logging and splitting marine sediment cores. *Mar. Geophys. Res.* 12, 85–100.
- Webster, J.M., George, N.P.J., Beaman, R.J., Hill, J., Puga-Bernabéu, Á., Hinestrosa, G., Abbey, E.A., Daniell, J.J., 2016. Submarine landslides on the Great Barrier Reef shelf edge and upper slope: a mechanism for generating tsunamis on the north-east Australian coast? *Mar. Geol.* 371, 120–129. <https://doi.org/10.1016/j.margeo.2015.11.008>.
- Widess, M.B., 1982. Quantifying resolving power of seismic systems. *Geophysics* 47, 1160–1173.
- Wiemer, G., Kopf, A., 2015. Altered marine tephra deposits as potential slope failure planes? *Geo-Mar. Lett.* 35, 305–314.
- Wiemer, G., Kopf, A., 2017a. Influence of diatom microfossils on sediment shear strength and slope stability. *Geochem. Geophys. Geosyst.* 18, 333–345. <https://doi.org/10.1002/2016GC006568>.
- Wiemer, G., Kopf, A., 2017b. On the role of volcanic ash deposits as preferential submarine slope failure planes. *Landslides* 14, 223–232.
- Wilson, C.K., Long, D., Bulat, J., 2003. The Afen slide - a multistaged slope failure in the Faroe-Shetland channel. In: Locat, J., Mienert, J. (Eds.), *Submarine Mass Movements and their Consequences*, Advances in Natural and Technological Hazards Research, 19. Springer Science+Business Media, Dordrecht, pp. 317–324.
- Wilson, C.K., Long, D., Bulat, J., 2004. The morphology, setting and processes of the Afen Slide. *Mar. Geol.* 213, 149–167. <https://doi.org/10.1016/j.margeo.2004.10.005>.
- Winkelmann, D., Stein, R., 2007. Triggering of the Hinlopen/Yermak Megaslide in relation to paleoceanography and climate history of the continental margin north of Spitsbergen. *Geochem. Geophys. Geosyst.* 8 (6), Q06018. <https://doi.org/10.1029/2006GC001485>.
- Winkelmann, D., Jokat, W., Niessen, F., Stein, R., Winkler, A., 2006. Age and extent of the Yermak Slide north of Spitsbergen, Arctic Ocean. *Geochem. Geophys. Geosyst.* 7 (6), Q06007. <https://doi.org/10.1029/2005GC001130>.
- Winkelmann, D., Geissler, W., Schneider, J., Stein, R., 2008. Dynamics and timing of the Hinlopen/Yermak Megaslide north of Spitsbergen, Arctic Ocean. *Mar. Geol.* 250, 34–50. <https://doi.org/10.1016/j.margeo.2007.11.013>.
- Wu, N., Jackson, C.A.L., Johnson, H.D., Hodgson, D.M., Clare, M.A., Nugraha, H.D., Li, W., 2021. The formation and implications of giant blocks and fluid escape structures in submarine lateral spreads. *Basin Res.* <https://doi.org/10.1111/bre.12532>.
- Yin, K.S., Zhang, L.M., Wang, H.J., Zou, H.F., Li, J.H., 2021. Marine soil behaviour classification using piezocone penetration tests (CPTu) and borehole records. *Can. Geotech. J.* 58, 190–199. <https://doi.org/10.1139/cgj-2019-0571>.
- Zampetti, V., Schlager, W., van Konijnenburg, J.H., Everts, A.J., 2004. 3-D Seismic characterization of submarine landslides on a miocene carbonate platform (Luconia Province, Malaysia). *J. Sediment. Res.* 74 (6), 817–830. <https://doi.org/10.1306/040604740817>.

## Glossary

See *Turner and Schuster (1996); Masson et al. (2006); Lee et al. (2007); Murawski and Meyer (2010); Dugan and Sheahan (2012); Thakur et al. (2017); Clare et al. (2019).*

**Basal surface:** Deepest boundary of a submarine landslide.

**Case study or study:** May include only one or several independent research papers that all deal with the same submarine landslide or slide complex.

**Failure mechanism:** A physical, chemical or other process that results in failure; the direct cause of a failure mode.

**Failure mode:** The cause of failure; the direct effect of failure mechanisms.

**Failure plane:** The surface or sediment horizon within the slope stratigraphy along which failure initiates. If no substantial erosion occurs the failure plane also acts as *glide plane*.

**Glide plane:** The surface within the slope stratigraphy upon which slide movement occurs. This surface can coincide with the *failure plane*, but does not have to be identical, e.g. if substantial erosion occurs during the slide movement, thereby remoulding and removing the failure plane.

**Liquefaction:** Sediment that normally behaves as a solid (i.e. with shear strength) behaves like a liquid. Occurs when a sediment loses strength under environmental conditions such as cyclic loading from earthquakes. Intergranular friction is lost with one another, and the particle weight is temporarily sustained by the pore fluid, causing transient pore pressures and subsequent failure.

**Permeability:** A measurement of the sediment's capability to let fluids pass through.

**Porosity:** Pore space of the sediment, and is the fraction of the volume of voids over the total volume.

**Pre-conditioning factor:** Long-term factors (e.g. sedimentation) that bring submarine slopes closer towards failure.

**Sediment horizon:** A bedding surface with a marked change in lithology, or a distinct layer or thin bed with a characteristic lithology or geotechnical properties within the stratigraphy.

**Sediment sequence:** Refers to alternating layers of varying physical and geotechnical properties, e.g. grain size, shear strength or porosity.

**Sensitive clay:** A clay where the remoulded shear strength is significantly less than its undisturbed shear strength. The ratio of undisturbed to disturbed strength is termed sensitivity.

**Slope failure:** Refers to the downward movement of slope material in response to gravitational stresses. Slope failure occurs when the downward driving forces exceed the resisting forces of the slope material.

**Strain softening:** Decrease in shear strength with increasing strain.

**Submarine landslide:** Gravity-driven mass movement that occurs in a variety of underwater slope settings worldwide.

**Submarine landslide complex:** Multi-failure complex, reference to a sedimentary body consisting of multiple mass failure deposits.

**Triggering mechanism:** An external stimulus that initiates slope failure.